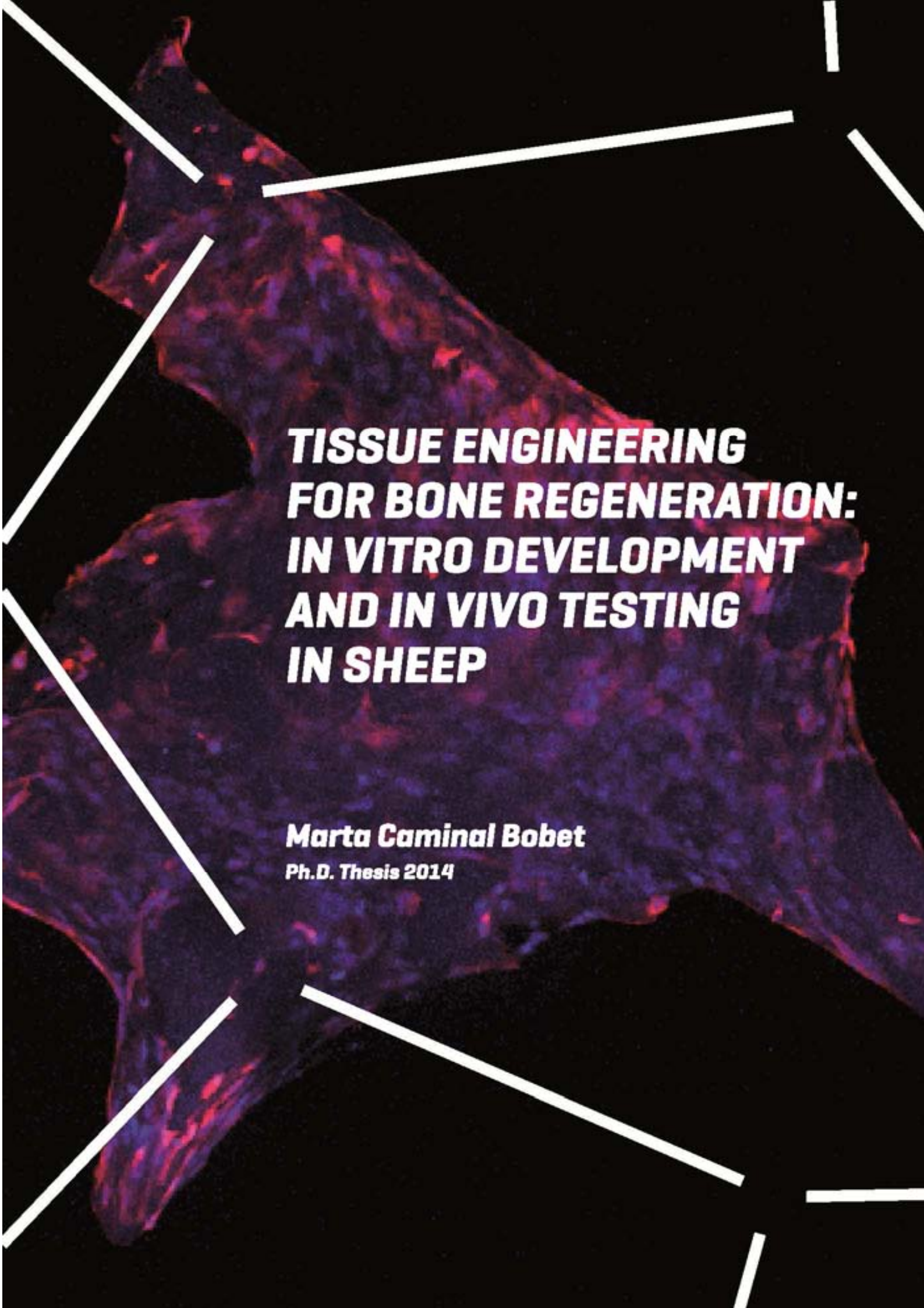

TISSUE ENGINEERING FOR BONE REGENERATION: IN VITRO DEVELOPMENT AND IN VIVO TESTING IN SHEEP

Marta Caminal Bobet

Ph.D. Thesis 2014

Universitat Autònoma de Barcelona

ESCOLA TÈCNICA SUPERIOR D'ENGINYERIA

Tissue Engineering for bone regeneration: *in vitro* development and *in vivo* testing in sheep

Programa de doctorat en Biotecnologia.

Departament d'Enginyeria Química.

MARTA CAMINAL BOBET

Bellaterra, Setembre de 2014

FRANCESC GÒDIA i CASABLANCAS, Catedràtic del Departament d'Enginyeria Química de la Universitat Autònoma de Barcelona i **JOAQUIM VIVES ARMENGOL**, Facultatiu del Banc de Sang i Teixits de Barcelona.

CERTIFIQUEM: Que la llicenciada **MARTA CAMINAL BOBET** ha dut a terme amb la nostra direcció, en els laboratoris del Departament d'Enginyeria Química, el treball que amb el títol: Tissue Engineering for bone regeneration: *in vitro* development and *in vivo* testing in sheep, es presenta en aquesta memòria, la qual constitueix la seva Tesi per optar al grau de Doctora en Biotecnologia.

I perquè en prengueu coneixement i tingui els efectes que correspongui, presentem davant de l'Escola de Doctorat de la Universitat Autònoma de Barcelona l'esmentada Tesi signant aquesta certificació a

Bellaterra, Setembre de 2014

Francesc Gòdia i Casablancas Joaquim Vives Armengol

No es poden deduir veritats amb cadenes de demostracions,
s'han d'experimentar.

(Antoine de Saint-Exupéry, El Petit Príncep)

AGRAÏMENTS

A la mare, al pare i a l'Aleix

TABLE OF CONTENTS

Table of contents

List of figures

List of tables

ABBREVIATIONS AND SYMBOLS

Abbreviatures and Symbols

AEMPS	*"Agencia Española del Medicamento y Productos Sanitarios*
ATMP	*Advanced Therapy Medicinal Products*
BA	*Bone Area*
BM	*Bone Marrow*
BME	*Basal Medium Eagle*
BrdU	*5-bromo-2'-deoxyuridine*
CD	*Cell Density*
CFU-F	*Colony-Forming Unit Fibroblast*
CPD	*Cell Population Doublilngs*
CSD	*Critical Size Defect*
DMEM	*Dulbecco's Modified Eagle Medium*
DMSO	*Dimethyl Sulfoxide*
DT	*Doubling Time*
EC	*European Commission*
ECACC	*European Collection Of Cell Cultures*
EF	*Expansion Factor*
FACS	*Fluorescence-activated cell sorting*
Fig	*Figure*
GAG	*GlycosAminoGlycans*
GCP	*Good Clinical Practices*
GFP	*Green Fluorescent Protein*
GLP	*Good Laboratory Practices*
GMP	*Good Manufacturing Practices*

GS	*Gold Standard*
H&E	*Hematoxylin and eosin*
hMNC	*Human MonoNuclear Cells*
hSer AB	*AB Human Serum*
IM	*IntraMuscular*
ISCT	*International Society for Cellular Therapy*
IV	*IntraVenous*
IVC	*Integral of Viable Cells*
LBA	*Lamelar Bone Area*
MNC	*MonoNuclear Cells*
MOI	*Multiplicity Of Infection*
MRI	*Magnetic Resonance Imaging*
MSC	*Mesenchymal Stromal Cells*
MTT	*3-[4,5-dimethylthiazol-2-yl]-2,5-diphenyl tetrazolium bromide*
OB	*Osteoblasts*
OC	*Osteoclasts*
oMNC	*ovine MonoNuclear Cells*
ON	*Osteonecrosis*
ONFH	*OsteoNecrosis of the Femoral Head*
PBS	*Phosphate Buffered Saline*
PEI	*"Producto en fase de investigación clínica" (Product in clinical research phase)*
PFA	*Paraformaldehyde*
q_p	*Specific Production Rate*

q_s	*Specific Consumption Rate*
ref	*Reference*
RM	*Regenerative Medicine*
SC	*SubCutaneous*
SEM	*Scanning Electron Microscopy*
SN	*Supernatant*
TA	*Total Area of tissue*
TE	*Tissue Engineering*
TEP	*Tissue Engineering Ppreparation*

SUMMARY

ENGLISH SUMMARY: Tissue engineering for bone regeneration: in vitro development and in vivo testing in sheep

Bone is a highly organized and specialized connective tissue, whose main function is the mechanics, providing attachment to muscles and therefore allowing the body to move. Currently the gold standard surgical treatment is based on the immobilization and introduction of bone grafts but it presents some complications, such as infections, non-unions, and donor site morbidity. Nowadays, millions of patients are suffering from bone defects and specifically, 10,000 to 20,000 new cases of osteonecrosis of femoral head (ONFH) are diagnosed only in the USA every year.

Regenerative medicine (RM) and tissue engineering (TE) are two areas of science fields focused on the developing of therapies to replace and regenerate lost or damaged tissues to improve the quality of life the patient. The combination of biomaterials, cells and signals is the key tool for the development of a RM and TE product. One of the most developed fields in RM is the orthopedic regenerative medicine, in specifically for bone tissue. There are different strategies combining autologous cells with scaffolds that have shown some efficacy for treating bone injuries. After discovery phase of any new advanced therapy medicinal products, there is the development phase that includes the conduction of preclinical studies (made to perform the proof of concept, safety and toxicology) and clinical studies before the registration of the new product.

First the components of the tissue engineered preparation (TEP) were determined and characterized in order to have a standardized material. It consists in MSC

(mesenchymal stromal cells) both human and ovine sources are used as a cellular component seeded in a deantigenized and lyophilized bone particles as a scaffold.

Then critical size bone defect (CSBD) was modeled in sheep in order to investigate the effect of the TEP in an extreme situation, demonstrating its safe ability to synthesize new bone and bone remodeling.

Afterwards TEP was tested in a relevant translational animal model of bone disease based on the method reported by Velez and collaborators for modelling ONFH in sheep demonstrating its efficacy and safety. Also demonstrating that MSC were involved in the synthesis of new bone, because labeled bone progenitors are shown after ONFH treatment, although paracrine mechanisms can not be discarded.

Therefore, the development of TEP could contribute to the overall RM to meet the requirements of an aging society.

RESUM EN CATALÀ: Enginyeria tissular per la regeneració òssia: desenvolupament in vitro i test in vivo en ovella.

L'os és un teixit connectiu altament organitzat i especialitzat, la funció principal és la mecànica, proporcionant l'afecció als músculs i per tant permetent que el cos es mogui. Actualment, el tractament quirúrgic estàndard es basa en la immobilització i la introducció d'empelts ossis però presenta algunes complicacions, com ara les infeccions, les no unions i la morbiditat de la zona donant. Avui en dia, milions de pacients pateixen defectes ossis i en concret, als EEUU es diagnostiquen entre 10.000 i 20.000 nous casos d'osteonecrosi del cap de fèmur (ONFH) a l'any.

La medicina regenerativa (RM) i l'enginyeria tissular (TE) són dos camps de la ciència que es centren en el desenvolupament de teràpies per reemplaçar i regenerar els teixits perduts o danyats per millorar la qualitat de vida del pacient. La combinació de biomaterials, cèl·lules i senyals és l'eina clau per al desenvolupament d'un producte RM i TE. Un dels camps més desenvolupats en RM és la medicina regenerativa ortopèdica, en concret per al teixit ossi. Hi ha diferents estratègies que combinen cèl·lules autòlogues amb matrius que han demostrat certa eficàcia en el tractament de lesions òssies. Després de la fase de descobriment de nous medicaments de teràpia avançada, i per tal d'aconseguir el registre del nou producte, hi ha la fase de desenvolupament, que inclou la realització d'estudis preclínics (fet per dur a terme la prova de concepte, la seguretat i toxicologia) i els estudis clínics.

En primer lloc es van determinar i caracteritzar els components de la preparació d'enginyeria tissular (TEP) amb la finalitat d'obtenir un producte estandarditzat. Aquesta preparació consisteix en un component cel·lular que són les cèl·lules

mesenquimals estromals (MSC), tant humanes com ovines unides en una matriu de partícules òssies desantigeneïtzades i liofilitzades.

Es va realizar un model de defecte ossi de mida crítica (CSBD) en ovella amb la finalitat d'investigar l'efecte de la TEP en una situació extrema, i es va demostrar la seva seguretat i capacitat per sintetitzar nou os i remodelar l'os existent.

Seguidament la TEP es va provar en un model animal rellevant de translació de la malaltia òssia basat en el mètode reportat per Vélez i col·laboradors per a la modelització de ONFH en ovelles demostrant la seva eficàcia i seguretat. També s'ha demostrat que les MSC estan involucrades en la síntesi d'os nou ja que es van trobar progenitors ossis marcats després del tractament de la ONFH, tot i així no es poden descartar els mecanismes paracrins.

Per tant, el desenvolupament de la TEP podria contribuir en general a la RM per tal de satisfer les exigències d'una societat que envelleix.

CHAPTER I

Introduction

1. CHAPTER I: INTRODUCTION

1.1 Regenerative medicine and tissue engineering

Regenerative medicine (RM) and tissue engineering (TE) are two science fields that emerged during the XXth century, having as a common challenge the development of therapies to replace and/or regenerate lost or damaged tissues. RM aims to contribute to the improvement of the quality of life of patients and to their healthy aging. It is a multidisciplinary field that attempts to facilitate to repair, replace and regenerate damaged or diseased cells, tissues and organs (Daar and Greenwood, 2007) in order to restore impaired function resulting from congenital defects, diseases, trauma injuries, ageing and others (Mason and Dunnill, 2008). Examples of such treatments are heart muscle repair after a heart attack (Assmus et al., 2002; Perin et al., 2004; Wollert et al., 2004), skin replacement after burn injury (Gurtner et al., 2007), movement restore after spinal cord injury (Saporta et al., 2003) and regeneration of pancreatic islets to produce insulin in people affected with diabetes (Halban, 2004). While regenerative medicine mainly focuses on stem cell therapy methodologies, tissue engineering combines biomaterial science concepts with cell biology and medicine. It was in 1988, at a National Science Foundation bioengineering panel meeting in Washington DC, that TE was first officially described as *the application of the principles and methods of engineering and life sciences toward the development of biological substitutes to restore, maintain or improve function* (Nerem, 1992). By 1993, Langer and Vacanti defined TE as an *interdisciplinary field that applies the principles of engineering and life sciences toward the development of biological substitutes that restore, maintain or improve tissue or whole organ function* (Langer

and Vacanti, 1993). In general, the term TE includes RM, so in this PhD both are used interchangeably.

RM and TE receive contributions from a number of research areas such as stem cell biology, material science, genetics and molecular biology, developmental biology and cell, tissue and organ transplantation shown in **Fig. 1-1**.

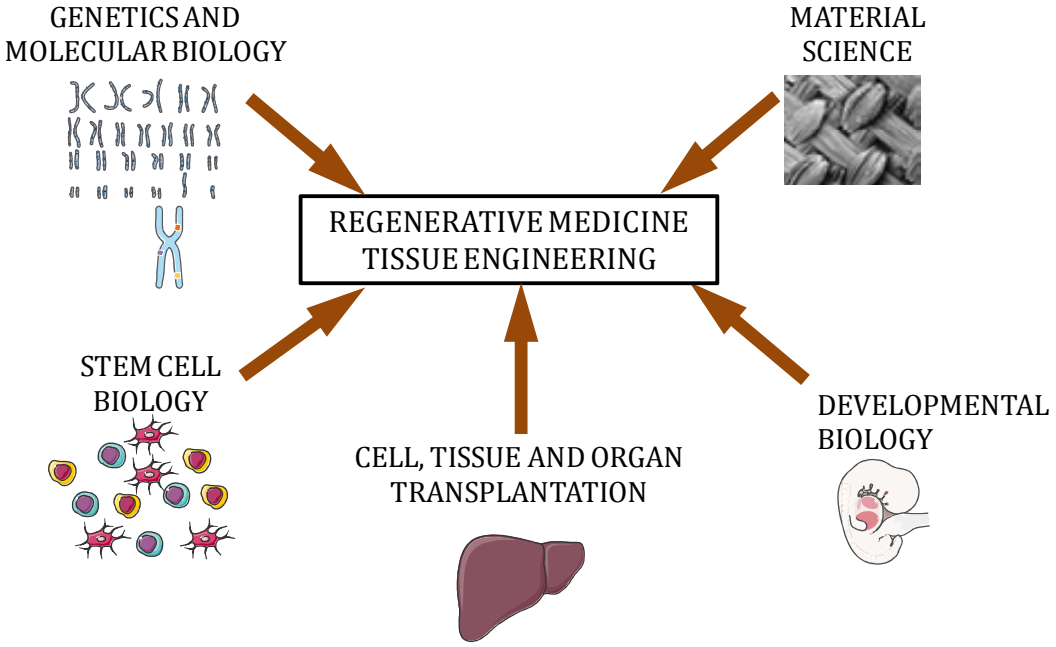

Fig. 1-1. A number of disciplines contribute to regenerative medicine. Figure based on (Daar and Greenwood, 2007) using artwork from "Medical Art Gallery" (Les Laboratoires Servier).

The first FDA (Food and Drug Administration) approval of a TEP (Tissue Engineering Preparation), with a living cellular component, was on 1998, when Organogenesis received the authorization for a hybrid product (Apligraf™) with living keratinocytes and fibroblasts for the treatment of venous leg ulcers. In 2000, Apligraf™ was approved by the FDA for a second major application in the treatment of diabetic foot ulcers (Parenteau and Naughton, 1999).

Since then, the number of publications on RM or TE (based on PubMed search; www.pubmed.gov) has grown exponentially, reaching 72,032 publications this

year as it is shown in **Fig. 1-2**. This proves the broad significance that RM and TE may have in future therapies for healing some diseases.

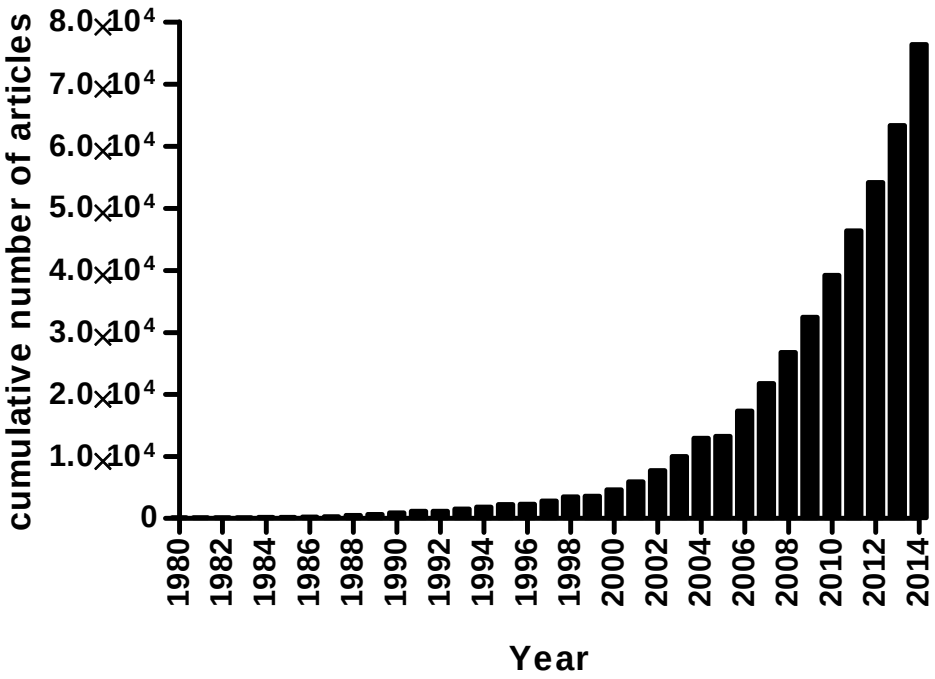

Fig. 1-2. Emerging interest in RM and TE. Cumulative number of PubMed (www.pubmed.com) entries that have been listed by the end of each year. Search terms: "Regenerative Medicine" OR "Tissue Engineering", accessed on 25/08/2014. The number for 2014 has been projected according to the recent development.

RM and TE comprise a combination of three key tools described below that could be used alone or in combination in new regenerative medicine treatments:

1) **Biomaterials** must provide structural support to the cells, retention and chemical signaling in order to promote the organization and differentiation of the cells that will facilitate the formation of a new functional tissue. New extracellular matrix produced by cells will be deposited as the biomaterial degrades.
2) **Signals** are required to enhance cell proliferation and/or differentiation. It includes growth factors and mechanical stimuli, among others.

3) **Stem Cells (SC) or progenitor cells** are necessary so they can differentiate into tissue specific cells to create new functional tissue. A stem cell is capable to self-renew and also differentiating to a mature cell.

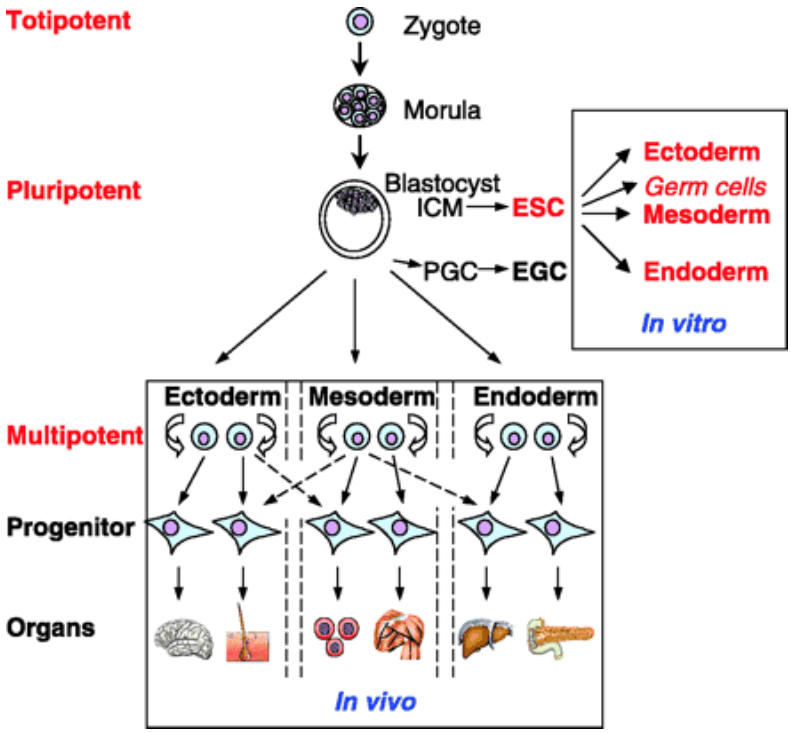

Fig. 1-3. Differences between toti, pluri and multipitent SC (Wobus and Boheler, 2005).

There are different types of stem cells, which are commonly classified by their potency. **Totipotent** stem cells (zygote) can create a complete and viable organism (including extraembryonic tissues). **Pluripotent** stem cells are derived from totipotent cells they can differentiate to any type of cell, except extraembryonic tissues, are the Embryonic Stem (ES) cells. **Multipotent** stem cells can differentiate to a wide variety of cells, but only those of a close family, for example Mesenchymal Stromal Cells (MSC) can differentiate into all cells in connective tissue, but not other kinds of cells. **Unipotent** stem cells can only turn into cells of their own type (See Fig.

1-3). Different types of cells have been used in order to repair different tissues in regenerative medicine and their proprieties are shown in **Fig. 1-4.**

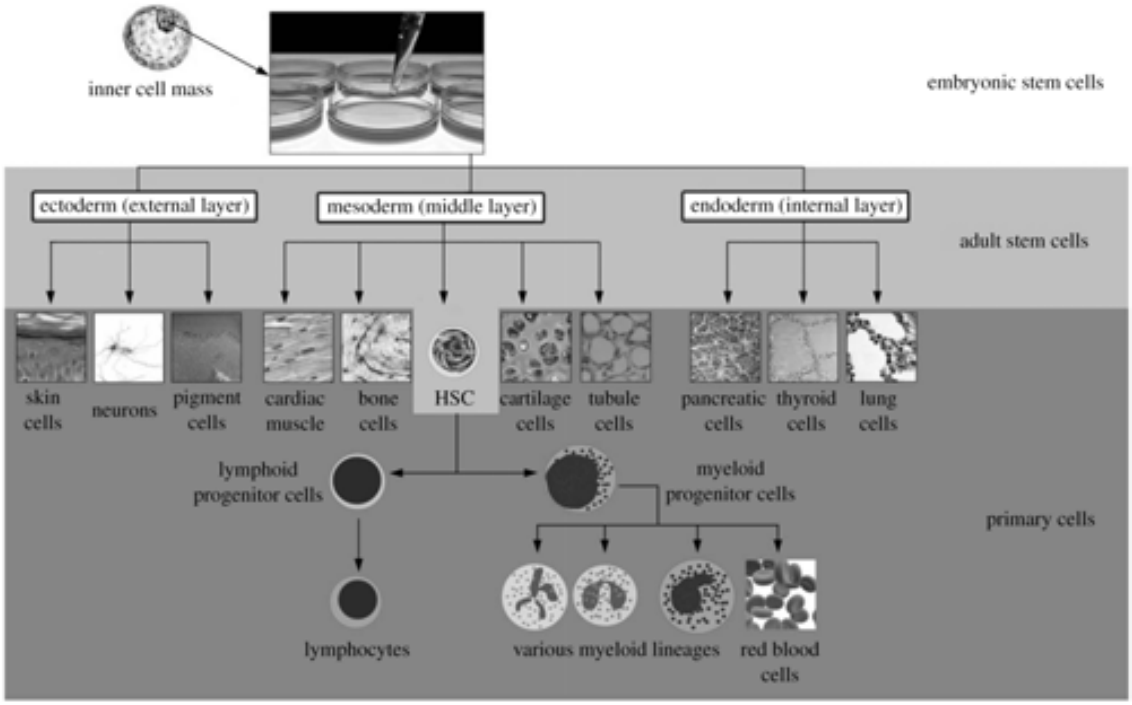

stem cell type	expansion potential	differentiation potential	cell availability	immunogenicity autologous	immunogenicity allogenic	teratogenicity	ease of regulation	ethical acceptance	bioprocess complexity	established clinical practice	regulatory approval
embryonic	+++	+++	+++	–	medium	yes	+	no	+++	no	no
adult											
– mesenchymal	+	++	+	low	high	no	++	yes	++	yes	yes
– haemopoietic	+	++	+	low	high	no	++	yes	++	yes	yes
– cord blood	+	++	++	low	low	no	++	yes	++	yes	yes
primary cells	–	–	+	low	high	no	+++	yes	+	yes	yes

Fig. 1-4. Properties of the different cell types used in regenerative medicine and tissue engineering applications.

Although the potential of ES cells for therapy is very promising, ethical reservations associated with the use of embryos and the allogeneic nature and with it rejection after transplantation has spurred the search for alternative sources of pluripotent stem cells. In August 2006 Takahashi and Yamanaka published a report claiming the induction of pluripotent stem (iPS) cells from mouse cells of adult and embryonic origin as the result of the transduction of four genes, namely Oct-3/4, Sox-2,c-Myc, and Klf (Takahashi and Yamanaka, 2006) and also demonstrate it from adult human dermal fibroblasts (Takahashi et al., 2007). Reprogramming adult cells to generate iPS has opened new therapeutic opportunities; and in 2013 Abad

and Serrano demonstrated that full reprogramming can occur *in vivo* reaching the pluripotency (Abad et al., 2013).

1.2 Bone tissue engineering

One of the most developed fields in regenerative medicine is the orthopedic regenerative medicine. A limited number of strategies combining autologous cells with a variety of synthetic scaffolds have shown some efficacy for treating long bone defects (Marcacci et al., 2007), fracture non-union (Quarto et al., 2001), osteonecrosis (Gangji and Hauzeur, 2005), cartilage (Chang et al., 2008), tendons (Young et al., 1998), muscles (De Bari et al., 2003), ligaments (Goh et al., 2003) and in spinal fusion surgery (Faundez et al., 2006; Putzier et al., 2008). However, there is a pressing need for additional high-quality, methodologically robust studies using cell-based therapies addressing bone regeneration. In this field of regenerative medicine, several types of stimulations and biomaterials have been studied but the cells mostly used are MSC which can be isolated from many different adult tissues and exhibit a great potential to give rise to cells of diverse lineages (Salem and Thiemermann, 2010).

It is necessary to following the requirements of the EMEA draft reflection on stem-cell based medicinal products (EMEA/CAT/571134/2009), it is necessary to perform non-clinical studies in order to adequately evaluate different aspects including proof of concept, immune rejection and safety, that were evaluated in this PhD project.

1.3 Bone

This thesis is in line with the regenerative medicine and in particular those related to bone regeneration. Regenerative medicine addressing bone repair, focuses on metabolic disorders (Casado-Diaz et al., 2008), non-union bone fractures (Kruyt et al., 2004), metastases and others.

1.3.1 Bone functions and structure

Bone is a highly organized and specialized connective tissue that has many functions in the body. The principal function of all bone types is mechanical, providing attachment to muscles and therefore allowing the body to move. Moreover in some parts of the body (skull, ribs, and pelvis) they have a protective function to vital structures such as brain, lungs, heart, bladder, viscera, etc. Additionally some bones (long and cancellous bones) are involved in the hematopoiesis process producing all blood cells that circulate in the body. Lastly all bones serve as a reservoir of calcium and participate actively in its homeostasis, as well as other metabolic functions. Bone is not a uniform tissue and has different structures. There are two main types of bone depending on its porosity and microstructure.

A. CORTICAL BONE

Cortical or compact bone (**Fig. 1-5A**) facilitates bone's main functions. As its name implies, cortical bone forms the cortex of most bones. Compact bone is much denser, stronger and stiffer than cancellous bone. Cortical bone contributes about 80% of the weight of a human skeleton.

B. SPONGY BONE

Spongy bone (also called cancellous or trabecular bone) (**Fig. 1-5B**) has a higher surface area, compared to compact bone, but is softer, weaker, and less stiff and dense than the cortical bone. It is typically found at the ends of long bones, proximal to joints and within the interior of vertebrae. Cancellous bone is highly vascular and it frequently contains bone marrow, where hematopoiesis takes place.

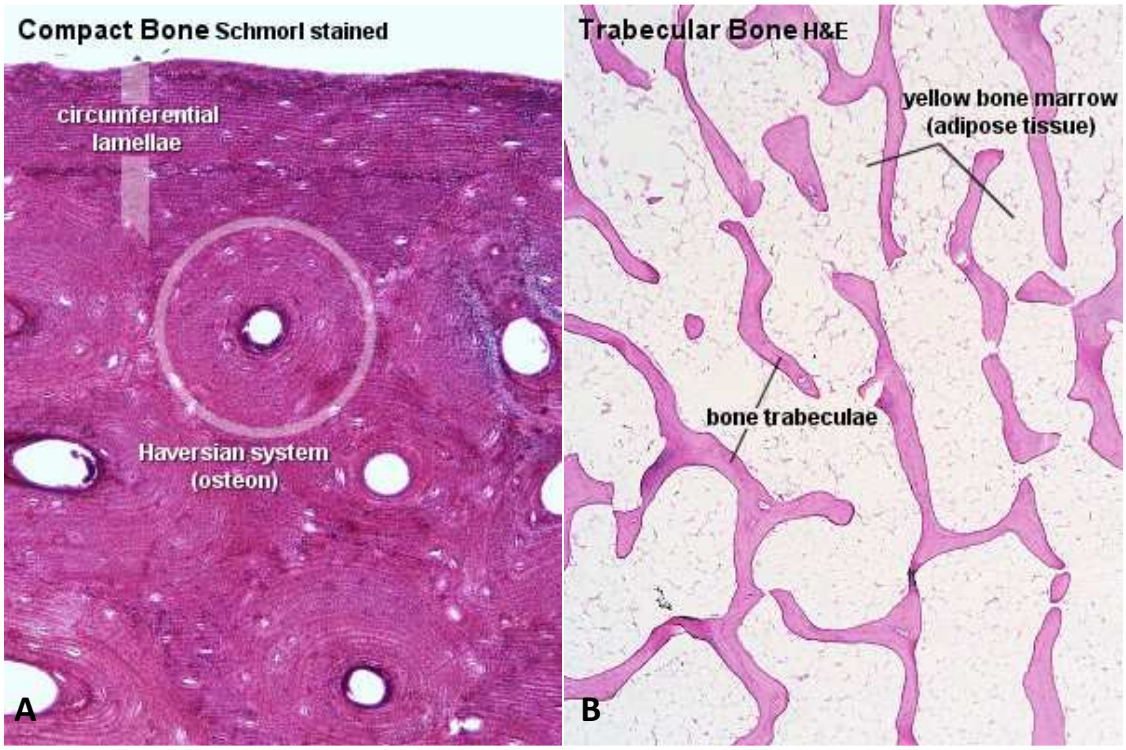

Fig. 1-5. A) Histological Schmorl staining of human compact bone. Osteon highlighted with a circle. B) Histological H&E image of spongy bone. Purple area shows the trabeculaeand wite area the bone marrow Image from School of Anatomy and Human Biology - The University of Western Australia http://www.lab.anhb.uwa.edu.au/mb140/corepages/bone/bone.htm#Histological

1.3.2 Bone matrix

Bone matrix is composed of organic and inorganic matter. The organic matter consists of type I collagen fibers embedded in a matrix containing proteoglycans and glycoproteins. Collagen fibers are made up of bundles of fibrils than confer resistance to pulling forces. The inorganic matter is made up of stiffening

substances that are crucial to avoid bending and compression. The bone mineral is hydroxyapatite, and it this association of hydroxyapatite with collagen fibers which is responsible for the hardness of bone.

1.3.3 Bone cell types

Bone tissue is composed of four principal cell types (see **Fig. 1-10**):

- **Osteoblasts:** the bone forming cells, located on the surfaces of bone lying side by side like a simple cuboidal epithelium. These cells are responsible for the synthesis of organic components of the bone matrix. When active, they show high levels of alkaline phosphatase activity.
- **Osteocytes**: the cells occupying the lacunae in the bone matrix. They possess long thin cytoplasmic processes — the filopodia located in thin cylindrical spaces or canals in the bone matrix — the canaliculi. Nutrients and oxygen pass between the blood vessels and distant osteocytes by the arrangement of the canaliculi. Osteocytes also break down the bone matrix by osteocytic osteolysis to release calcium for calcium homeostasis.
- **Osteoclasts**: the large, multi-nucleated cells formed by fusion of monocytes. They lie in shallow depressions on the bone surface called the Howship's lacunae.
- **Osteoprogenitor cells**

Both osteoblasts and osteocytes have MSC origin whilst osteoclasts come from hematopoietic stem cells (HSC).

1.3.4 Bone formation (osteogenesis)

Some of the most obvious structures derived from the paraxial mesoderm are bones.

There are three distinct lineages that generate the skeleton. The somites generate the axial skeleton, the lateral plate mesoderm generates the limb skeleton, and the cranial neural crest gives rise to the branchial arch and craniofacial bones and cartilage. There are two major modes of bone formation, or **osteogenesis**, and both involve the transformation of a preexisting mesenchymal tissue into bone tissue. The direct conversion of mesenchymal tissue into bone is called **intramembranous ossification**. This process occurs primarily in the bones of the skull. In other cases, the mesenchymal cells differentiate into cartilage, and this cartilage is later replaced by bone. The process by which a cartilage intermediate is formed and replaced by bone cells is called **endochondral ossification**.

A. Endocondral ossification

Endochondral ossification involves the formation of cartilage tissue from aggregated mesenchymal cells, and the subsequent replacement of cartilage tissue by bone (Horton, 1990). The process of endochondral ossification can be divided into five stages (**Fig. 1-6**). First, the mesenchymal cells are commited to become cartilage cells. This committment is caused by paracrine factors that induce the nearby mesodermal cells to express two transcription factors, Pax1 and Scleraxis. These transcription factors are thought to activate cartilage-specific genes (Cserjesi et al., 1995; Šošić et al., 1997). Thus, Scleraxis is expressed in the

mesenchyme from the sclerotome, in the facial mesenchyme that forms cartilaginous precursors of bone, and in the limb mesenchyme (**Fig. 1-6**).

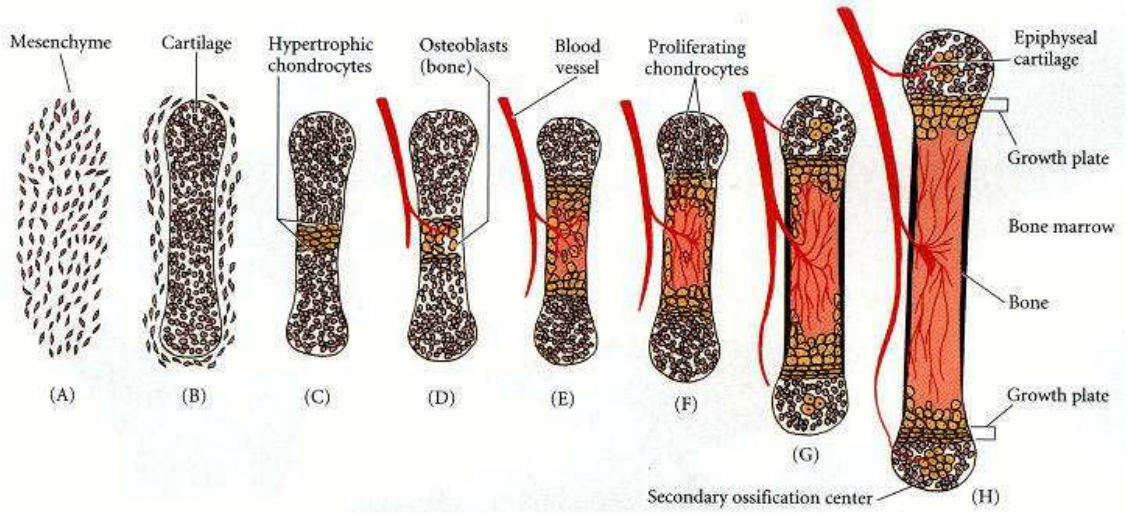

Fig. 1-6. Schematic diagram of endochondral ossification. (A, B) Mesenchymal cells condense and differentiate into chondrocytes to form the cartilaginous model of the bone. (C) Chondrocytes in the center of the shaft undergo hypertrophy and apoptosis while they change and mineralize their extracellular matrix. Their deaths allow blood vessels to enter. (D, E) Blood vessels bring in osteoblasts, which bind to the degenerating cartilaginous matrix and deposit bone matrix. (F-H) Bone formation and growth consist of ordered arrays of proliferating, hypertrophic, and mineralizing chondrocytes. Secondary ossification centers also form as blood vessels enter near the tips of the bone. (Gilbert, 2000).

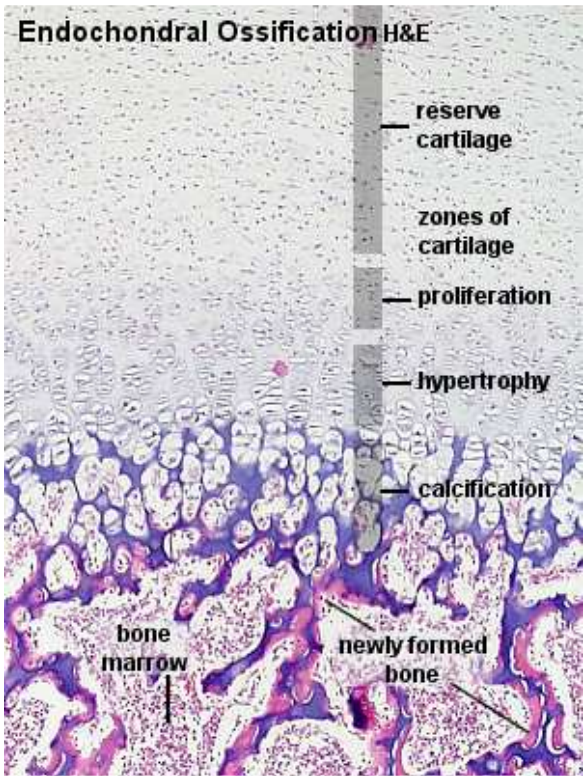

Fig. 1-7. Endochondral ossification. Histological H&E staining. Different zones of bone formation from bone epiphysis at the top, zone of reserve of cartilage, zone of proliferation, zone of hypertrophy, zone of calcification and zone of ossification at the bottom. Image from School of Anatomy and Human Biology - The University of Western Australia http://www.lab.anhb.uwa.edu.au/mb140/corepages/bone/bone.htm#Histological

B. Intramembranous ossification

Intramembranous ossification is the characteristic way in which the flat bones of the skull are formed. During intramembranous ossification in the skull, neural crest-derived MSC proliferate and condense into compact nodules. Some of the MSC develop into capillaries; others change their shape to become osteoblasts, committed bone precursor cells (**Fig. 1-8**).

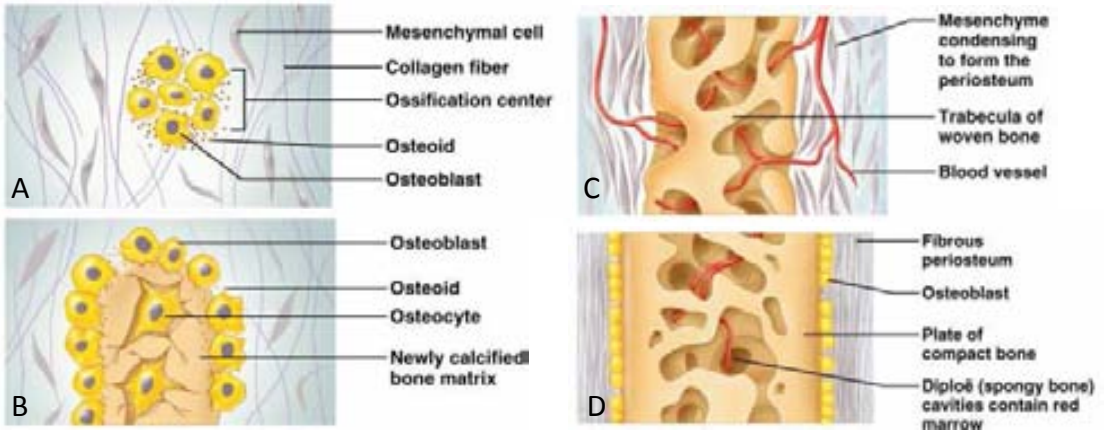

Fig. 1-8. Schematic diagram of intramembranous ossification. (A) Ossification centers appear in the fibrous connective tissue membrane. (B) bone matrix (osteoide) is secreted within the fibrous membrane and calcifies. (C) Woven bone and periosteum form. (D) Lamellar bone replaces woven bone, just deep to the periosteum. Bone marrow appears.

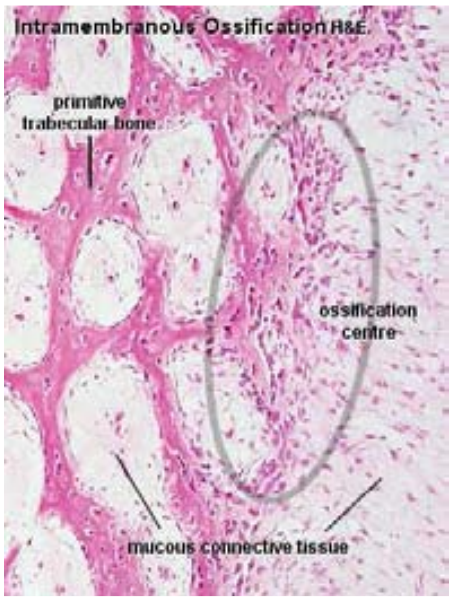

Fig. 1-9. Intramembranous ossification. Ossification center highlighted by a circle (containing osteoblast line) and primary trabecular bone as intense pink area at top left**.** Image from School of Anatomy and Human Biology - The University of Western Australia http://www.lab.anhb.uwa.edu.au/mb140/corepages/bone/bone.htm#Histological

The osteoblasts secrete a collagen-proteoglycan matrix that is able to bind calcium salts. Through this binding, the prebone (osteoid) matrix becomes calcified. In most cases, osteoblasts are separated from the region of calcification by a layer of the osteoid matrix they secrete. Occasionally, though, osteoblasts become trapped in the calcified matrix and become terminally differentiated osteocytes—bone cells. As calcification proceeds, bony spicules radiate out from the region where ossification began. Furthermore, the entire region of calcified spicules becomes surrounded by compact mesenchymal cells that form the periosteum (a membrane that surrounds the bone). The cells on the inner surface of the periosteum also become osteoblasts and deposit osteoid matrix parallel to that of the existing spicules. In this manner, many layers of bone are formed.

C. Bone remodellinig

The renewal of bone is responsible for bone strength throughout our life. Old bone is resorbed and new bone is formed. During childhood and the beginning of adulthood, bone becomes larger, heavier and denser, bone formation is then more important than bone resorption and at a certain age, bone mass starts to decrease loosing the capacity to form new bone.

Two main types of cells are responsible in bone remodeling cycle: A) osteoblasts, involved in bone formation and B) osteoclasts involved in bone resorption. Preosteoclasts are stimulated and differentiated under the influence of cytokine and growth factors to mature into active osteoclasts. Osteoclasts digest mineral matrix, the old bone. And then osteoblasts are responsible for bone matrix synthesis (collagen). Two other non-collagenous proteins are also formed:

osteocalcin and osteonectin and finally protein matrix is mineralized (see **Fig. 1-10**).

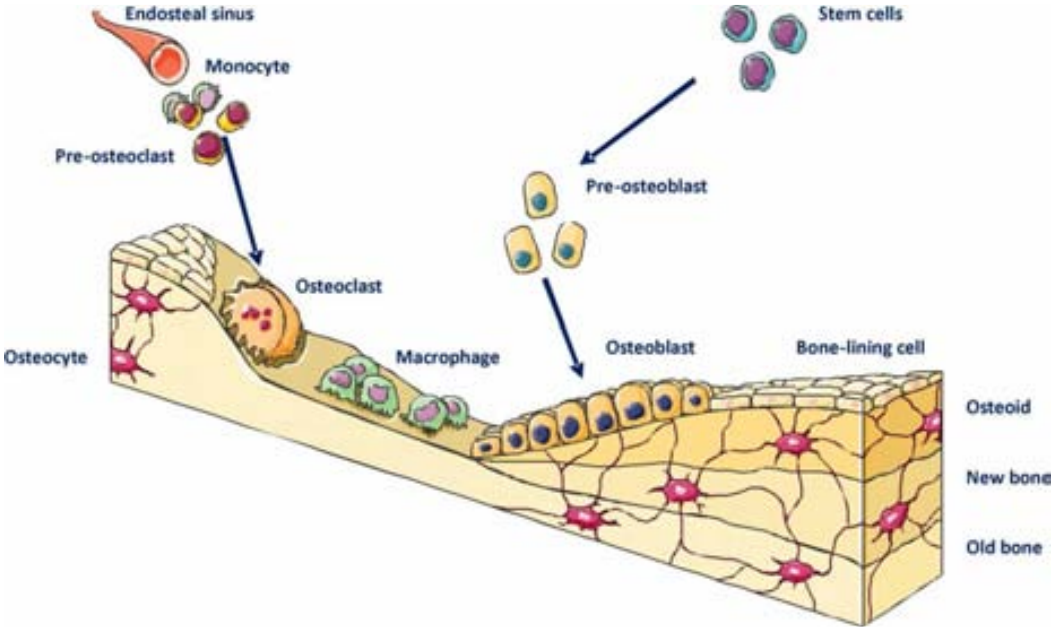

Fig. 1-10. Bone remodeling sequence. A cartoon depiction of the sequential action of osteoclasts and osteoblasts to remove old bone and replace it with new bone. (Stępien, 2011)

1.3.5 Current treatments in bone lesions

The grafting of bone in skeletal reconstruction has become a common task of the orthopedic surgeon. Over 800,000 grafting procedures are performed each year, for surgical reconstruction or replacement, as often the result of trauma, pathological degeneration, or congenital deformity of the tissue (Laurencin et al., 1999). Currently the gold standard surgical treatment is based on the immobilization and introduction of bone grafts (autologous, homologous, heterologous or synthetic grafts) (Nandi et al., 2010). With respect to graft transplants, vascularized autografts are at frequently used at present with a high success rate, but presenting some complications, such as infections, non-unions, and donor site morbidity (Kim et al., 2009). For this reason, this procedure is often

not applicable in large reconstructions due to important quantity of bone required and increased donor side morbidity.

Today, established surgery protocols are based on the immobilization and introduction of bone grafts (autologous, homologous or heterologous grafts), implants of different biomaterials or bone transport methods, to stimulate cicatrization (Finkemeier, 2002), and promote revascularization (Glowacki, 1998). Unfortunately, these techniques show limited success, and none of them has proven to be fully satisfactory, probably due to the delay in the formation of subcondral bone and the embolism of the tissues to repair as a consequence of the failure in the neovascularization of the treated area. Nowadays, millions of patients are suffering from bone defects (450.000 bone grafts are implanted per year in US only), and the clinical need to treat them efficiently will increase with population aging. Moreover, osteonecrosis of the femoral head (ONFH) is a disease characterized by death of the osteocytes and the bone marrow, is caused by inadequate blood supply to the affected segment of the subchondral bone and this may lead to articular surface collapse 10,000 to 20,000 new cases are diagnosed only in the USA every year (Malizos et al., 2007).

1.4 Bone Regenerative medicine

The optimal combination of cells, scaffold and signals in not yet completely known for bone regeneration, although initial results from several groups on tissue engineering to treat bone defect are highly promising. Indeed some approaches have already been reported showing successful results at pre-clinical and even clinical phases (Cancedda et al., 2007). Also some relevant work has been done combining gene therapy with bone scaffolds for bone regeneration (Kimelman et

al., 2007). The most important challenge in this field is the understanding and characterization of the whole process of bone regenerative medicine. For that reason it is important to consider:

a) The type of cells to be used, taking into account the clinical doses
b) The nature, structure and characteristics of the scaffold used, which must be resorbable and with low immunogenic response. In bone regeneration, the scaffold has to display osteoconductive and osteoinductive characteristics.
c) The signals or compounds, which should promote cell growth, osteogenesis and/or angiogenesis.

An ideal regenerative medicine product for bone regeneration should combine the three characteristics described before.

1.4.1 Cells

MSC is likely the most used cell, type in bone regenerative medicine. These cells can be derived from different source tissues including bone marrow (BM), cartilage, fat, muscle and others as shown in **Fig. 1-11**. In the present work MSC are used in a preclinical study with the objective of demonstrating their potential in future clinical applications.

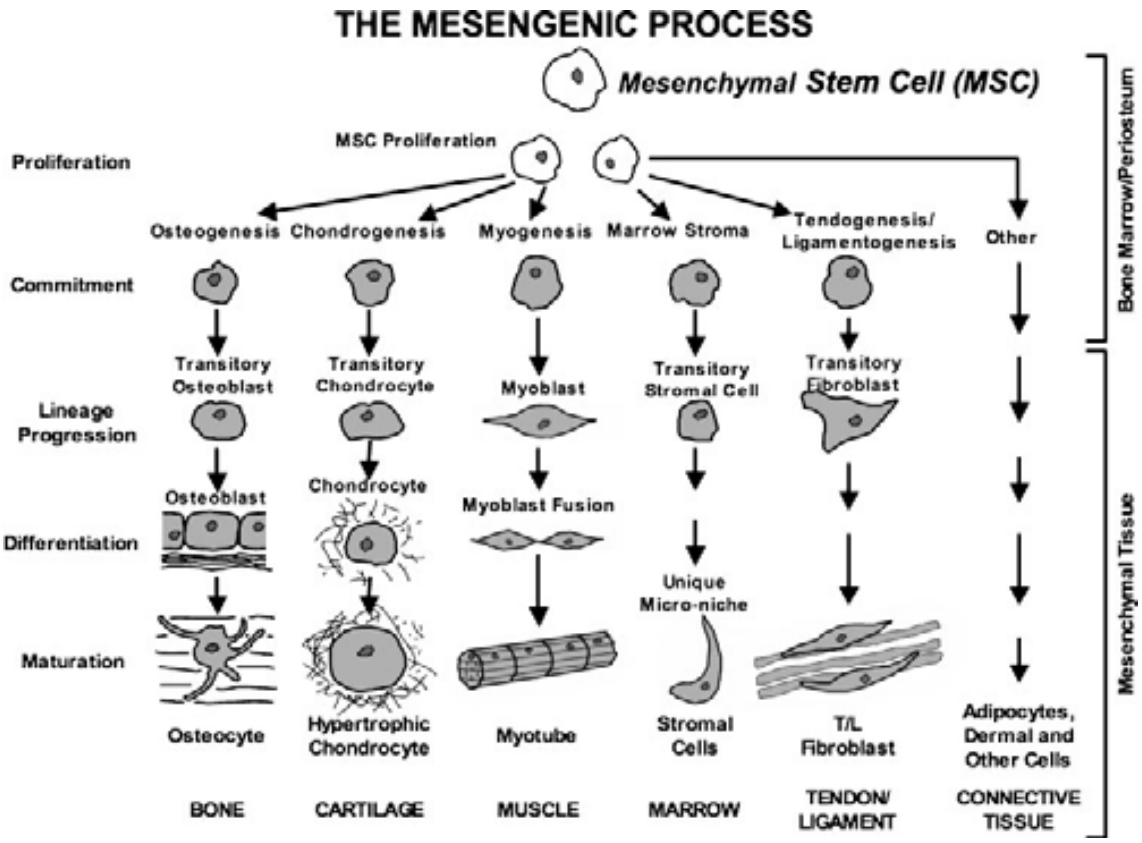

Fig. 1-11: MSC lineages. Different tissues were MSC could be found and also differentiate (Caplan, 2005).

The term MSC refers to a number of cell types with common features. For this reason, International Society for Cellular Theraphy (ISCT) had defined minimal criteria for the characterization of MSC (Dominici et al., 2006), listed below:

1. *In vitro a*dherence to plastic
2. Specific surface antigen expression ($CD105^+$, $CD73^+$, $CCD90^+$, $CD45^-$, $CD34^-$, $CD14^-$, $CD19^-$, HLA-DR^-)
3. Multipotent differentiation potential (osteoblasts, chondroblasts and adipocytes).

Cells derived from the bone marrow contain several cellular sub-populations of stem cells that can differentiate into mesenchymal, endothelial, endodermic or neurodermic lineages (Jiang et al. 2002). The percentage of these populations in respect to other mature cells (lymphocytes, neutrophils and granulocytes) is very low. In the mononuclear fraction of bone marrow, the percentage of multipotent

mesenchymal stem cells falls in the range of 0.001-0.0001 % (Alhadlaq and Mao 2004). The contents of osteoprogenitor cells and endothelium progenitor cells in bone marrow is therefore low. Additionally, the concentration of all types of stem cells in the bone marrow declines strongly with age and health condition (Caplan 2007). Finally, the efficiency and time required for tissue regeneration highly depends on the number of immature cells available in the graft (Dennis et al. 2007). These data offer clear evidence for the need to expand the cells to be used in the grafts *in vitro*, in order to obtain the necessary levels to reach the therapeutic application. Therefore, the development of the appropriate methodology to expand the two cell types targeted in this project, BM-MSC and BM-MNC is a critical part of the work. Normally, the expansion on multipotent mesenchymal progenitor cells is done in systems based on the intensive subculture of the adherent fraction of the BM-MNC. In this way, MSC are obtained as the adherent fraction of BM-MNC, and the non-adherent cells are washed out every 24-48 hours. The composition of the nonadherent fraction is quite diverse: osteoblasts and/or osteoprogenitor cells, fat cells, fibroblasts, reticular cells, macrophages, endothelial progenitor cells (Seshi et al. 2000). Some of them possess clear therapeutic applications in regenerative but are usually discarded in the process for the selection of MSC. Additionally, it has been shown that the mesenchymal progenitors of bone marrow (CFU-F, CFU-O) can survive and expand in suspension cultures supplemented with cytokines. The expansion of BM-MNC in suspension cultures allows the synergistic growth of the different progenitor population, hematopoietic and mesenchymal (Baksh et al. 2005). In suspension cultures, the supplementation of the culture media with cytokines and growth factors (SCF, TPO, FLT, VEGF) allow to expand the initial population of hematopoietic

stem/progenitor cells (CD133+, CD34+), that in turn can generate endothelial cells under the proper signaling (Loges et al. 2004).

1.4.2 Scaffolds

In regards to the scaffold, it is also a very important part of any tissue engineering approach, and should combine several properties. The scaffold should be biocompatible to avoid any rejection, should have structural integrity, and serve as a temporary framework for the cells until the newly formed bone is generated. An ideal scaffold should have a proper balance between mechanical properties, a porous structure, and degradability while remaining osteoconductive. As an example, a bioceramic material like hydroxyapatite provides high strength and loading resistance, but is not reabsorbed and remains in the treated defect for several years after callus formation. On the other side, tri-calcium phosphate based scaffolds have a greater capacity to be reabsorbed, but they are too fragile to sustain the weight load (Piattelli et al., 1996). Different efforts are in progress (Lee and Shin 2007) to find biomaterials (either single compounds or composites) allowing to increase reabsorbability of the implant without resistance loss. Also bone allografts either decalcified or not, in order to regenerate new bone (Yuan et al., 2007). They have the advantage of being osteoconductives, and in some cases osteoinductives and also have a high reabsorbation capacity due its human nature. These bone allografts will be studied with gluing compounds, such as fibrin in order to amalgamate the pices of bone in order to have a shaped structure.

1.5 Development of new bone regenerative products

The majority of new bone regenerative products under development are products in which cells are combined with a biomaterial or scaffold. These innovative products pose novel challenges that may have significant bearing on how clinical products are developed, is for this reason that adequate regulatory framework has developed with the dual aim to promote development of new products to repair significant healthy problems as bone injuries and to protect the safety of people to whom these products have to be administered. For these reasons, each regulatory agency in the different countries adapted the rules for pharmaceutical products to the cellular products emerging a new category of advanced therapy medicinal products (ATMP) implanted by the end of 2007. In concrete, in Europe the ATMP are defined and regulated by the European Commission (EC), the European Regulation No 1394/2007 (including gene therapy medicinal products, somatic cell therapy medicinal products and tissue-engineered products). Tissue-engineered products, intended as products that contain or consist of engineered cells or tissues, and presented as having properties for, or administered to human beings in order to regenerate, repair or replace human tissues.

As shown in **Fig. 1-12**, the discovery phase of the possible ATMP where *in vitro* experiments were performed is followed by a development phase. In this phase pre-clinical and clinical experiments are performed before the registration of the ATMP. Preclinical studies are conducted to perform the proof of concept, safety and toxicology, evaluating the risk-benefit of the new ATMP. According to 21 CFR (Code of Federal Regulations) Part 58, all preclinical toxicology studies are to be

conducted in compliance with Good Laboratory Practices (GLP) to assure the veracity of the results.

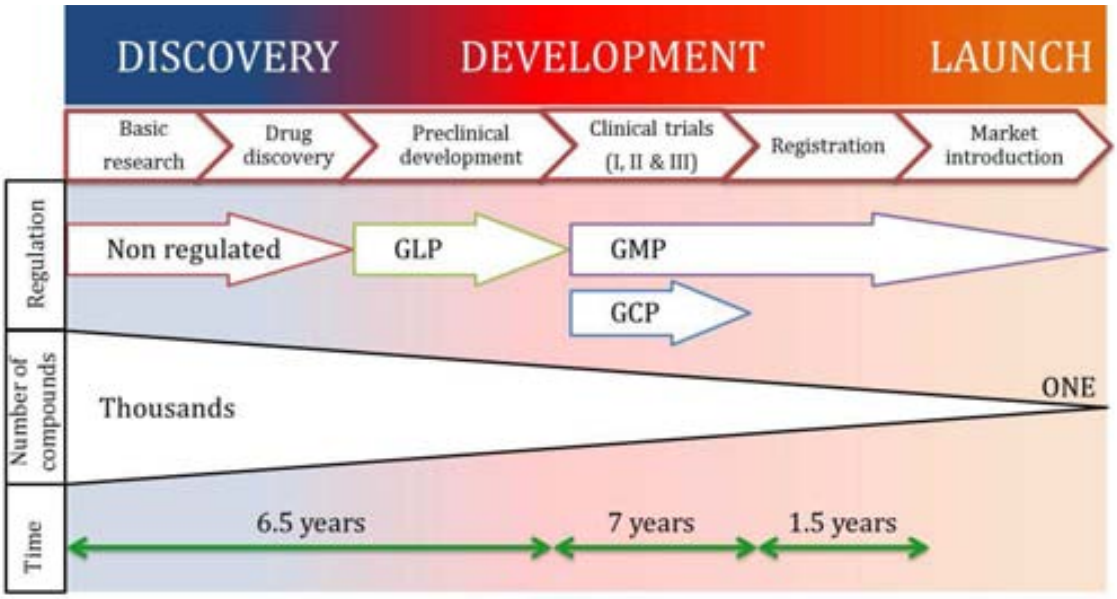

Fig. 1-12. Development process of a bone regenerative product

Once preclinical studies both *in vitro* and *in vivo* are successfully overcome, a report must be submitted to the corresponding regulatory agency depending on the country with the dual intended to demonstrate the safety of the ATMP and to get license to launch clinical trials in humans. In the clinical trials tolerance dose, effectiveness, efficacy and toxicity are tested with an increasing number of patients in each of the phases. There is also a post-marketing research after ATMPS has been submitted and approved by the Regulatory agency. The fact that high number of cells is produced from a single donor, there is a need to guarantee the traceability and safety from the donation to the implantation, either autologous products or allogenic products. That is why both during clinical trials and marketing all products have to be produced in compliance with Good Manufacturing Practices (GMP).

Although this is the classical way to operate, sometimes all phases have to be overlapped in order to answer some suggested questions by the corresponding regulatory agencies. ATMPs development is a long way to go to the market and most of them will fail to succeed.

1.5.1 Animal models in bone preclinical studies

Although there is *in vitro* technology to study different aspects of the development process of bone regenerative products, in order to study the function of the implant characterize the interactions between cells and scaffolds require the use of animal models.

Animal studies are extremely important in the assessment of safety and prove of concept in bone regenerative products. Before an animal model is developed to demonstrate the efficacy and identify toxicity of either cells or scaffold it is important to have that product well characterized, due to its selection may not be trivial.

It should be noted that there is no animal species defined for the task to assess safety and perform prove of concept, therefore scientific justification of the chosen specie or species should be provided.

In general, preclinical translational testing is performed in large skeletally mature animals, rather than rodents or rabbits. Large animal models were developed to verify the practicability of tissue engineering approaches closer to the real clinical situations. Dog, goat, sheep, and pig are the most utilized species (O'Loughlin et al., 2008). Adult sheep offer the advantage of being of a more similar body weight, so mechanical forces are similar to humans and having long bones of dimensions

suitable for the implantation of human implants and prostheses (Newman et al., 1995) and new bone regenerative products. Moreover sheep animal model is the one that has the most similar anatomy and physiology to human having the less neurovegetative sensitivity level, as previously justified in some bone studies that this model has been used (Reichert et al., 2009).

The proposed animal model is one that approaching more human anatomy and physiology, neurovegetative less sensitivity level has, as has been justified anteriorided in all bone pathology studies that have used this animal model.

An optimal model system will closely mimic the pathological condition addressed, and it should not be able to heal spontaneously. Taking in consideration the critical importance of weight load resistance among bone functions, it is proposed here to use a large animal for the *in vivo* tests, particularly sheep. This study focuses on two animal models designed to assess the regeneration product in two relevant specific cases:

1) Critical size large bone defects (CSBD) that will not heal throughout the animal's life. This model mimics the large bone defects associated with the failure of hip implants, segmental bone defects and tumor surgery.
2) Osteonecrosis of the femoral head (ONFH), pathology associated with the lack of vascularization in the bone that leads to a no regeneration of the bone.

Critical-sized defects are defined as “the smallest size intraosseous wound in a particular bone and species of animal that will not heal spontaneously during the lifetime of the animal”(Rimondini et al., 2005). It has been defined as a segmental

bone deficiency of a length exceeding 2–2.5 times the diameter of the affected bone (Lindsey et al., 2006). Nevertheless, a critical defect in long bone cannot simply be defined by its size but may also be dependent on the species phylogenetic scale, anatomic defect location, associated soft tissue and biomechanical conditions in the affected limb as well as age, metabolic and systemic conditions, and related morbidities affecting defect healing (Lindsey et al., 2006).

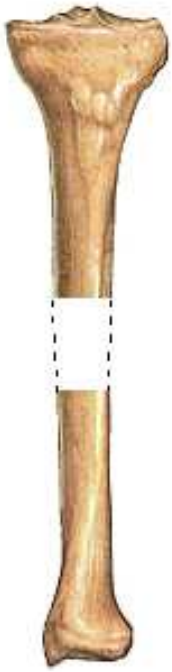

Fig. 1-13. Scheme of a tibia critical size defect. The defect produced will be used to test the bone regeneration product

ONFH model try to mimics the disease progression in humans and was first designed in ostrich model by Conzemius (Conzemius et al., 2002) and then adapted to an easy accessible quadruped model that has similar human physiologic characteristics, sheep by Velez (Vélez et al., 2011). Two relevant specific cases will be treated for regeneration. The model utilized crigenation with liquid nitrogen combined with vascular ligation which induced consistent necrotic lesions that

progressed to end-stage osteonecrosis. Once the model is created a core decompression and bone regenerative product injection would be performed.

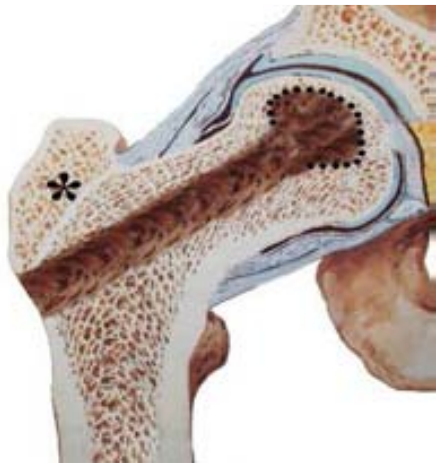

Fig. 1-14. Scheme of a human femoral head core decompression. The resulting hole will be used to inject bone regeneration product

In addition to the animal model choice, it is also highly important to understand which is the bone regeneration mechanism that takes place when the bone regenerative product is administered. It is important to know if either the administered cells are performing the bone regeneration or they are releasing some factors that recruit new cells capable of regenerating bone tissue. In order to overcome this fact, it is very important to track the cells since they are administered. For cell tracking, different labeling systems have been developed. On one hand there BrdU (5-bromo-2'-deoxyuridine) is a synthetic nucleoside analogue of thymidine and it is commonly used in the detection of proliferating cells (Kee et al., 2002; Li et al., 2008; Lehner et al., 2011). On the other hand, GFP (Green Fluorescent Protein), a 27-kDa monomeric protein isolated from jellyfish, has become popular as a reporter system in fixed and liver tissue since the cloning of its gene (Shimomura et al., 1962). GFP is a protein no expressed by the MSC that should be transfected to those cells in order to express it. Currently, two basic

approaches are used for gene delivery: transfection of plasmid-based expression constructs and infection of cells with viral expression constructs (e.g., retrovirus or lentivirus), each harboring the gene of interest. Retroviruses are one of the most commonly used vectors in gene therapy approacthes. They have the ability to integrate into the host genome in a stable fashion to the dividing cells. Otherwise lentiviruses, a retrovirus subclass, they have the ability to integrate into the genome of non-dividing cells.

CHAPTER II

Aim and Objectives

2. CHAPTER II: AIM AND OBJECTIVES

The aim of the project presented here was to develop a 3D tissue engineered product (TEP) loaded with mesenchymal stromal cells (MSC) and further test the feasibility, efficacy and safety of its use for bone regeneration in large animal models.

In order to address this question, three specific objectives were defined:

1) Development and characterisation of the TEP, which involved the establishment of human and ovine mesenchymal stromal cells and manufacture of hybrid bone matrix and MSC constructs (as reported in **Chapter II**).

2) Validation of the feasibility of using the TEP *in vivo*, in a standard test of long bone critical size defect (as reported in **Chapter III**).

3) Evaluation of efficacy, safety and mechanism of action in a relevant translational animal model of bone disease based on the method reported by Velez and collaborators for modelling osteonecrosis of the femoral head in sheep (Velez et al., 2010) (as reported in **Chapter IV**).

The objectives of this thesis were chosen to provide perspectives in order to satisfy the demands on nearby bone tissue engineering, particularly within the context of a growing aging population, associated with degenerative skeletal diseases.

CHAPTER III

In vitro studies

3. In vitro studies

The first step in the development of a new regenerative medicine product is to determine which would be the components and characterize them in order to have a standardized material. In this case the product consists in two components, the cellular and the scaffold one. For the cellular component MSC (mesenchymal stromal cells) both human and ovine sources are used. In addition different scaffolds from bone source were used in order to perform all experiments.

For the preclinical phases of the product, it is necessary to use ovine cellular source, so it is for that reason that it is necessary to ensure that hMSC and oMSC are equivalents. Also the regenerative medicine product must be comparable both with sheep cells and human cells.

3.1 Cellular source optimization

Protocols for human isolation of MNC (Mononuclear cells) and cultivation of MSC are extended around the scientific community, but these are not standardized for oMSC (ovine MSC). It is necessary then to develop the protocols from MO obtain, then the isolation and seeding of oMNC and finally the cell expansion once required dose is achieved.

3.1.1 oMNC isolation

Human MNC isolation consists in different stages clearly established in the literature, although these phases must be improved for the ovine MNC isolation. The protocol, starting from a BM (Bone marrow) with anticoagulant obtained from

the sheep sternum, consists in a dilution of the BM with PBS; subsequently a centrifugal gradient is performed.

BM from different sheep were used to determine the MNC isolation. The parameters studied in order to adapt the oMNC isolation protocol were: 1) PBS dilution of the initial BM (1:1 and 1:3), 2) Ficoll:diluted BM ratio (1:1 and 1:2.5), 3) Ficoll gradient density (1.077, 1.083 and 1.191 g/mL) and 4) Centrifugal force (200*g*, 330*g* and 670*g*). All experiments had a fixed variable, so were performed with the same centrifugal time of 35 minutes.

Fig. 3-1-A illustrates that at as lower the PBS dilution of initial BM higher the number of MNC obtained by BM volume. Moreover, 1:1 ratio of diluted BM:Ficoll was more effective than the ratio 1:2.5 achieving higher number of cells in the first option. In addition **Fig. 3-1-B** highlights that the better Ficoll density was 1.077 g/mL getting better or similar MNC concentration than the other two densities. Also there was some correlation between the centrifugal force and the MNC obtained, obtaining more cells with higher force with the exception of 330 *g* in 1.077 g/mL Ficoll case. Nevertheless taking a look of the cellular ring obtained (see **Fig. 3-1-C**), in 670 *g* it is a clearly localized ring was not shown neither in 200 *g* nor in 330 *g* centrifugal force.

Since the variable centrifugal force was the one that determines the presence or not of the MNC ring, a new experiment has been performed with higher centrifugal force in order to improve the number of cells obtained. In this case 1000 *g* was tested and compared to the other 200 *g*, 330 *g* and 670 *g* as shown in **Fig. 3-2**. It can be observed that 1000 *g* has a statistically higher ($p<0.001$) cell number obtaining in comparison to the other three centrifugal forces achieving a maximum

of $1.6 \cdot 10^7$ MNC/BM mL and a minimum of $5.3 \cdot 10^6$ MNC/BM mL ($9.1 \cdot 10^6 \pm 5 \cdot 10^6$ MNC/BM mL). Furthermore, the MNC ring was clearly observed in 1000 *g*, compared to 200 *g*, 330 *g* and 670 ring (see **Fig. 3-1-C**).

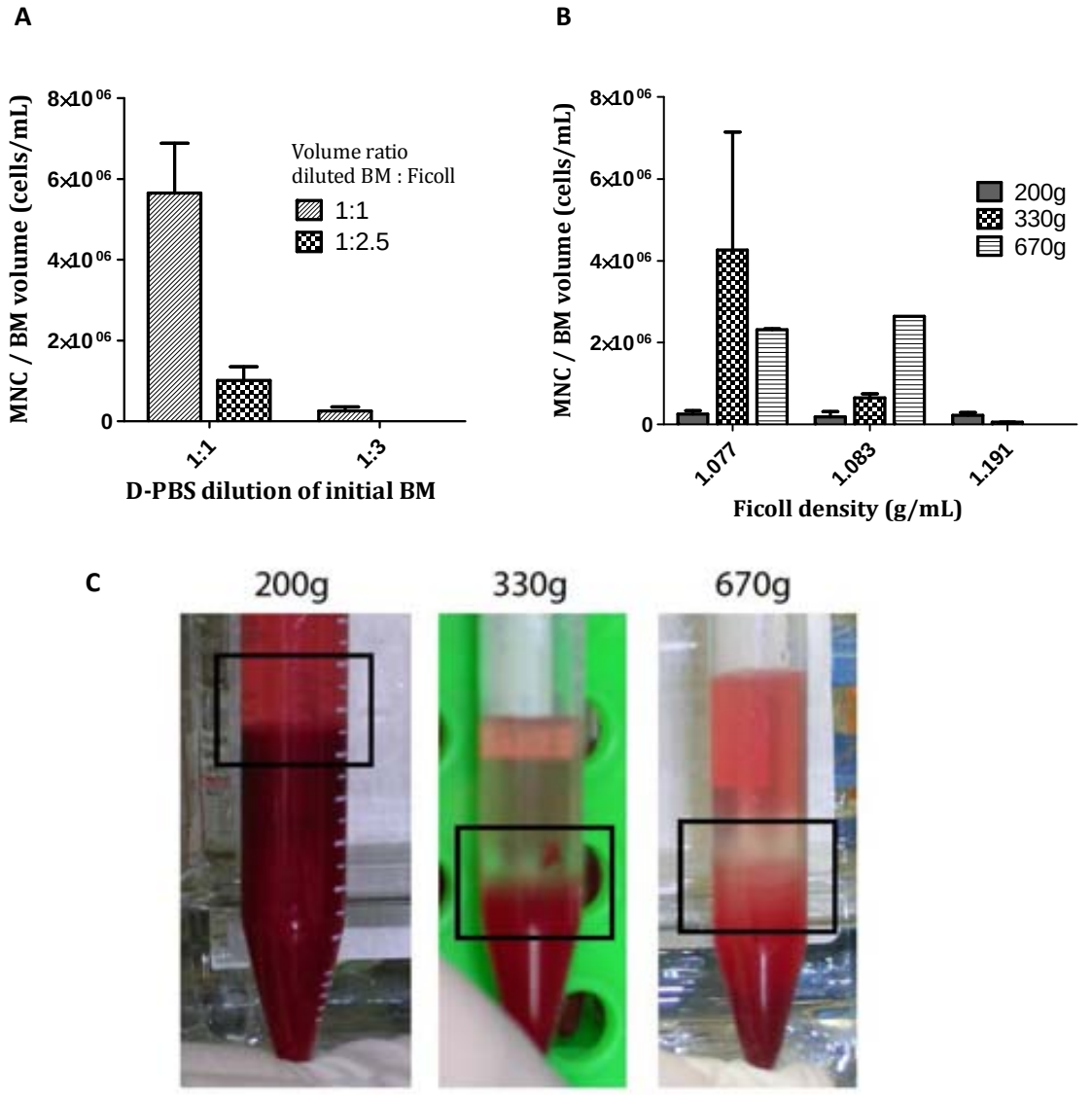

Fig. 3-1. Parameter determination of MNC isolation. A) Graph showing the dependence between the number of MNC obtained with the PBS dilution and the Ficoll ratio. B) Graph showing the dependence between the MNC obtained with the centrifugal force and the Ficoll density. C) Image showing the MNC ring observed in different centrifugal forces applied, the square indicates were the ring must be present.

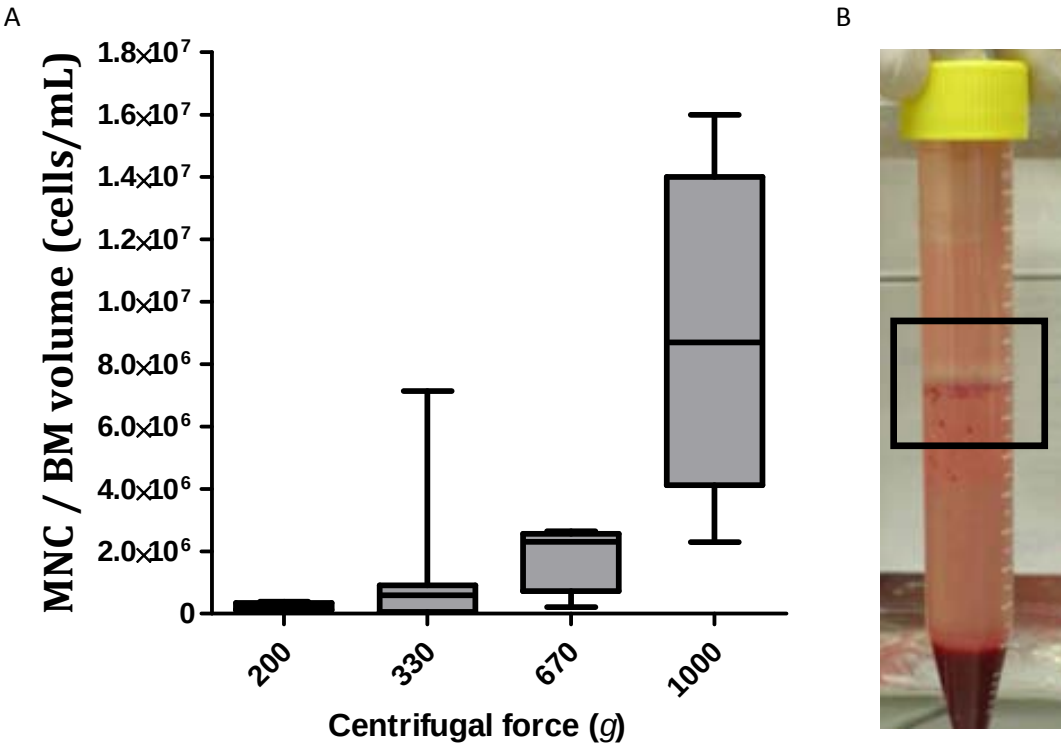

Fig. 3-2. A) Effect of centrifugal force on the obtaining of MNC. The results obtained for 1000 *g* centrifugal are statistically significant ($p<0.001$). B) MNC ring aspect in the case of 1000 *g*.

After these experiments the MNC isolation protocol was defined as described in materials and methods. Once the protocol was defined, the ratio of MNC / BM volume from 56 different samples was calculated and plotted. High variability among this ratio is observed, as shown in Fig. 3-3, ranging from $2.62 \cdot 10^5$ to $2 \cdot 10^7$ ($5.77 \cdot 10^6 \pm 5.31 \cdot 10^6$).

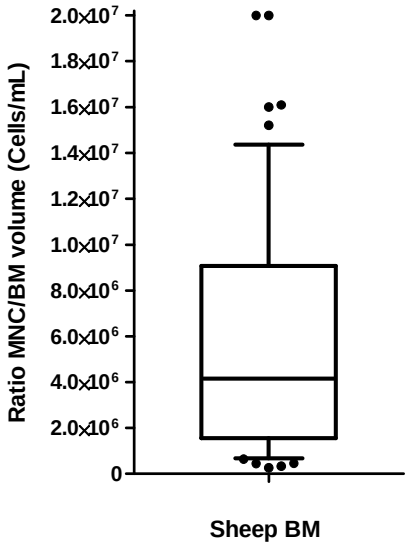

Fig. 3-3: Ratio MNC/BM volume (n=56). Outliers are represented as ●.

3.1.2 oMNC seeding

Once MNC are isolated the MSC are selected by its capacity to adhere to the plastic surface. Different protocols were performed in order to determine the best seeding density and the time passed before non-adherent cell wash. The variables analyzed are listed below:

Cell seeding density: $1 \cdot 10^5$, $2 \cdot 10^5$, $4 \cdot 10^5$ and $6 \cdot 10^5$ MNC/cm^2.

Washing time: 3 and 5 days after seeding.

The number of cells and expansion factor at day 10 was analyzed besides the maxim specific growth rate (μ_{max}), were analyzed in order to determine which the best options were.

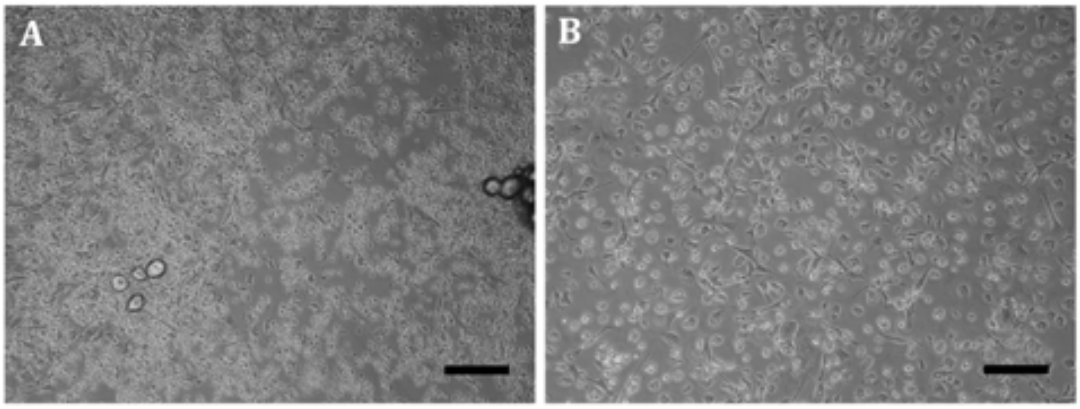

Fig. 3-4: oMSC culture from MNC, seeding at $4 \cdot 10^5$ MNC/cm^2. A) Represents the cell culture before the washing, were most of the cells are not attached. B) Just after the cell wash at day 5. Scale bars, 200 µm. (Original magnification, 100x).

Washing time was very important for the cells because as it is represented in **Fig. 3-4-A**, before washing, none interested cells were deattached and occupying surface not allowing cells to grow normally as it can see in **Fig. 3-4-B**. Cellular activity was monitored by the measuring some metabolites as glucose (cell substrate present in the media) and lactate (cell subproduct liberated to the media) present in the culture media at different time. Also cell number was measured by direct cell count in the Haemocytometer.

Next, in **Fig. 3-5** growth kinetic profile BM MNC culture for different cell seeding density and 3 days washing time is shown. The growth profile is in sigmoid curve and in all cases cell number is related to the glucose and lactate concentration. The more cell number increases the higher lactate production and glucose consumption are. Focusing on the final culture cell number (day 10) it is slightly shown that it is lower at low seeding density, achieving $3 \cdot 10^4$cells/cm^2 in the lower density and $6 \cdot 10^4$cells/cm^2 in the two higher cell seeding densities. It was confirmed with the pictures on **Fig. 3-6** where it is shown cell density just after the washing at the day 3 in the first column, where it is illustrated that more cells are attached in the surface in higher cell seeding density condition.

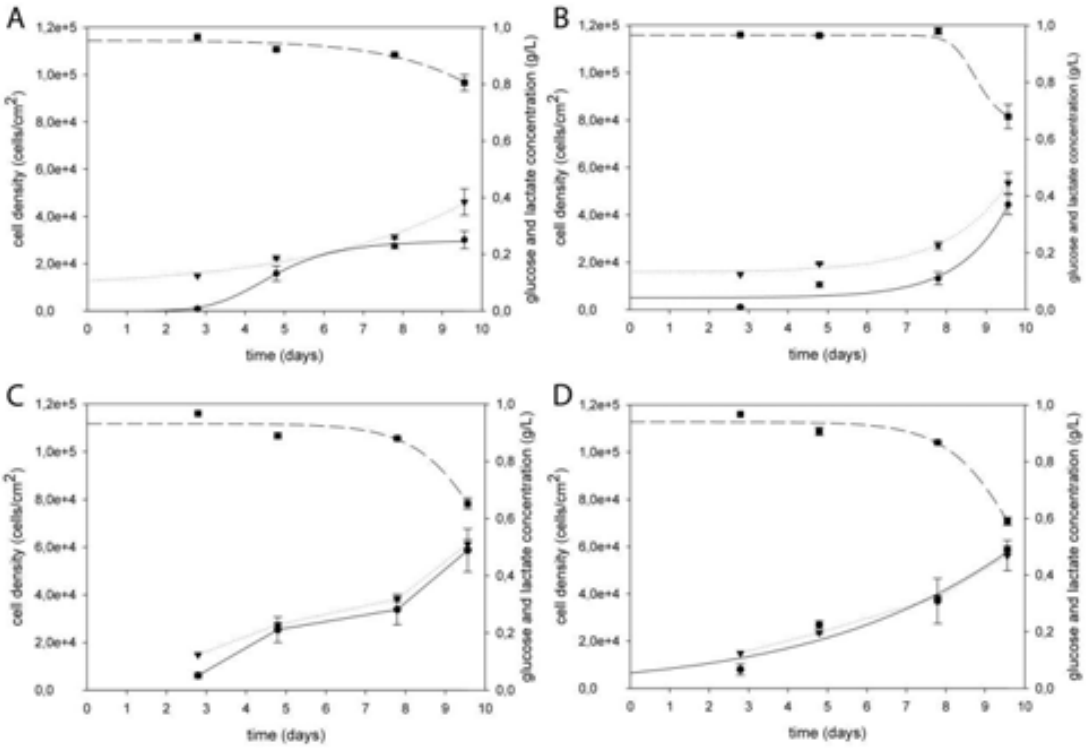

Fig. 3-5: Growth kinetics profile from BM oMNC at different cell seeding density ($1 \cdot 10^5$, $2 \cdot 10^5$, $4 \cdot 10^5$ and $6 \cdot 10^5$ MNC/cm2) and 3 days washing time after the seeding. Cell density (●), glucose concentration in media (■) and lactate concentration in media (▼).

In addition, consistent with the results of previous graphics, by day 10, the conditions with the highest cell density at the end of the culture are those whose seeding density was $4 \cdot 10^5$ and $6 \cdot 10^5$.

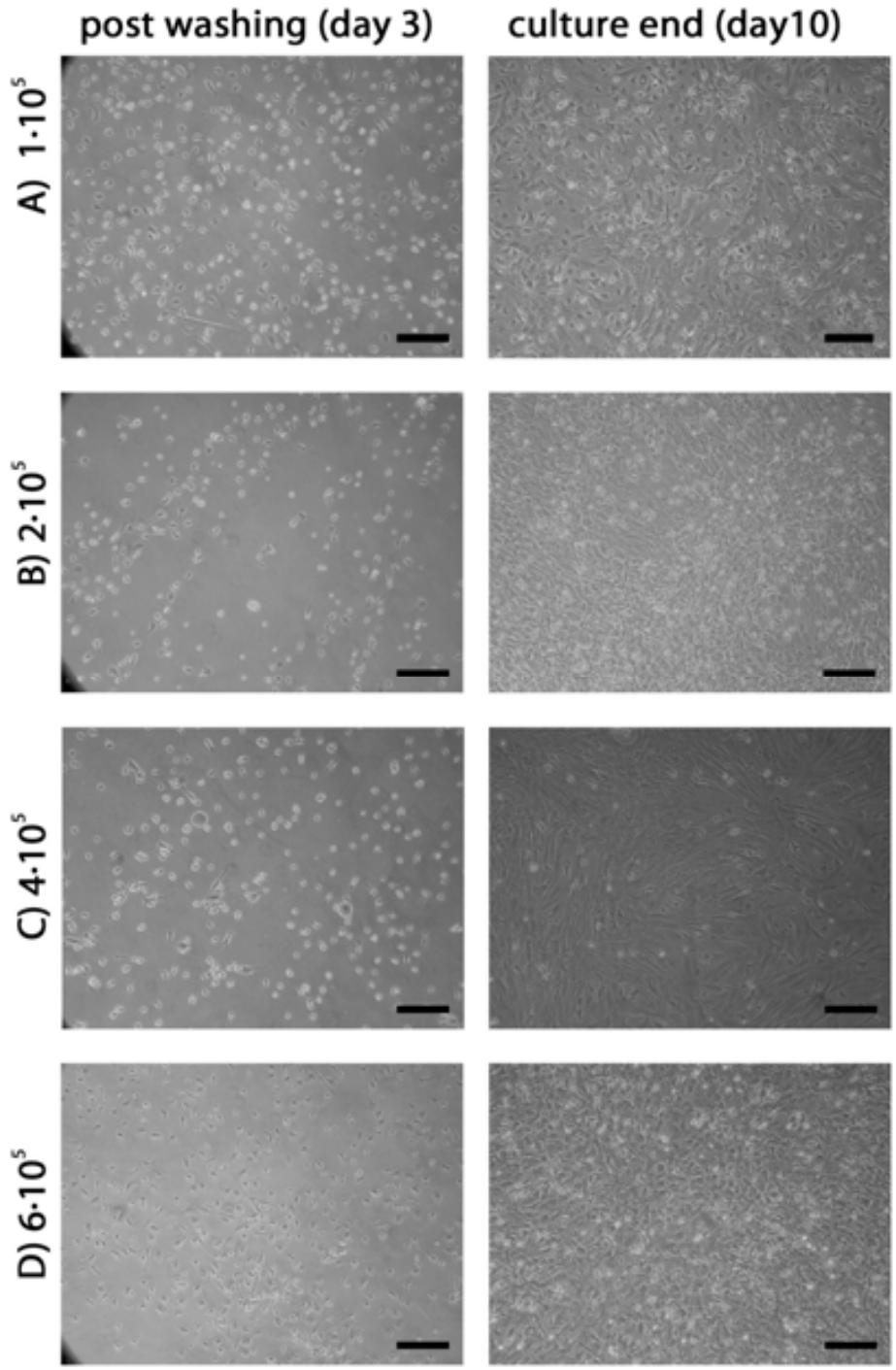

Fig. 3-6: oMSC culture from MNC. Different cell seeding density. A)$1 \cdot 10^5$, B)$2 \cdot 10^5$, C)$4 \cdot 10^5$ and D)$6 \cdot 10^5$ MNC/cm^2. At the first column cells just after MNC washing at day 3 after cell seeding. At the second column cells at the end of the culture, there are some spaces with a confluent monolayer of cells. . Scale bars, 200 μm. (Original magnification, 100x). Scale bars, 200 μm. (Original magnification, 100x).

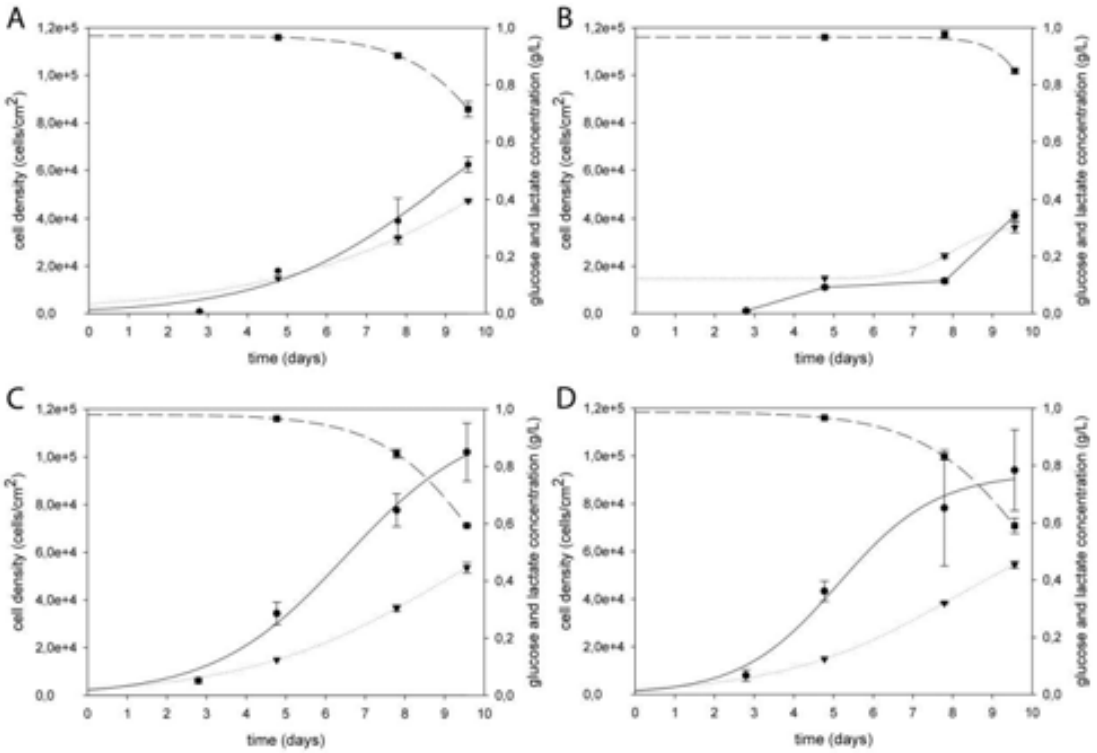

Fig. 3-7: Growth kinetics profile from BM oMNC at different cell seeding density ($1 \cdot 10^5$, $2 \cdot 10^5$, $4 \cdot 10^5$ and $6 \cdot 10^5$ MNC/cm^2) and 5 days washing time after the seeding. Cell density (●), glucose concentration in media (■) and lactate concentration in media (▼).

Comparing these results with the results of washing at 5 days is possible to observe that as seen in the graphs on **Fig. 3-7**, as seen in **Fig. 3-4**, cell growth follows a sigmoid trend and it is related to the glucose consumption and lactate production.

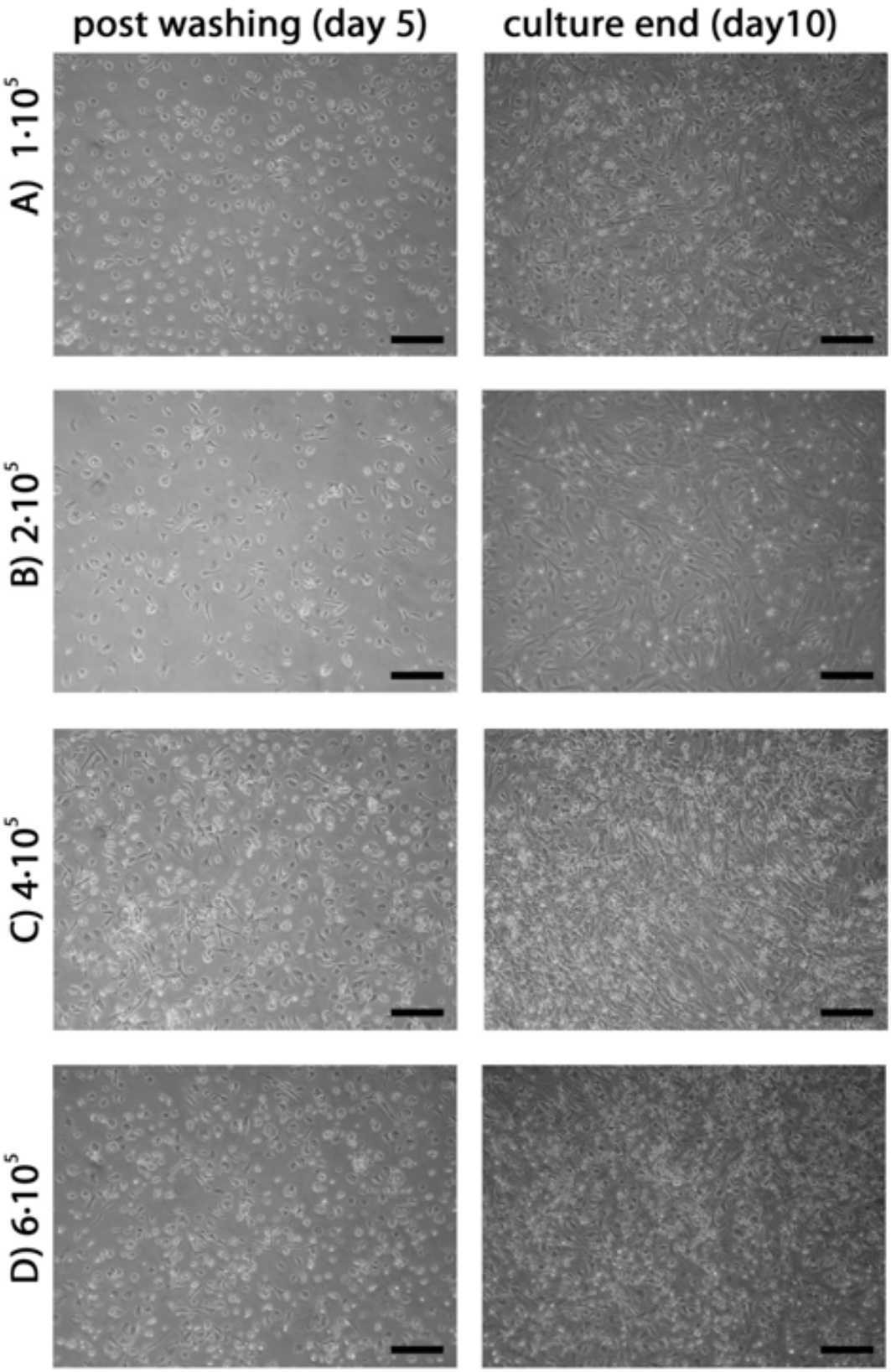

Fig. 3-8: oMSC culture from MNC. Different cell seeding density. A)$1{\cdot}10^5$, B)$2{\cdot}10^5$, C)$4{\cdot}10^5$ and D)$6{\cdot}10^5$ MNC/cm^2. At the first column cells just after MNC washing at day 5 after cell seeding. At the second column cells at the end of the culture, there are some spaces with a confluent monolayer of cells. Scale bars, 200 μm. (Original magnification, 100x).

Furthermore, with the exception of $4 \cdot 10^5$ cells/cm^2 condition in which irregular cell growth was shown, in the other conditions the same pattern was followed, obtaining more cells as higher was the cell density, being similar the conditions $4 \cdot 10^5$ and $6 \cdot 10^5$ where about $1 \cdot 10^5$ MSC/cm^2 were obtained, confirmed by images on **Fig. 3-8**.

All these parameters are summarized in **Table 3-1**, were it can be observed that the μ_{max} is higher in the seeding conditions of $4 \cdot 10^5$ cells/cm^2 in both washing conditions, besides obtaining in both cases the higher final cell number at day 10. It is for these reasons that the condition $4 \cdot 10^5$ cells/cm^2 and 5 days washing time, was chosen to perform the cell expansions in the following experiments, as described in Materials and Methods.

Cell seeding (CMN/cm^2)	Washing time (days)	μ_{max} (days^{-1})	Doubling time (days)	Cell number (day 10)
$1 \cdot 10^5$	3	0.14	5.0	$3.0 \cdot 10^4$
$2 \cdot 10^5$	3	0.47	1.5	$4.4 \cdot 10^4$
$4 \cdot 10^5$	3	0.53	1.3	$8.5 \cdot 10^4$
$6 \cdot 10^5$	3	0.27	2.6	$5.9 \cdot 10^4$
$1 \cdot 10^5$	5	0.26	2.7	$6.2 \cdot 10^4$
$2 \cdot 10^5$	5	0.25	2.8	$4.1 \cdot 10^4$
$4 \cdot 10^5$	5	0.54	1.3	$8.6 \cdot 10^4$
$6 \cdot 10^5$	5	0.34	2.0	$9.4 \cdot 10^4$

Table 3-1: Culture parameters summary on different cell seeding density and washing time.

3.1.3 oMSC Growing

Once oMSC were isolated, it was necessary to expand them in order to obtain a high cell number. Different seeding densities were tested ($1 \cdot 10^3$ and $2.5 \cdot 10^3$ cells/cm^2) in DMEM + 10% autologous serum (see **Fig. 3-9**). More cells were produced in higher density condition compared to the lower one. Culture images in **Fig. 3-10** corroborate this effect, where at the beginning of the culture (day 2) differences were observed between the cultures (more cells were present in the $2.5 \cdot 10^3$cells/cm^2 culture), which were maintained until the end of it.

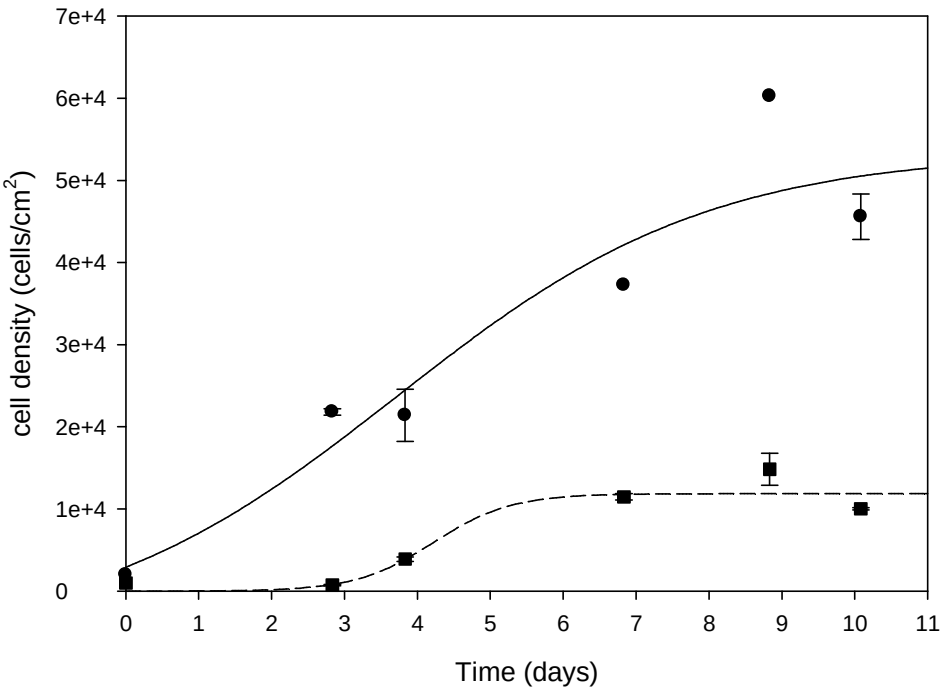

Fig. 3-9: Different seeding densities growth curves, $2.5 \cdot 10^3$ (●) and $1 \cdot 10^3$ (■) cells/cm^2. DMEM + 10% autologous serum. Passage 1.

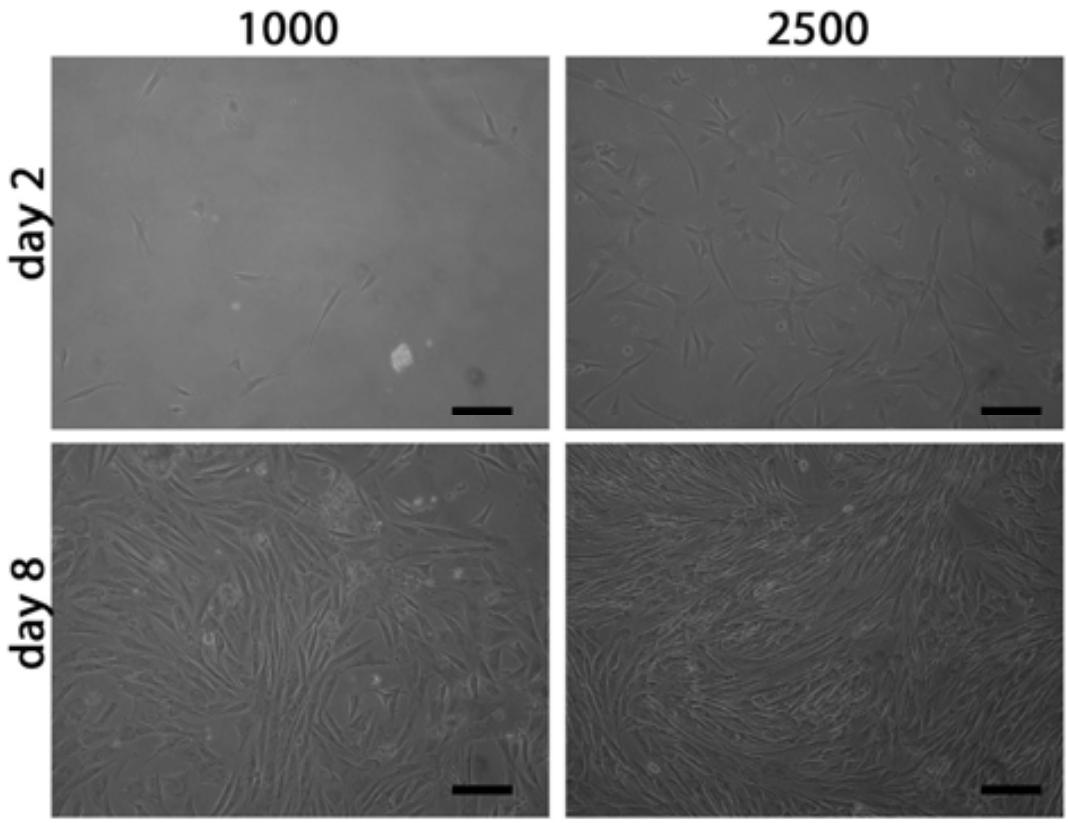

Fig. 3-10: Growth curves images of $1 \cdot 10^3$ and $2.5 \cdot 10^3$ cells/cm^2 seeding density at different time points (2 and 8 days). Scale bars, 200 µm. (Original magnification, 100x).

Subsequently different medium supplements were tested in order to find the one that could generate high cell growth. The supplements tested were FBS, autologous serum and a pool of different ovine sera at a 10% concentration. It can be seen in **Fig. 3-11** that the FBS and pool serum worked similarly, obtaining a maximum of $5 \cdot 10^4$ cells/cm^2 at 6th day of culture, whereas autologous serum failed to achieve the same cell density at the end of the culture. This effect is also seen on the images taken during the culture showed in **Fig. 3-12** where FBS and pool serum conditions showed high cell density compared to the autologous serum.

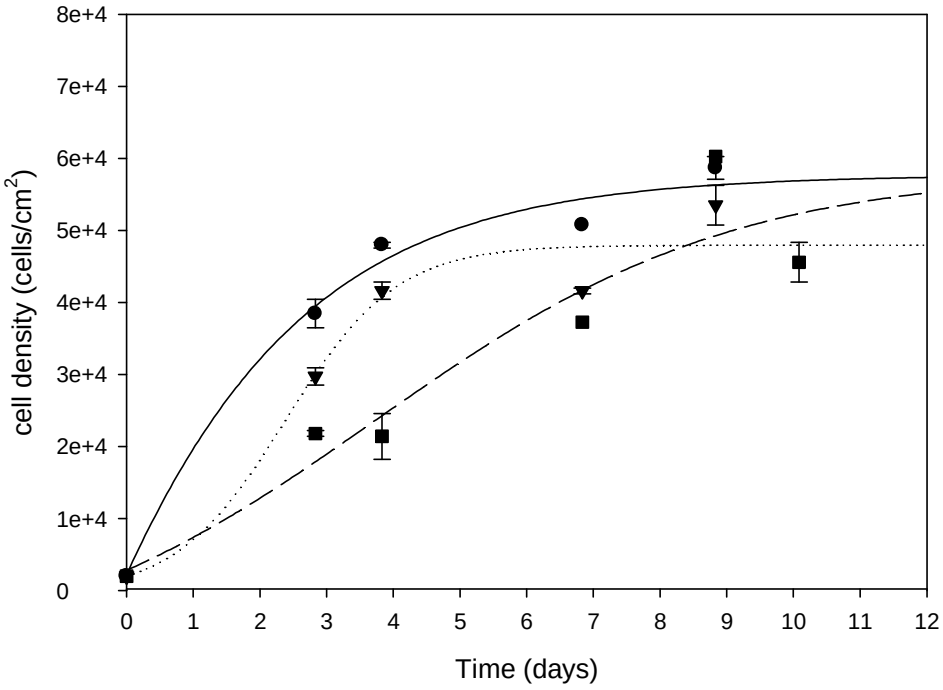

Fig. 3-11: Growth curves evaluation between different culture supplements.DMEM + 10% FBS (●), + 10% autologous serum (■) and + 10% serum pool (▼). Cell seeding $2.5 \cdot 10^3$ cells/cm^2. Passage 1.

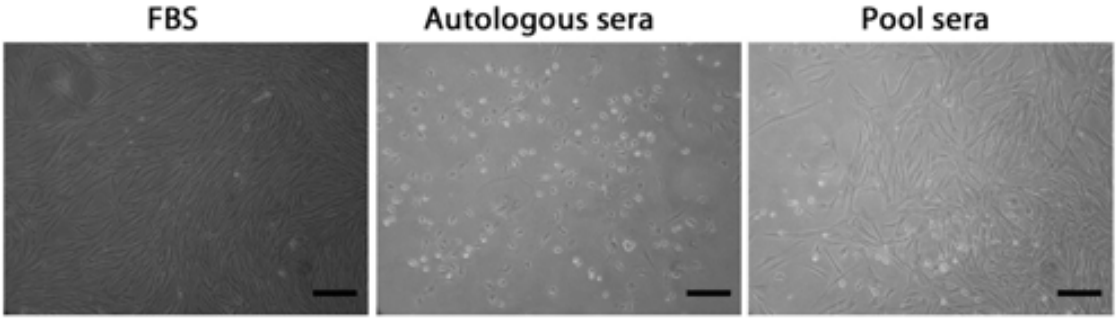

Fig. 3-12: End culture images for different media supplementation, FBS, autologous sera and pool sera. Scale bars, 200 µm. (Original magnification, 100x).

Furthermore, culture parameters calculated as shown in **Table 3-2.** It can be observed that the maximum growth rate was much higher in the case of FBS and autologous serum supplements compared to autologous serum, although the expansion factor is slightly similar in all cases.

Condition	μ_{max} (days^{-1})	Doubling time (days)	Expansion factor
FBS	0.88	0.8	29.3
Autologous serum	0.38	1.8	30.1
Pool serum	0.83	0.8	26.8

Table 3-2: Culture parameters summary on different culture supplements. Maximum growth rate (μ_{max})

3.2 oMSC Characterization

Human MSCs are broadly characterized and described in the literature, but it has to be proven through various test that sheep cells obtained from bone marrow isolated and expanded in a similar manner similar really MSC. The tests performed were the capacity to forms colonies (cfu-f), its multipotenciality and immunophenotype.

3.2.1 CFU

One of the properties that characterize the MSC is to have capacity to form colony-forming unit fibroblast. The assay is shown in **Fig. 3-13** where three different MNC from different sheep were assayed, obtaining an average of 0.009±0.002% cfu-f efficiency with no significant differences between individuals.

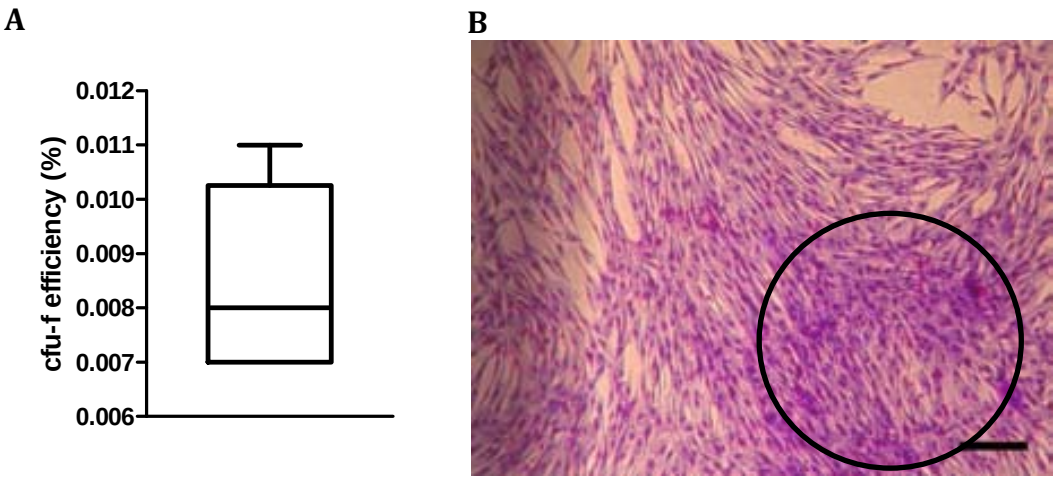

Fig. 3-13: Cfu-f assay. A) Cfu-f from three different sheep starting from MNC isolated from BM. B) image of a cfu-f, cristal violet staining. The circle indicates a stained cfu-f. Scale bars, 200 μm. (Original magnification, 100x).

3.2.2 Multipotenciality

MSC are also characterized to hold the potential to differentiate to at least three lineages, adipogenic, condrogenic and osteogenic. oMSC were assayed to differentiate to those three lineages and as seen in **Fig. 3-14**.

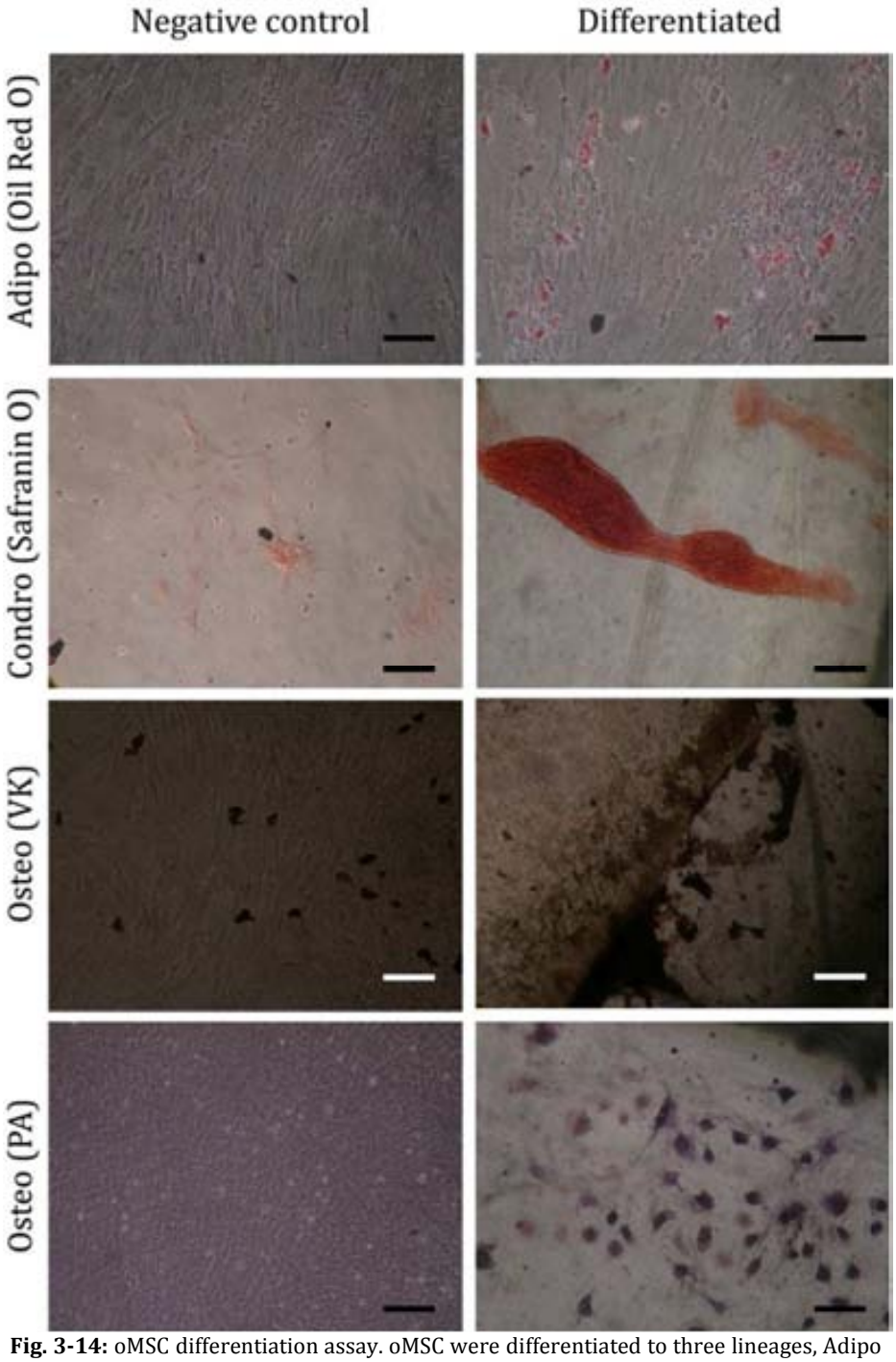

Fig. 3-14: oMSC differentiation assay. oMSC were differentiated to three lineages, Adipo (adipogenic) with Oil Red O staining, Condro (Chondrogenic) with Safranin O staining and Osteo (osteogenic) with Von Kossa (VK) and Alkaline Phosphatase (PA). Scale bars, 200 µm. (Original magnification, 100x).

Adipogenic lineage differentiation was demonstrated by cytoplasm lipid vacuoles staining by Oil Red O in the differentiated condition whereas non in the negative control. Moreover, chondrogenic micromass pellets were stained by Safranin O in and non in negative control because those were not present. And finally osteogenic differentiation was performed by two staining, Von Kossa and Alkaline Phosphatase suggesting the capacity of these cells to differentiate to all three lineages.

3.2.3 Immunophenotype

By FACS (Fluorescence-activated cell sorting), oMSC derived from three different sheep were analyzed to determine the expression levels of CD44, CD45, CD90 and HLA-DR. As shown in **Fig. 3-15** and **Table 3-3** high levels of CD44 and CD90 were expressed, however CD45 and HLA-DR were slightly detected, in conjunction with the MSC expression pattern described.

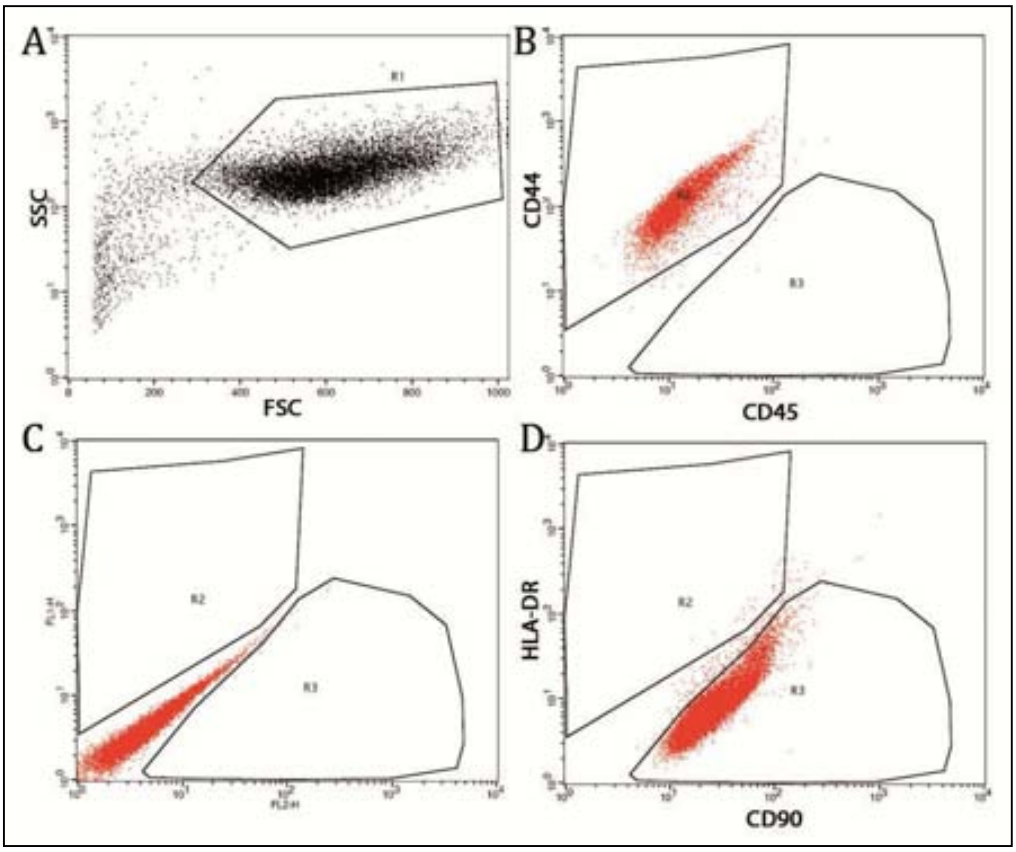

Fig. 3-15: oMSC immunophenotype characterization by FACS. A) Delimitation of cells population by forward and side scatter. C) Gate positioning for unstained population. B) CD44-FITC and CD45-PE staining. D) HLA-DR-FITC and CD90-PE staining.

Expression levels slightly differ in different cell lines even so obtaining high levels of CD44 and CD90 in all cases as shown in **Table 3-3**.

	CD44+	CD90+	CD45+	HLA-DR+
N=1	99.63%	98.30%	0.03%	0.22%
N=2	82.00%	99.49%	0.01%	0.00%
N=3	91.23%	82.45%	0.05%	0.24%
mean	90.95%	93.41%	0.03%	0.15%

Table 3-3. Summary of different oMSC cell lines phenotype.

3.3 MSC Colonization

Once cells were characterized, the bone regeneration product must be developed. In order to keep the cells in the lesion site, either CSD or the decompressed ONFH,

it is important to attach de cells into the surface of a scaffold, in this case a bone scaffold.

3.3.1 Scaffold types

Two different types of scaffolds were analyzed for this aim, both of them human bone particles from tissue donors, deantigenized and lyophilized. The first one are fragments of cancellous bone ranging from 0.5-1 cm and the second one is cortical bone powder ranging from 0.5-1mm. Approximately $4 \cdot 10^6$ cells were offered to each of the scaffolds (Fragments and powder) and supernatant (SN) cells were monitored over the time as an indirect data of the colonized cells of both scaffold type. **Table 3-4** shows the summary of the cell inoculums offered to each scaffold, the cell number in the SN at the end of the experiment and the immobilized cells in the scaffold resulting from the subtraction of the other two parameters.

	cell inoculums	**SN cells**	**immobilized cells in bone scaffold**
Fragments	$4.1 \cdot 10^6$	$2.6 \cdot 10^6$	$1.5 \cdot 10^6$
Powder	$3.8 \cdot 10^6$	$1.8 \cdot 10^6$	$2.0 \cdot 10^6$

Table 3-4: Colonization summary. Fragments referring cancellous bone ranging from 0.5-1cm and powder referring to cortical bone powder ranging from 0.5-1mm. SN: Supernatant.

Cell colonization lasted 24 hours, meanwhile a kinetic immobilization assay were performed in order to set the moment that all cells are colonized as shown in **Fig. 3-16**. It can be observed that more cells are being colonized in the powder bone ($2.0 \cdot 10^6$) compared to bone fragments ($1.5 \cdot 10^6$), since bone powder had larger free surface for colonization compared to bone fragments. Besides, in both cases the maximum colonized cells is observed after 8 hours of colonization.

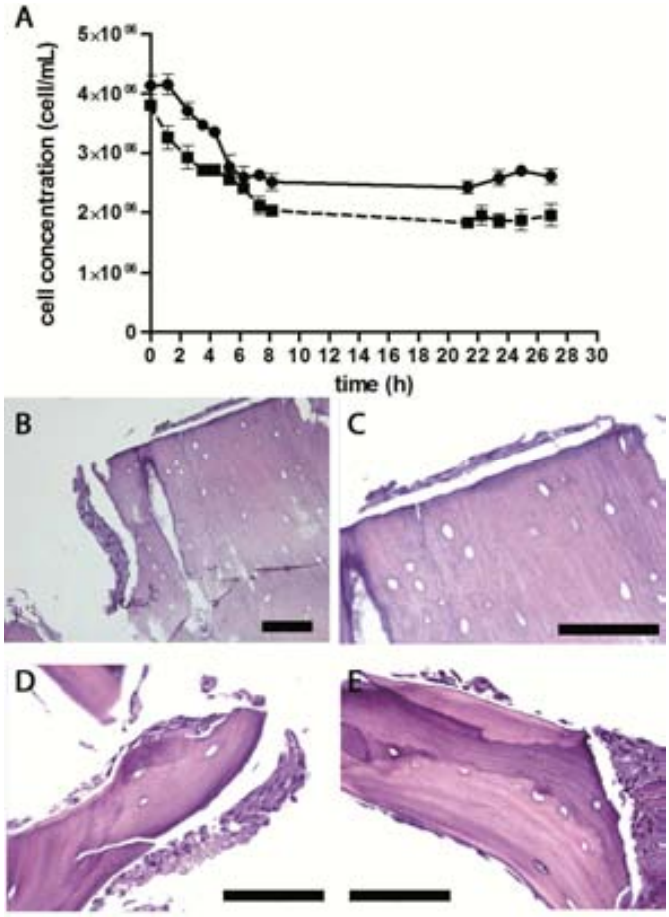

Fig. 3-16: oMSC colonization in different scaffolds. A) Bone colonization in two scaffold types, bone fragments (●) and bone powder (■), supernatant cell concentration is represented. B) and C) Hematoxylin-Eosin staining of colonized bone fragments. D) and E) Hematoxylin-Eosin staining of colonized bone powder. Scale bars, 50 µm.

Also particles and powder colonized was histologically analyzed in order to check that cells are attached to the bone scaffold surface after 24 hours in the same way in both scaffolds, as seen in **Fig. 3-16**.

3.3.2 Colonization kinetics

Additionally, different inoculums were offered to bone powder to choose the one that achieve a high number of cells immobilized in the scaffold. Three different cell numbers were assayed, $3 \cdot 10^6$ cells/mL (high concentration), $2 \cdot 10^6$ cells/mL (medium concentration) and $1 \cdot 10^6$ cells/mL (low concentration). Higher number

of cells are immobilized as higher the inoculums is, $2.5 \cdot 10^6$ cells having colonized in the $3 \cdot 10^6$ cell/mL condition as seen in **Table 3-5.**

	cell inoculums	SN cells	immobilized cells in bone scaffold
high	$3.6 \cdot 10^6$	$4.7 \cdot 10^5$	$2.5 \cdot 10^6$
medium	$1.7 \cdot 10^6$	$9.4 \cdot 10^4$	$1.6 \cdot 10^6$
low	$9.0 \cdot 10^5$	$6.1 \cdot 10^4$	$8.4 \cdot 10^6$

Table 3-5: Colonization summary. High: $3 \cdot 10^6$ cells/ml, mediu: $2 \cdot 10^6$ cells/ml and low: $1 \cdot 10^6$ cells/mL. SN: Supernatant.

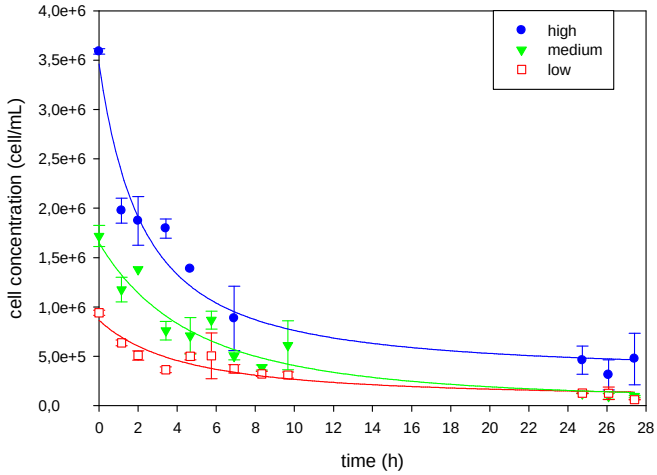

Fig. 3-17: Colonization kinetics in different inoculums. High (blue): $3 \cdot 10^6$cells/ml, medium (green): $2 \cdot 10^6$ cells/ml and low (red): $1 \cdot 10^6$ cells/mL. Supernatant cell concentration is represented as an indirect measure of cell immobilization in bone powder.

On **Fig. 3-17** it can be seen that colonization lasted 28 hours but it is at approximately 8 to 10 hours after the colonization starts when almost all cells are immobilized in the three conditions.

3.3.3 Colonization system

Up to now agitated colonization was used in order to allow a better homogenization of the cell suspension that entails a better colonization of the cells but also it could interfere in the cell adhesion. Therefore two different colonization systems were tested; the stirred one and the no agitated one. The colonization

product was analyzed by confocal microscopy (see **Fig. 3-18**) where no differences were shown in the cell colonization homogeneity in both colonization systems.

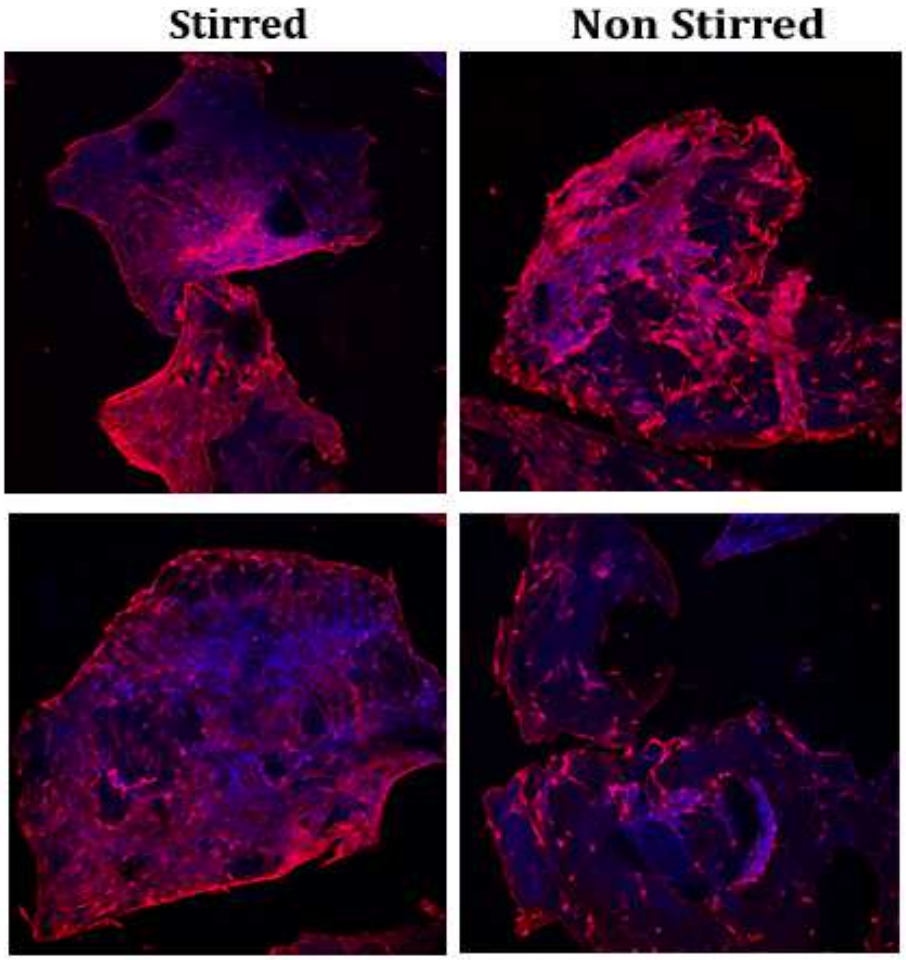

Fig. 3-18: Confocal microscopy images of bone powder colonization of oMSC. Speen-shaped cells in red could be seen homogeneously over the whole bone surface.

3.4 Cell labeling

Cell labeling is a significant fact for understanding *in vivo* bone regeneration mechanism as a way of checking whether cells remain at the site of implantation and if they participate in this regeneration process. Different cell tracking strategies have been tested, they were BrdU labeling and eGFP expression.

3.4.1 BrdU labeling

As BrdU is incorporated into the replicating cells when new DNA is synthesized substituting for thymidine, it was necessary to use a cell culture in the exponential phase during at least 0.8 days (Doubling time with either pool sera or FBS as analyzed in **Table 3-2**) for BrdU labeling of almost all the cells.

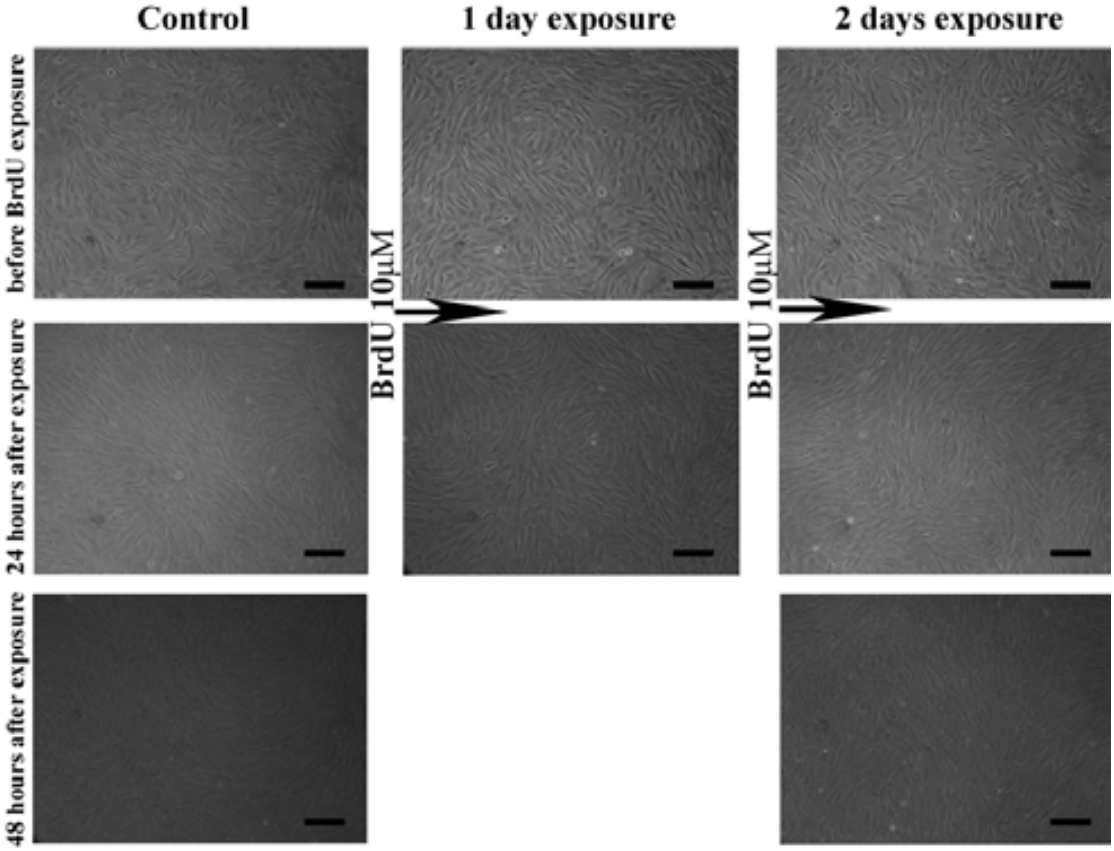

Fig. 3-19: oMSC exposure to BrdU in stationary phase. Control, 1 and 2 days BrdU exposure. No differences are shown between different exposures neither at 24h and 48h. Scale bars, 200 μm. (Original magnification, 100x).

BrdU cell toxicity was analyzed by morphological tracking of oMSC cultures exposed to BrdU during 1 and 2 days. **Fig. 3-19** shows no evident differences between BrdU exposed cells and control even though the cultures were in the stationary phase in which there is no cell division and therefore BrdU is not able to be incorporated into the DNA of the cell. Then, to characterize the effect of BrdU in cell growth effectively, after cell exposure at BrdU during different times and they

were plated at 1000 cells/cm^2 density. Growth curves were analyzed both microscopically (**Fig. 3-21**) and kinetically (**Fig. 3-20**) for 14 or 15 days.

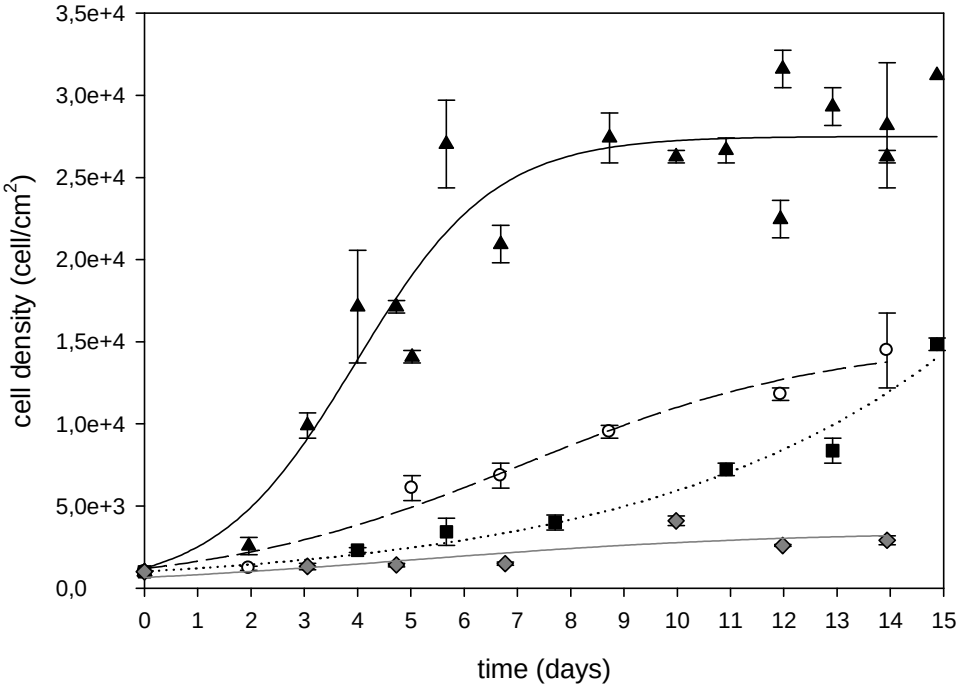

Fig. 3-20: oMSC growing after different days of BrdU exposure. Control cell growing (▲), 2 days (○), 3 days (■) and 4 days (◆) BrdU exposure.

As shown in **Fig. 3-20** cell growth is affected by exposure to BrdU. After 15 days of cell culture, cells with exposures to BrdU of 2 and 3 days showed a 3-fold decrease on final cell density compared to the control. Moreover no significant growth was found in the 4 days exposure condition having less than 2 duplications throughout the culture time. This data was also confirmed macroscopically, as shown in **Fig. 3-21**. In the beginning of the culture no differences were shown in the cell density except that morphological differences were observed between control (BrdU-) and 3 and 4 days BrdU exposure, showing in the last case bigger cells and accumulation of cytoplasmic vacuoles. At the end of the culture, no significant morphological changes were observed between conditions even so the longer BrdU exposure, the lower the cell density achieved at the end of the culture.

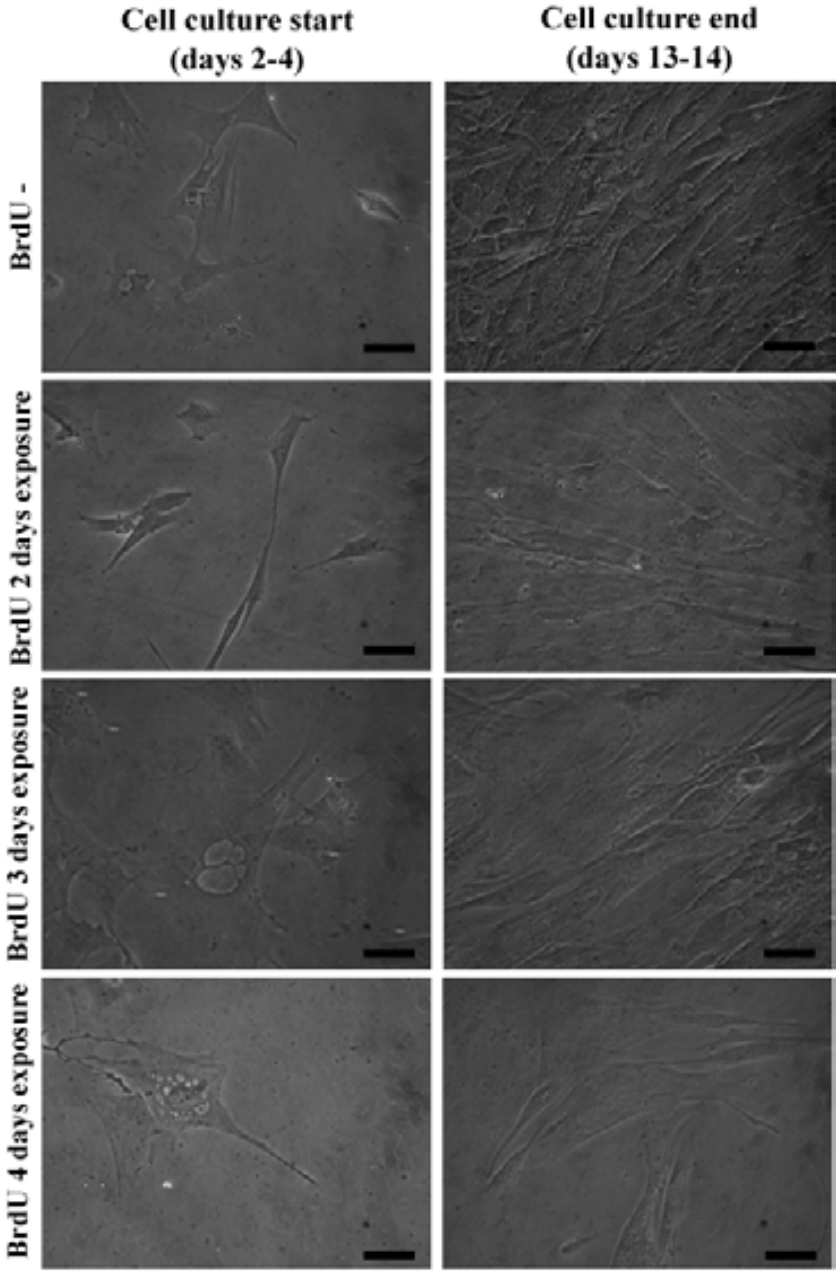

Fig. 3-21. Photographs showing cell density and morphology both the start and end of the cell culture with different BrdU time exposures, 0 (control without BrdU), 2, 3 and 4 days. Scale bars, 100 μm. (Original magnification, 200x).

3.4.2 eGFP labeling

Another system to label cells had to be developed due to failure in oMSC BrdU labelling. The technology chosen was reporter gen (Green Fluorescent Protein; eGFP) tranfection by retroviral and lentiviral vectors. At 5 days after transfection, eGFP expression was identified by fluorescence microscopy both in retroviral and lentiviral

transfections (**Fig. 3-22**). The retroviral transfected oMSC showed no eGFP expression whilst it was manifested in the lentiviral transfected ones.

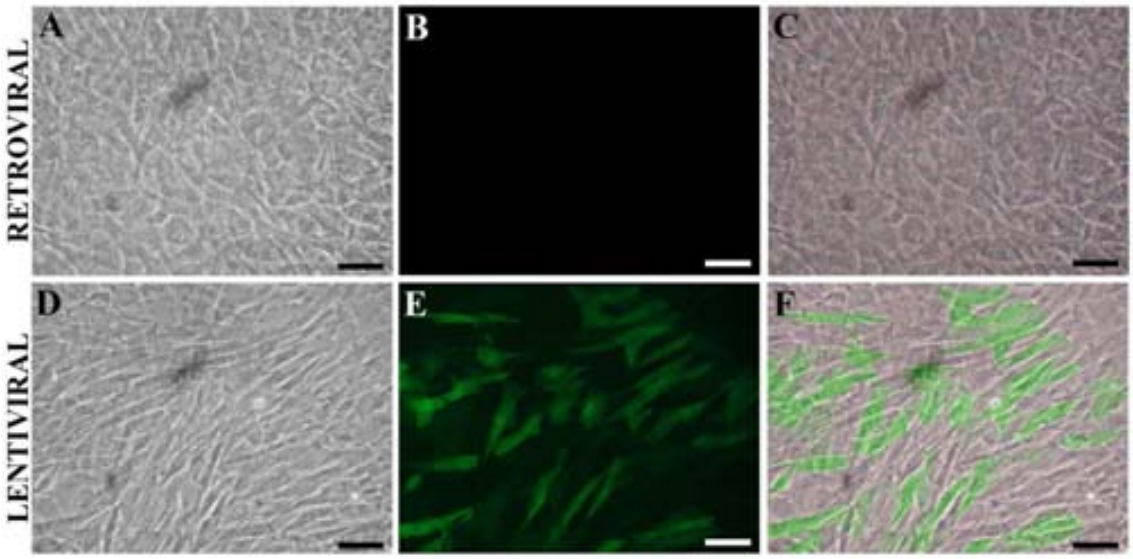

Fig. 3-22: oMSC eGFP retroviral (A, B and C) and lentiviral transfection (D E and F). Microscopic images of pase contrast (A and D), fluorescence microscope images (B and F) and image overlap (C and F). Scale bars, 200 μm. (Original magnification, 100x).

Cells expressing eGFP were analyzed by FACS in order to quantify the percentage of eGFP positive cells in the culture as shown in **Fig. 3-23**. One phase after infection at MOI=25, the eGFP+ cells percentage were 37.76%. Thus lower eGFP expression in older conditions, new experiments were performed in order to improve the transduction efficiency. Different MOI were assayed in oMSC ranging from 250, 500 and 1000 and achieving 75%, 84% and 95% eGFP positive cells at the culture end after infection, as can be seen in **Table 3-6**. Since there were no significant differences in the eGFP expression between the three MOI conditions, MOI chosen for the following experiments was 250 due to the lower consumption of virus obtaining a similar high eGFP expression.

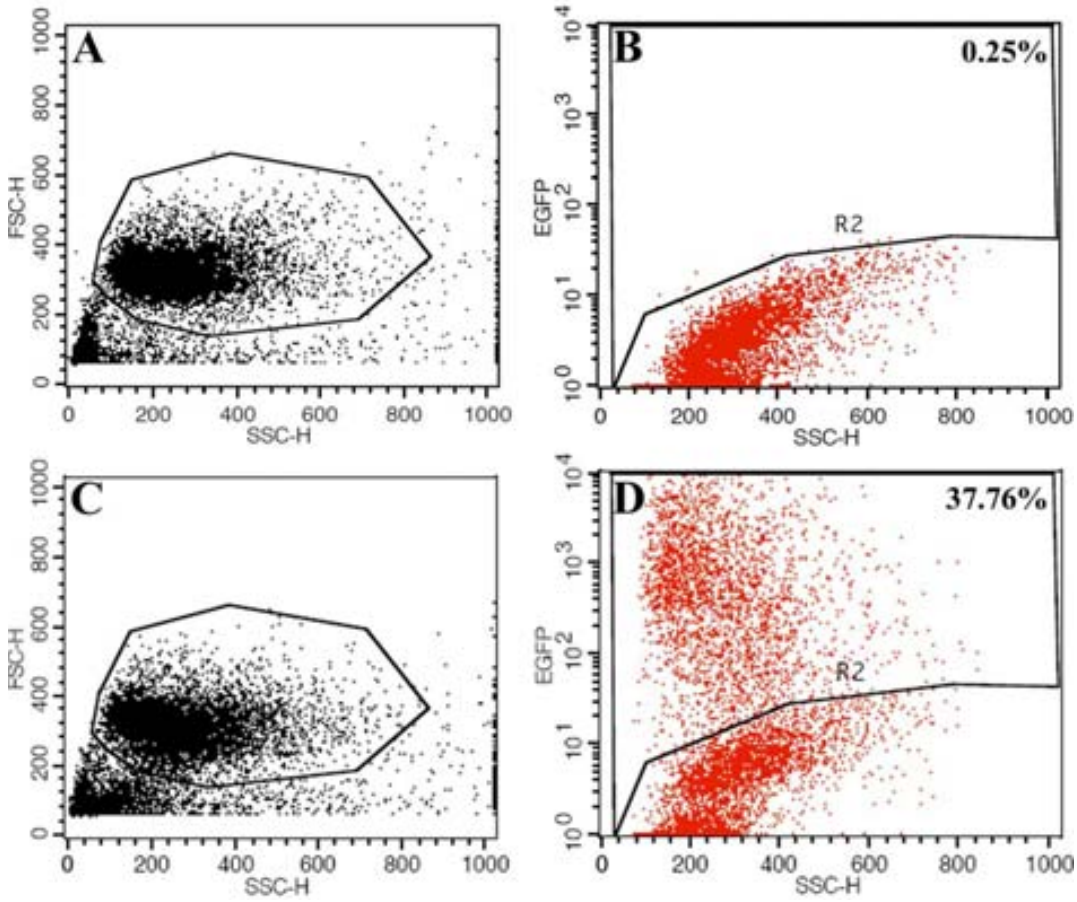

Fig. 3-23: Detection of oMSC eGFP-expressing cells by flow cytometry. Negative control, non-transfected oMSC (A-B) and oMSC eGFP+ cells (C-D). Cells gated for forward and side scatter (A and C) and subsequently for eGFP expression (B and D). MOI = 25.

MOI	250	500	1000
%eGFP+ cells	75%	84%	95%

Table 3-6: eGFP positive cells percentage with different MOI infections.

For evaluation of expression stability of the eGFP gene over time, two different cell lines expressing eGFP at different levels, were allowed to grow until passage 18 and eGFP expression was analyzed at passage different passages. Cells grown normally until passage 18 although eGFP expression starts to decrease from passage 10 (**Fig. 3-24**). oMSC eGFP+ cells also express CD44+ and CD90+ the same as those unlabeled cells.

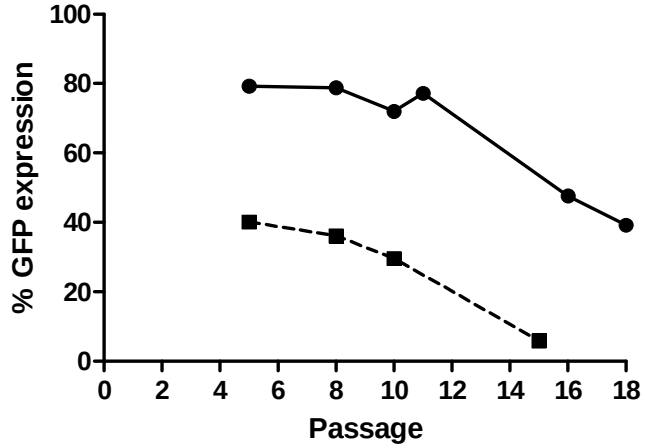

	Passage 4
CD44+	High*
CD90+	97,55%
CD45+	ND
HLA-DR+	ND

Fig. 3-24: A) eGFP stability over passages in two oMSC different lines, 73 (●) and 74 (■). B) Immunophenotype of oMSC expressing eGFP. ND = No determined. * Determined in the same channel as eGFP and observing a high displacement of the cell population but not quantified.

To further asses the eGFP expression stability in different conditions, transfected oMSC were cultured in differentiation medium towards adipogenic, osteogenic or chondrogenic lineage. On cellular level the expression of eGFP was detected at the end of differentiation cultures and oMSC eGFP transfected lines were capable to differentiate to the three lineages, this fact was confirmed by performing different stains, Oil Red O for adipogenic lineage, Von Kossa staining for osteogenic lineage and Safranin O for chondrogenic lineage (see **Fig. 3-25**).

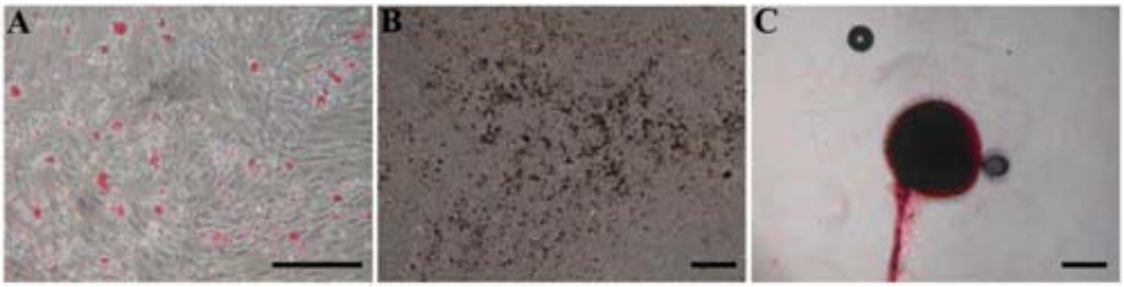

Fig. 3-25: Differentiation assay of oMSC expressing eGFP. A) adipogenic by Oil Red O staining, B) Osteogenic by Von Kossa staining and C) Chondrogenic differentiation by Safranin O. Scale bars, 400 µm.

Additionally, adipogenic cells did not switch off the eGFP gene expression in the course of differentiation, since the fluorescent signal was found both in differentiated areas of the culture as well as in cells showing no signs of

differentiation. The fluorescence signal for instance, was co-localised with fat vacuoles within the same cell during adipogenic differentiation, as seen in **Fig. 3-26**.

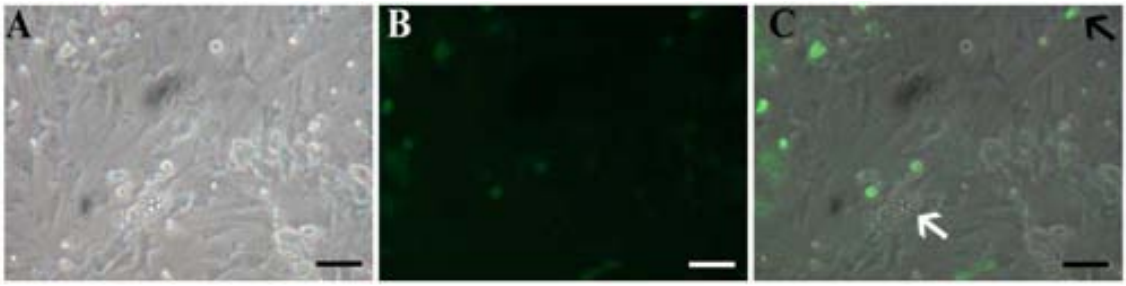

Fig. 3-26: Colocalization of eGFP signal in differentiated and non differentiated cells. Microscopic images of phase contrast (A), fluorescence microscope images (B) and image overlap (C), white arrow indicates co-localization of eGFP signal and fat vacuoles in the same cell during adipogenic differentiation and black arrow represents eGFP signal in a no differentiated cell without fat vacuoles. Scale bars, 100 µm. (Original magnification, 200x).

Cell labeling was further developed for the future *in vivo* use. Once the cells are implanted in the animal model, the technique to analyze eGFP expression must be through immunohistochemistry approach since no information will be obtained by FACS using a cell suspension. It is for this reason that the test product was mimicked in order to develop the immunohistochemical technique. Cells were colonized in bone fragments and eGFP and non eGFP expressing cells were identified by immunohistochemistry and Hematoxylin and eosin (H&E) counterstain as shown in **Fig. 3-27**.

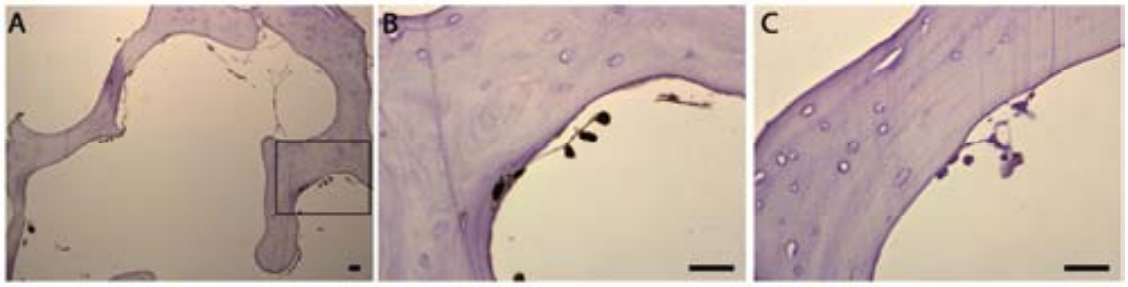

Fig. 3-27: eGFP Immunohistochemistry of bone particles colonized by oMSC expressing eGFP, H&E counterstaining. A) overview of eGFP staining , B) A enlargement showing more detailed eGFP cells in brown and C) negative control without secondary antibody showing cells not stained in brown.

3.5 oMSC comparison with human cells

The product developed for bone regeneration is a model of human autologous cells to be tested in large animal models; therefore the characterization of oMSC compared to hMSC was studied. First, the main culture parameters were calculated as summarized in **Table 3-7**. It can be observed that hMSC grow slower than oMSC as they have a higher μ_{max} and a lower doubling time, also show a smaller expansion factor.

Condition	μ_{max} (days^{-1})	Doubling time (days)	Expansion factor
hMSC (hSerB pool serum)	2.7	2.6	8.7
oMSC (ovine pool serum)	0.83	0.8	26.8

Table 3-7: Main culture parametersfor hMSC and oMSC. Maximum growth rate is expressed as μ_{max}.

However, as shown in **Fig. 3-28¡Error! No se encuentra el origen de la referencia.**, the cellular morphology is very similar to the oMSC, and GFP labeled hMSCs have similar immunophenotype and are able to differentiate into osteogenic lineage, chondrogenic and adipogenic.

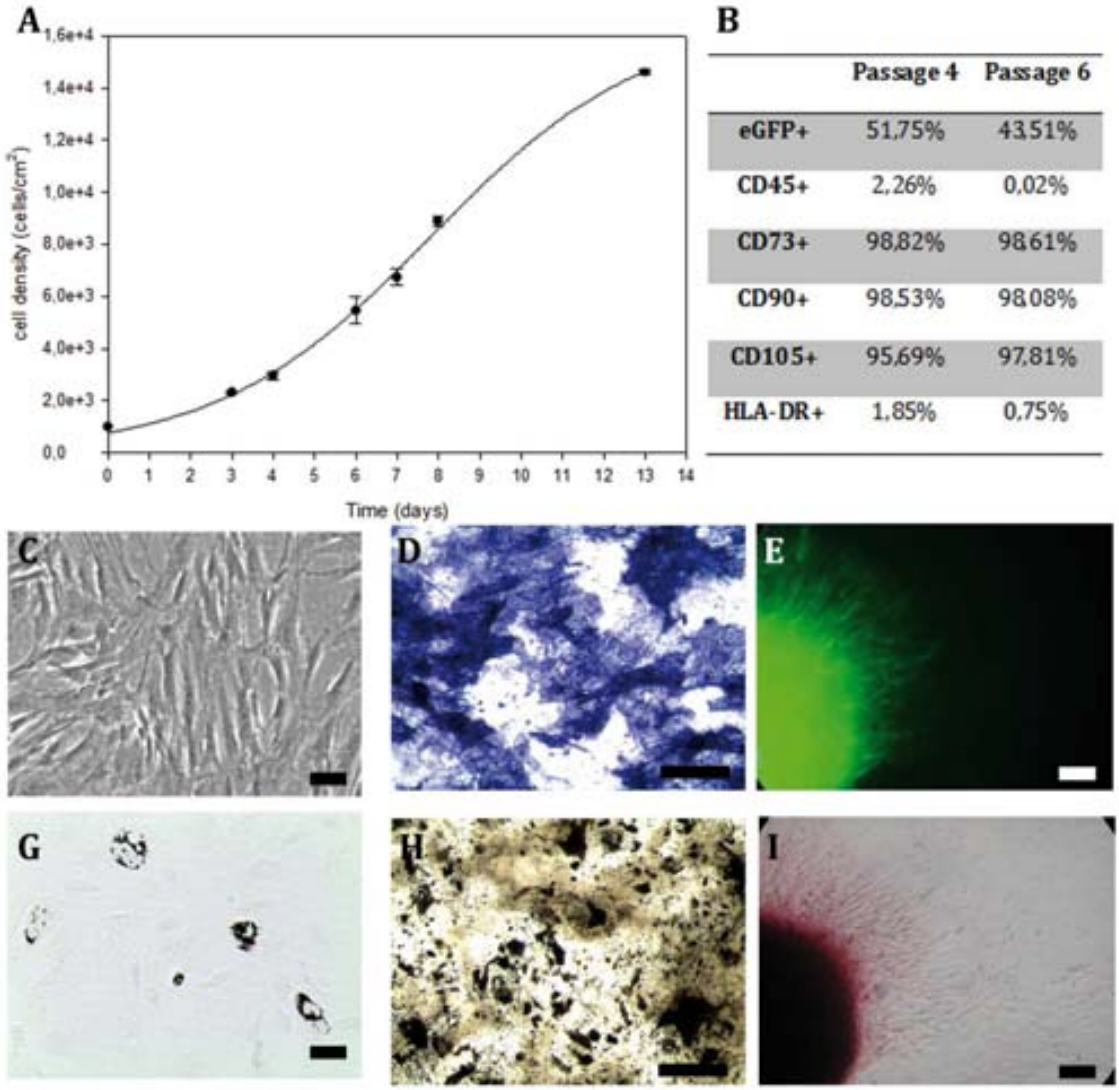

Fig. 3-28: Characterization of hMSC. A) hMSC growing. B) Summary of eGFP expression and immunophenotype in passage 4 and 6. C) hMSC morphology. G) Adipogenic differentiation, Oil Red-O staining. D) and H) Osteogenic differentiation, alkaline phosphtase and von Kossa assay respectively. E) and I) Chondrogenic differentiation, eGFP expression and Safranin O staining respectively.

After cell characterization and development of a proposed TEP for bone regeneration a further *in vivo* study to validate the feasibility of its use and bone remodeling capacity was tested in a standard model of critical bone size defect as described in next Chapter III.

CHAPTER IV

Results: Critical Size Bone Defect

4. CHAPTER IV: CRITICAL SIZE BONE DEFECT

By definition, a critical size bone defect (CSBD) is the smallest defect in a particular bone and species that will not heal spontaneously during the lifetime of that animal (Schmitz and Hollinger 1986). CSBD has been re-described as a defect that has less than 10% bone regeneration during the lifetime of the animal. For practical purposes if 10% of regeneration has not been reached by one year, it is unlikely to occur, more practically, a defect that will not heal over the duration of the study (Gosain, Song et al. 2000).

In the present PhD project a CSBD was modeled in order to investigate the effect of oMSC in an extreme situation. The aim of the study was to examine the induction of the physiological mechanisms of bone regeneration by administration of cells with potential to differentiate into osteoblasts and bone matrix osteoinductive and osteoconductive. This study was designed with two specific goals: 1) evaluate the **efficacy** in bone regeneration of a tissue engineering product (TEP) and 2) assess the **safety** of those TEP.

TEP consists of a particulate deantigenized human bone colonized by oMSC and blended with fibrin glue, applied to a large translational animal model. The model consisted of a critical size defect in the tibia generated by a surgical excision of a bone portion of approximately 2.5 cm long (according to the definition of CSBD) and stabilized with internal fixation. Two reference groups were included in the study comparison to the TEP group: A) the gold standard in human practise (autologous bone injert) and B) another group composed by the same scaffold as the TEP but without cells.

This animal study was approved by the Ethics Committee on Animal Experimentation in Vall d'Hebron (Registration Number 47/09 CEEA).

4.1 Experimental design

Sixteen female sheep (*Ovis aries*, Ripollesa breed) were used to perform this study. All animals were 20 months old and weighted between 30.4 kg and 41.8 kg (37.1±3.5 kg) (see **Table 4-1**). A critical size defect was created in the right tibia of all sheep (2.4±0.2 cm height, 1.7±0.3 times the diameter of the tibia), as resumed in **Table 4-1**. Sheep were randomized in three groups showed in **Table 4-1** and **Table 4-2**.

Sheep ID	Weight (kg)	Defect height (cm)	Tibiae diameter (cm)	Defect high/ diameter	Treatment group	Observations
1	38	2.0	1.9	1.1	GS	Fixation plates not well placed
2	41	2.5	1.7	1.5	GS	N/A
3	37	2.5	1.5	1.7	S	N/A
4	38	2.5	1.6	1.6	GS	Infection observed in the clinical follow-up
5	35	2.5	1.5	1.7	TEP	N/A
6	41	2.1	1.5	1.4	GS*	Infection observed in the clinical follow-up
7	36	2.3	1.5	1.6	TEP	Infection observed in the clinical follow-up
8	36	2.5	1.4	1.8	S	N/A
9	42	2.4	1.4	1.7	TEP	N/A
10	40	2.3	1.5	1.6	TEP	N/A
11	36	2.5	1.4	1.9	S	N/A
12	37	2.5	1.4	1.9	S	N/A

Sheep ID	Weight (kg)	Defect height (cm)	Tibiae diameter (cm)	Defect high/ diameter	Treatment group	Observations
13	31	2.5	1.6	1.6	TEP	N/A
14	30	2.5	1.2	2.2	S	Infection observed at the end of the study
15	33	2.5	1.5	1.7	TEP	N/A
16	40	2.5	1.3	2.0	TEP	N/A
Average	37.1	2.4	1.5	1.7	N/A	N/A
Standard deviation	3.5	0.2	0.2	0.3	N/A	N/A

Table 4-1. Ovine specimens included in the study and the correspondent weight, treatment group and observations. GS: Gold Standard, S: Scaffold, TEP: Tissue Engineered Product. *heterologous gold standard. N/A: Not applicable.

This experimental model was first developed using frozen extremities in order to reduce the number of animals and refine the surgical technique in line with the 3Rs principles. This permitted to select the most appropriate fixation system which consisted of LP osteosynthesis plates. Moreover all surgical operations were carried out by the same surgeon in order to minimize the variability in the study and all the operations were iconographyed in order to perform further analysis.

Treatment group	Treatment	Treated sheep number
GS	Gold Standard	4
S	Scaffold	6
TEP	Tissue engineered product	6

Table 4-2. Study treatments summary.

4.2 Cell isolation and expansion

Table 4-3, **Fig. 4-1** and **Fig. 4-2** summarise the most relevant aspects of the cell isolation and expansion of oMSC. In order to obtain the clinical dose of oMSC, cells from each animal were isolated from the bone marrow (BM) and then expanded *in vitro.*

After BM extraction, MNC were isolated on a Ficoll gradient and the number of MNC recovered for a given volume of BM with an average of $9.6 \cdot 10^6 \pm 4.9 \cdot 10^6$ MNC/mL BM, obtaining in all the cases more than $2 \cdot 10^6$ MNC/mL BM. After MNC isolation, oMSC were expanded under sterile conditions, judged by visual check under the microscope. No signs of bacterial or yeast contamination were observed in any the cellular lines used to manufacture the TEP. All cellular expansions were performed using the same lot of ovine sera previously tested for a proper expansion. In order to achieve the clinical dose two passages were performed in a total of 20 days, passage -1 (p-1) and passage 0 (p0). Clinical doses were achieved in all cellular lines expanded in order to manufacture the TEP. Expansion data are showed in **Table 4-3** were duplication number and expansion factor was illustrated for both passages (-1 and 0), in which only passage 0 (p0) is calculated using the initial oMSC seeded and passage -1 (p-1) is estimated as the average of passage 0 (4 duplications), due to the lack of information of the initial oMSC number in the BM.

Sheep ID	Cell population doublings	Expansion factor
5	11	78
7	11	83
9	10	77
10	11	79
13	10	76
15	11	79
16	10	77
AVERAGE	11	78
Standard deviation	0.3	2.2

Table 4-3. Summary of oMSC expansion. All data is showed for the two passages of the expansion.

Uniformity in the cell population doublings was evident in all cell lines with an average of 11±0.3 duplications. Also expansion factor presented consistency with an average of 78±2.2. Cell densities achieved at p-1 and p0 were shown in **Fig. 4-1**. Cellular density reached at p-1 is more variable than at p0. Also density at p0 was always higher than p-1 density for each specimen. At P0 sheep 11, 12 and 14 cell lines were not performed because cells were not needed for the TEP manufacturing because they are included in the scaffold group.

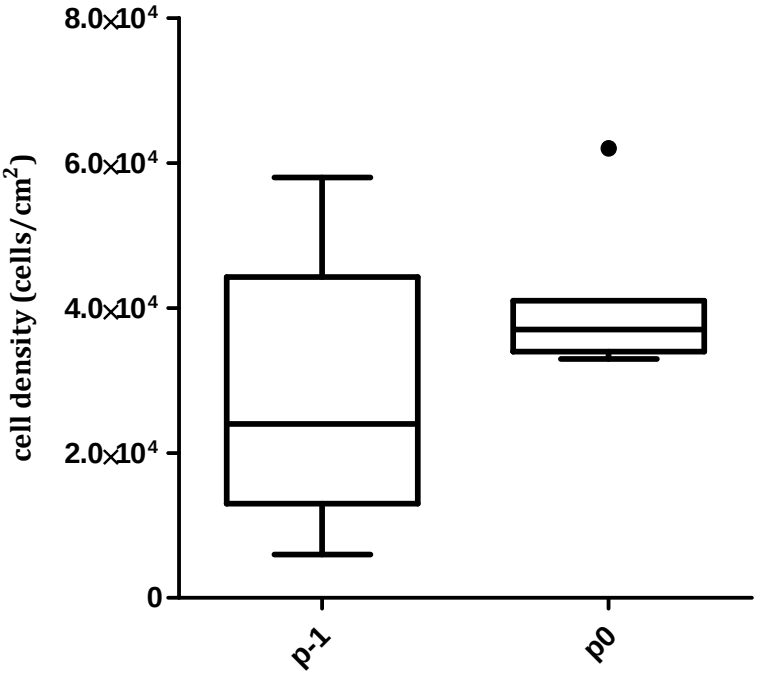

Fig. 4-1. Cellular densities achieved for each oMSC line during the study. Passage -1 (p-1) and passage 0 (p0).

The relationship between the cell density reached in each passage and the MNC number in volume of BM is shown in **Fig. 4-2**. Cell density achieved in p-1 is much more variable than in p0. The higher the number of MNC obtained for mililiter of BM, the more cell density is obtained at p0 (p=0.1007). However no relationship was found at p-1 (p=0.2858): In both passages the slope of the linear regression is similar indicating a similar behaviour in p-1 (0.0015) and p0 (0.0014).

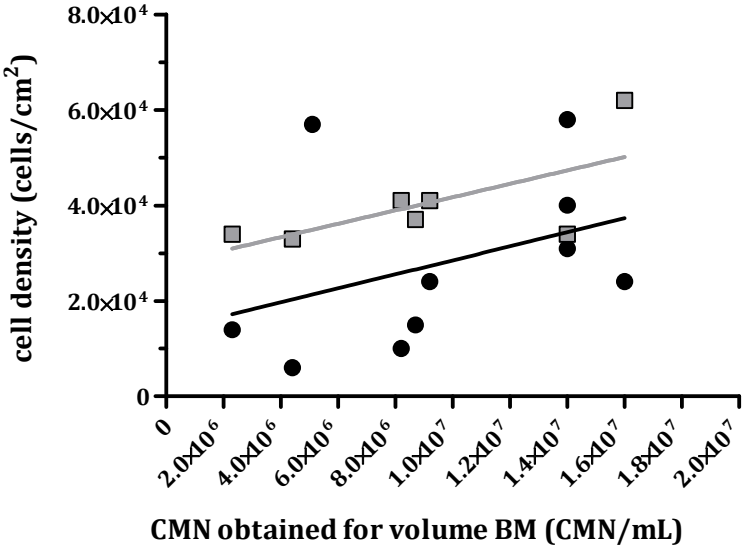

Fig. 4-2. Cellular densities achieved for each oMSC line during the study depending on the initial **MNC** concentration in **BM**. Passage -1 in black (p=0.2858) and passage 0 in gray (p=0.1007).

4.3 Colonization

Number of oMSC retained in 3cc of bone graft for each sample is shown in **Fig. 4-3**. Such numbers resulted from the subtraction cells in suspension at the end of the colonisation reaction to the inoculated cells.

$1.8 \cdot 10^7$ total oMSC were used as inoculum for the colonisation and an average of $1.7 \cdot 10^7 \pm 3.8 \cdot 10^5$ oMSC were attached to the scaffold after 21 hours whilst non-attached cells had a viability of 58%±5%. Low variability was observed between all samples, therefore ensuring high uniformity among all.

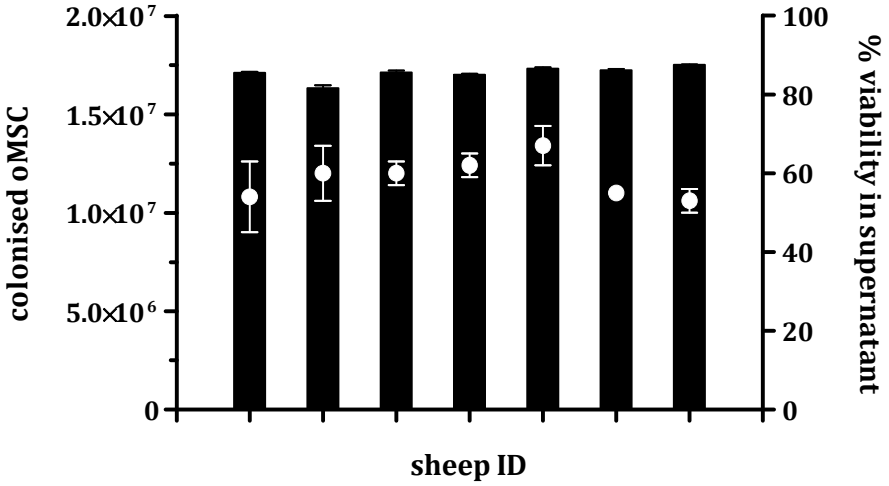

Fig. 4-3. oMSC number colonized for 3cc of scaffold, in each specimen that it was used to treat a critical size defect of a sheep (gray bars) and non-colonised (supernatant) cells viability (white points), for each manufactured TEP.

4.4 Manufacture of cell seeded and cell-free construct

After scaffold colonisation and the respective washes, bone colonised particles were blended together with fibrin glue, modeled in a 3-D cylindrical structure with a central hole, as it is shown in **Fig. 4-4 A – C**. To ensure the high viability of the living cells in the TEP, preparation and waiting times were timed. Neither of them exceeded one hour as it is shown in **Fig. 4-4 D**, ensuring the high viability of cells incorporated in the product. Cell viability was double-checked by the MTT assay performed with bone particles colonized with hMSC over time (**Fig. 4-5**) which evidenced that cell viability remained unaltered during the first 4 hours post-colonization.

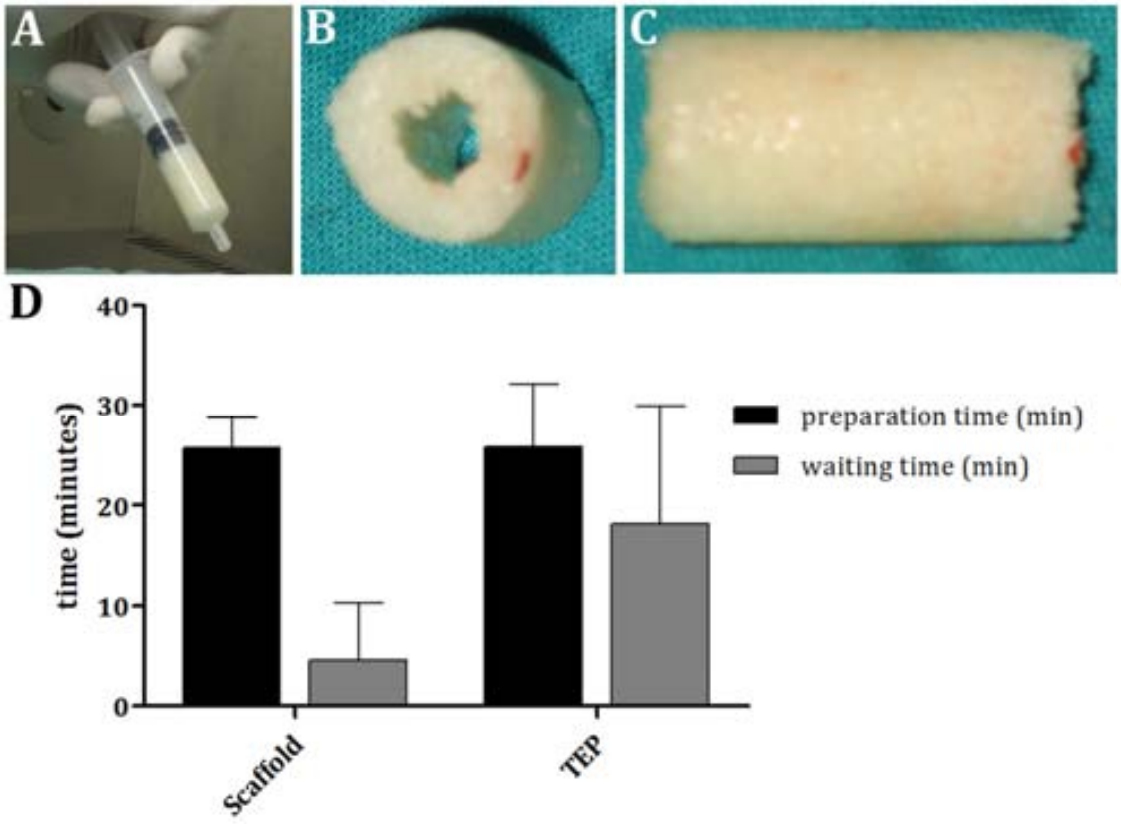

Fig. 4-4. Tissue engineered product fabrication. A-C) Tissue engineered product shape with a central hole. D) Graph showing the elapsed time between the preparation of the construct (black) and the preparation and the introduction into the sheep critical size defect (gray).

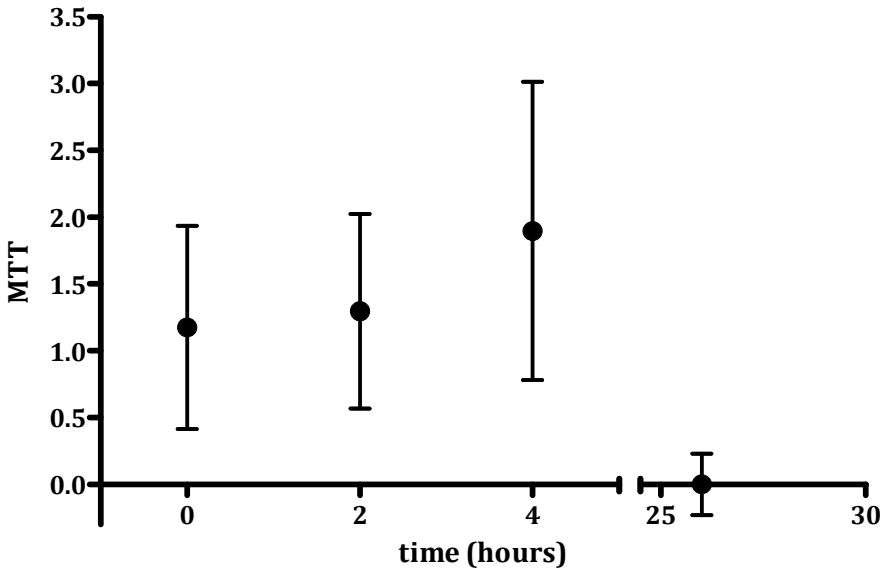

Fig. 4-5. MTT assay of bone particles colonised with hMSC over time. One way ANOVA * statistically significant difference $p<0.05$ Bonferroni post-test in comparison with time 0, 2 and 4 hours.

4.5 Critical size defect creation and administration

Both procedures for A) treating with the gold standard and B) the other two experimental groups were performed successfully by fixing the tibia by two osteosynthesis plates (see **Fig. 4-6**).

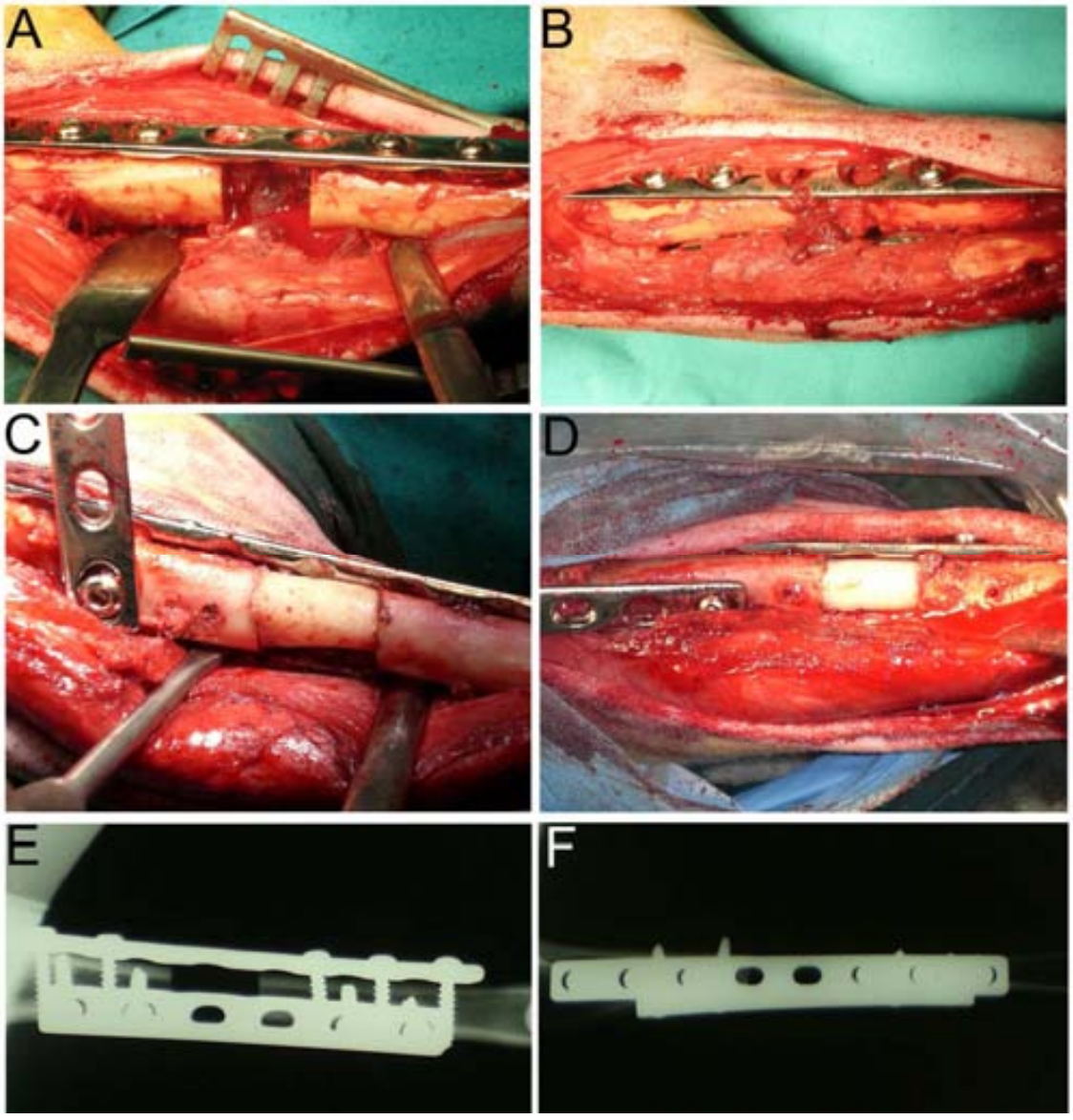

Fig. 4-6 Graph showing the induction of critical size defects (A) and the different treatments, gold standard (B), scaffold (C) and Tissue engineered product (D). X-ray image illustrating the position of the osteosyntesis plates, on coronal (E) and sagital (F) plane after surgery.

4.6 Clinical follow up

All animals (with the exception 4, 6, 7 and 14) tolerated well the surgery and implantation of the constructs. During the course of the treatment sheep were undergone a clinical follow up consisting in treated tibiae x-ray, blood analysis for biochemical and cellular analysis and weight control.

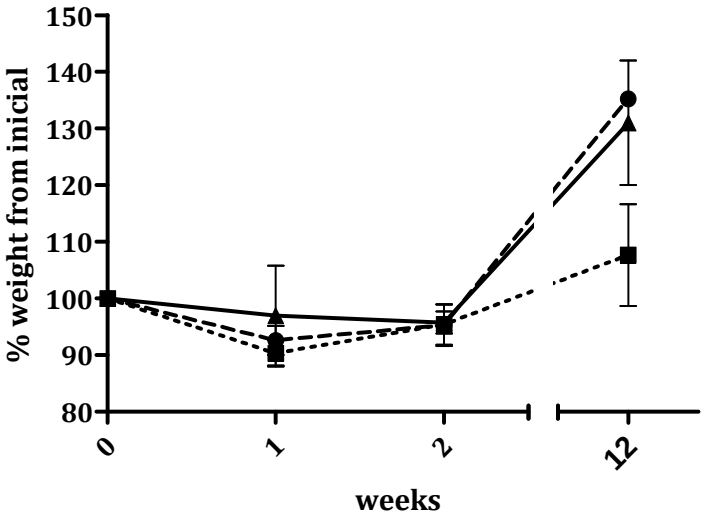

Fig. 4-7. Weight gain percentage representation throughout the study, with reference to the weight of the day 0 (surgery). GS: Gold Standard (▲), S: Scaffold (■), TEP: Tissue engineered product (●). No significant differences were found between any group ($p<0.05$).

Evolution of the percentage of variation of the initial weight (day of surgery) during all treatment period is shown graphically in **Fig. 4-7**. Although no significant differences were found ($p<0.05$) there is an evidence that both TEP group and GS group had similar weight gain compared with scaffold group that shows a slow weight recuperation.

Only three out of sixteen ewes (4: GS, 6: GS and 7: TEP), divided into the three groups described in **Table 4-1** and **Table 4-2**, had to be sacrificed before the end of the study, due to infection of the critical size defect after the implantation of the

construct, and sheep 14: S that infection was found at the end of the study during the euthanasia.

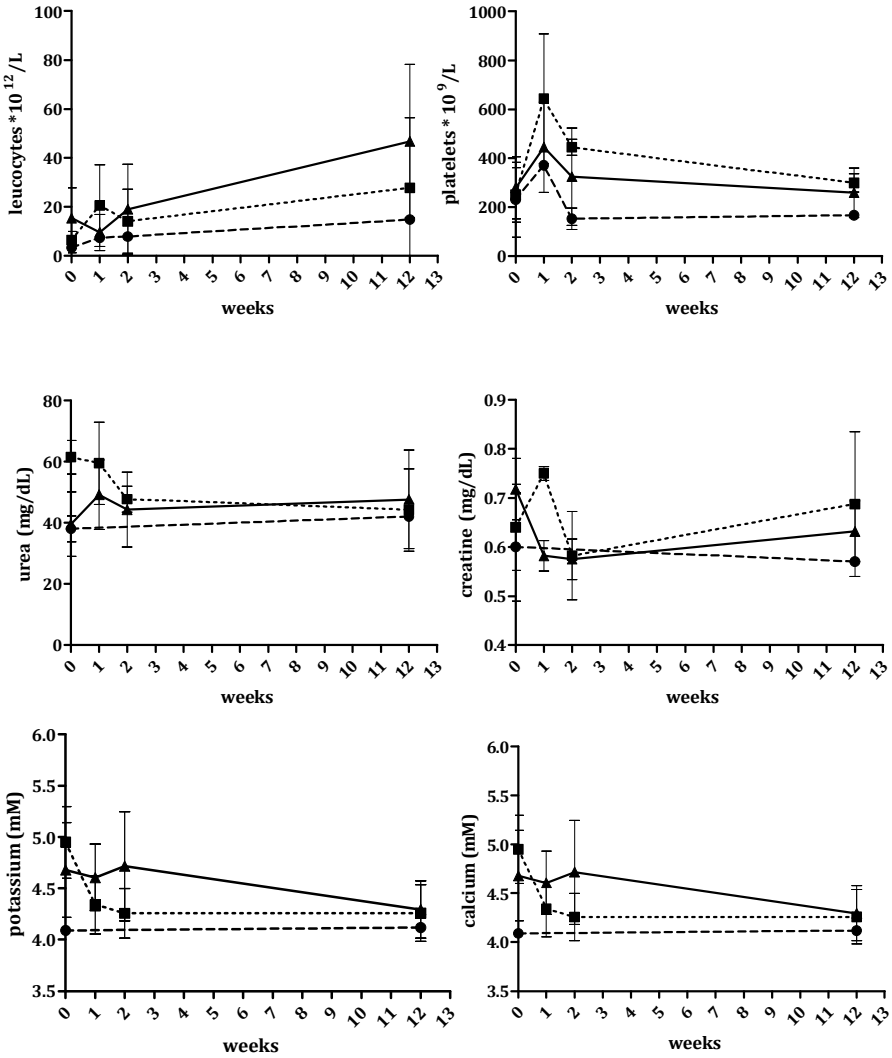

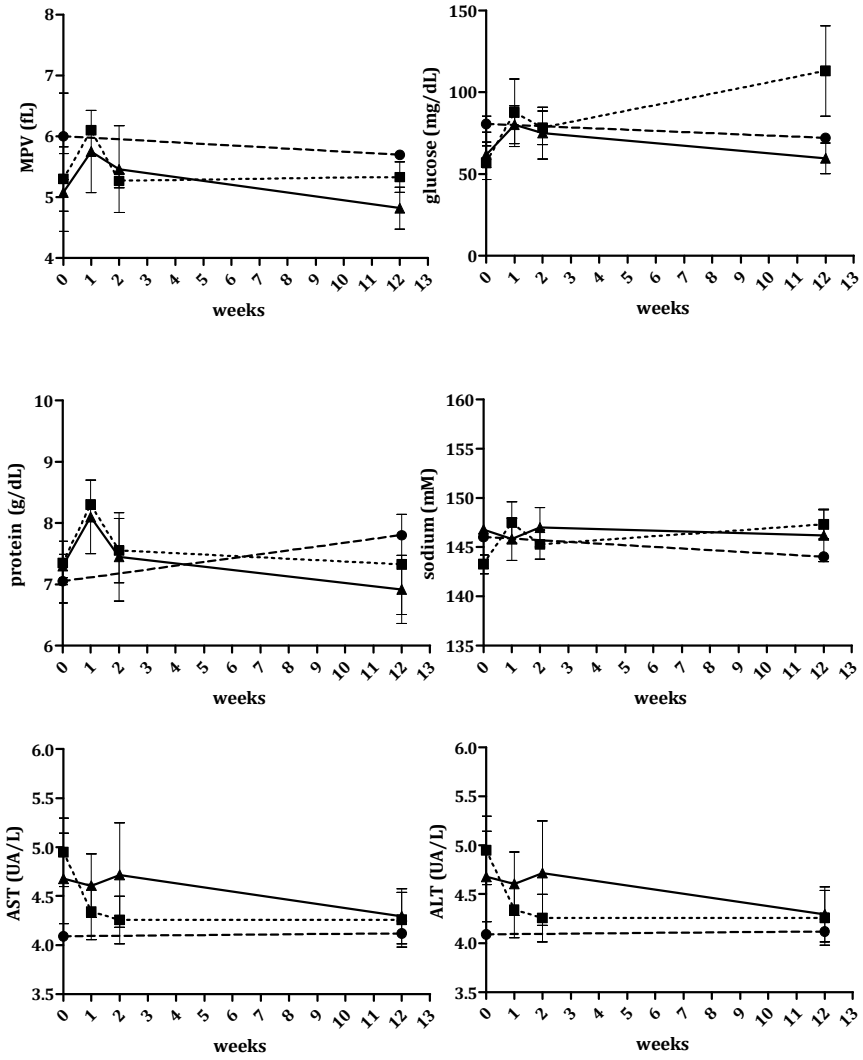

Fig. 4-8. Blood tests analysis. For the three experimental groups GS: Gold Standard (▲), S: Scaffold (■), TEP: Tissue engineered product (●) over time. MPV: Mean platelet volume; AST: Apartate aminotransferase; ALT: Alanine aminotransferase; UA: Units of activity.

Moreover, as judged radiographically plate fixation remained stable during the course of treatment (**Fig. 4-10**) even for sheep number 1 treated with gold standard that had an incorrect alignment (**Fig. 4-9**).

Fig. 4-9. Wrong positioning of the osteosynthesis plates in sheep 1.

In the radiological follow up, any tumorigenic signal was not observed in neither the TEP group nor both control groups (**Fig. 4-9** and **Fig. 4-10**).

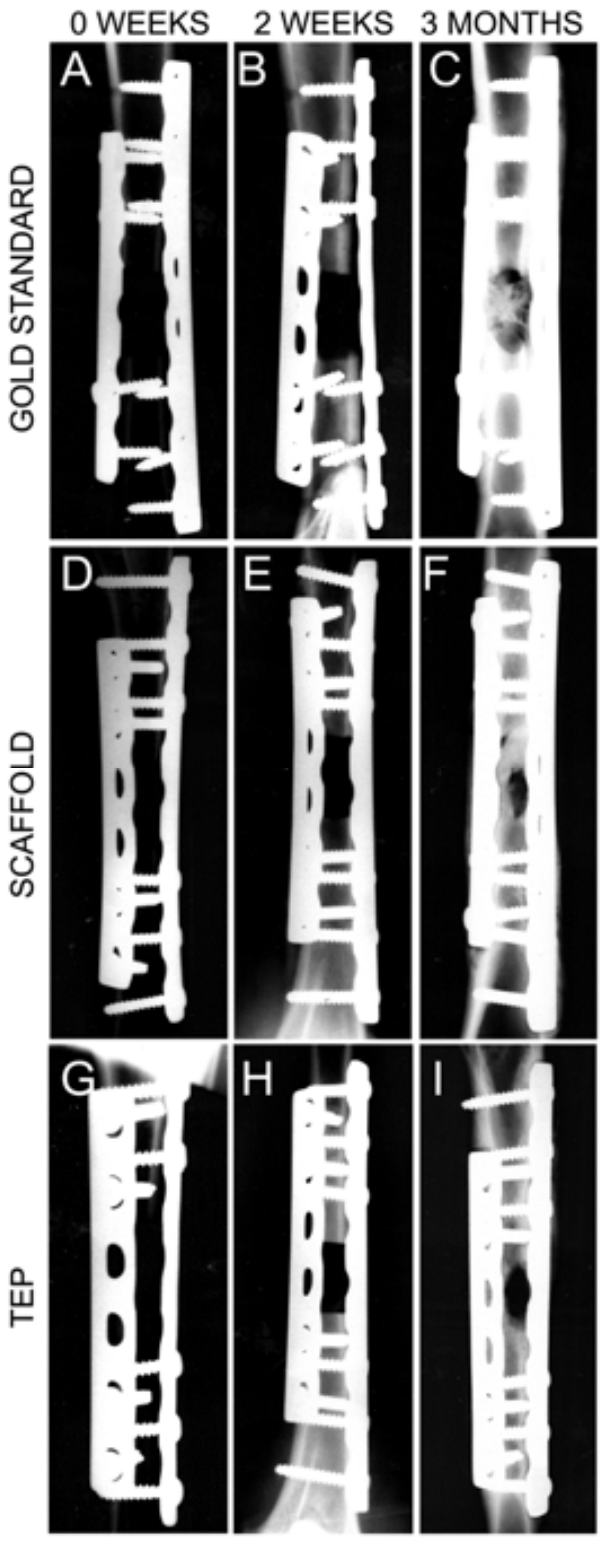

Fig. 4-10. Follow up X-ray photographs of treatment at time zero (A, D and G), 2 weeks (B, E and H) and at the end of the experiment (C, F and I) for the three experimental groups, gold standard (A, B and C) sheep 2, scaffold only (D, E and F) sheep 61 and tissue engineered product (G, H and I) sheep 55.

4.7 Mechanical properties

Once animals were euthanasied, specimens for biomechanical testing were obtained from sheep listed in **Table 4-1**.

Macroscopically, bone union was observed between construct and adjacent bone. Later, pathologic examination confirmed this at the microscopic level (4.8. Macroscopical and Histological results).

Torsion test allowed obtaining information related to the treated bone strength normalized with the value of the torque of the untreated contralateral tibia of each animal. Statistical analysis of the results shown in **Fig. 4-11** was made by the Kruskal-Wallis nonparametric method to test whether data from three or more unrelated groups come from the same population did not show significant differences ($p < 0.1$) between GS and TEP groups, while there are significant differences between S and TEP group.

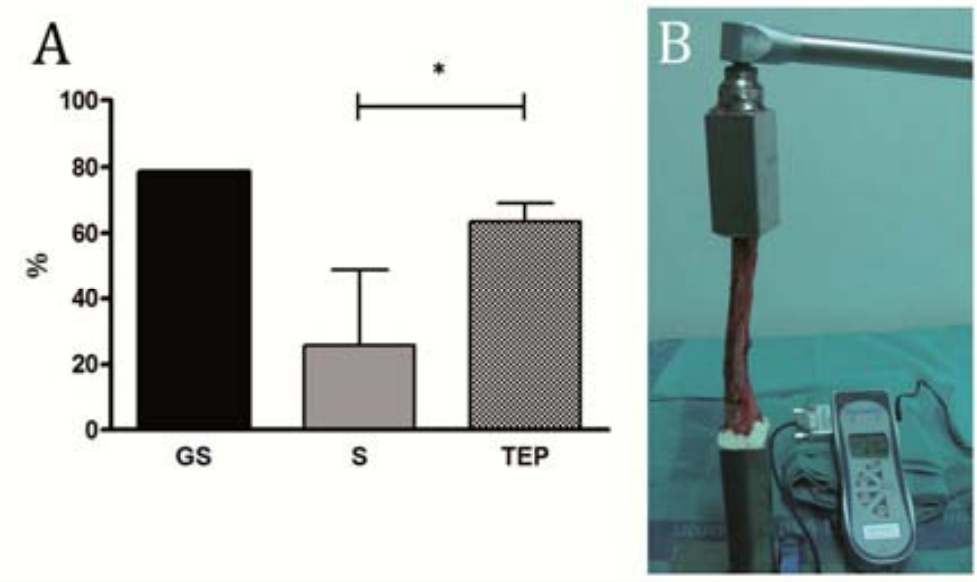

Fig. 4-11. Biomechanic test. A) Biomechanical strength percentage of the treated tibiae relative to contralateral tibiae. GS: Gold Standard (black), S: Scaffold (gray), TEP: Tissue engineered product (black and white). B) Image of the biomechanical torsion test performed. * Significant differences ($p<0.1$).

4.8 Macroscopical and Histological results

Tibias were cut off and the central part of treated ones were decalcified for 2 months and then split in two parts with a scalpel without breaking it (**Fig. 4-12**) before paraffining in order to have sectional cuts.

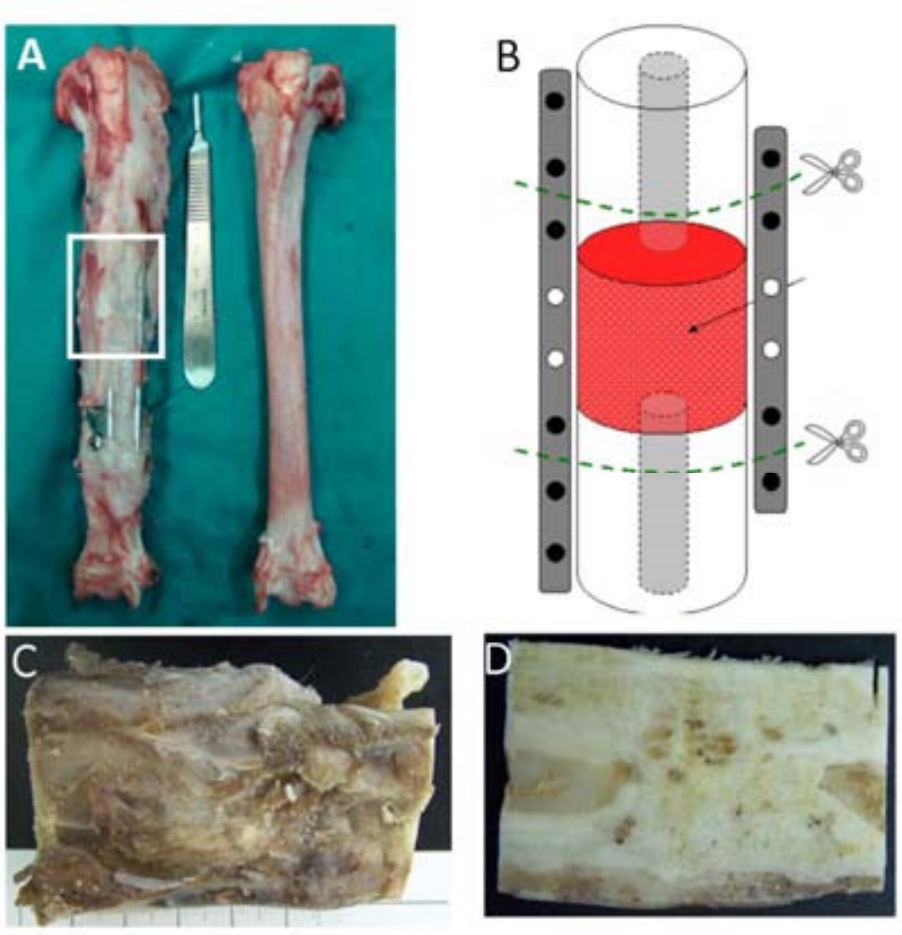

Fig. 4-12. Sample processing. A) Bare tibias, treated at left and non-treated one at right. B) Scheme of the tibia cuts before decalcification. C) and D) different views of the decalcified part of the tibiae. D) In the central part it is shown a different tissue corresponding to the construct.

Macroscopically all specimens of the TEP group and both control groups showed bone integration between naïve bone and new generated bone (**Fig.** 4-12 **D**)

Our experimental system does not allow us to distinguish between cells provided by the TEP and cells that migrated to the injured area. Although it was observed in histological sections, intense bone remodeling activity accompanied by

vascularization in GS and PA, having superior bone regeneration degree in individuals belonging to the group gold standard. In contrast, it is significant that the scaffold group showed only residual ossification while in TEP group, provided with oMSC, bone regeneration around scaffold particles was observed (see **Fig. 4-13**, **Fig. 4-13** and **Fig. 4-14**).

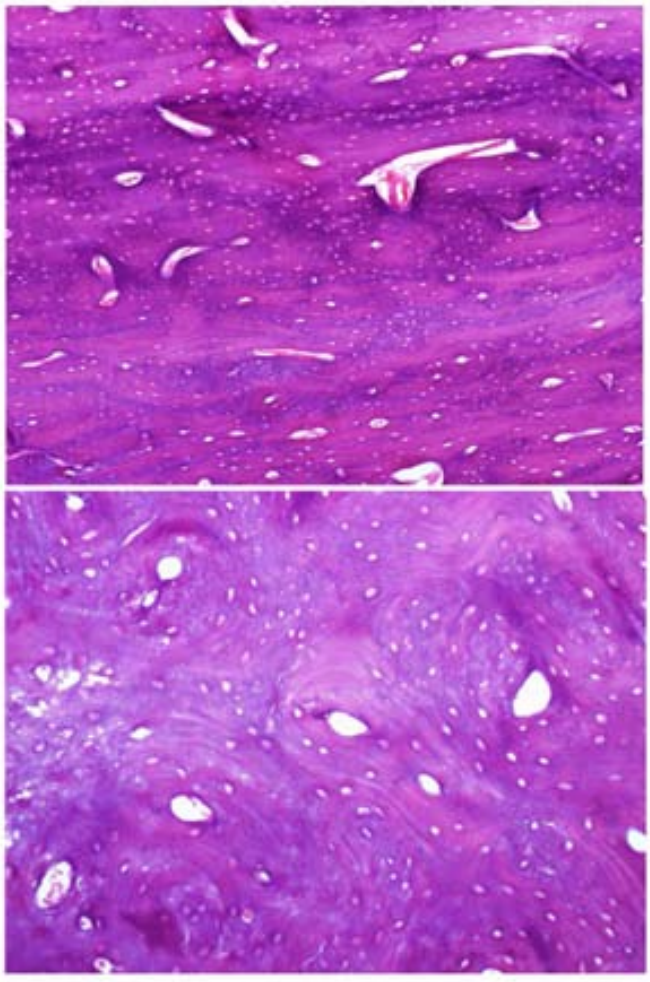

Fig. 4-13. Representative images of the results gold standard showing staining with hematoxylin / eosin for histological sections of bone.

Therapeutic intervention is based on the biological principles of bone regeneration, in which cells are involved, extracellular matrix and osteoinductive signals. It is relevant to note that the contribution of oMSC in TEP favored regeneration of the injured tissue (**Fig.** 4-15), compared with scaffold group (**Fig.**

4-14) and similar to the gold standard group treated with autologous cancellous graft (**Fig.** 4-13).

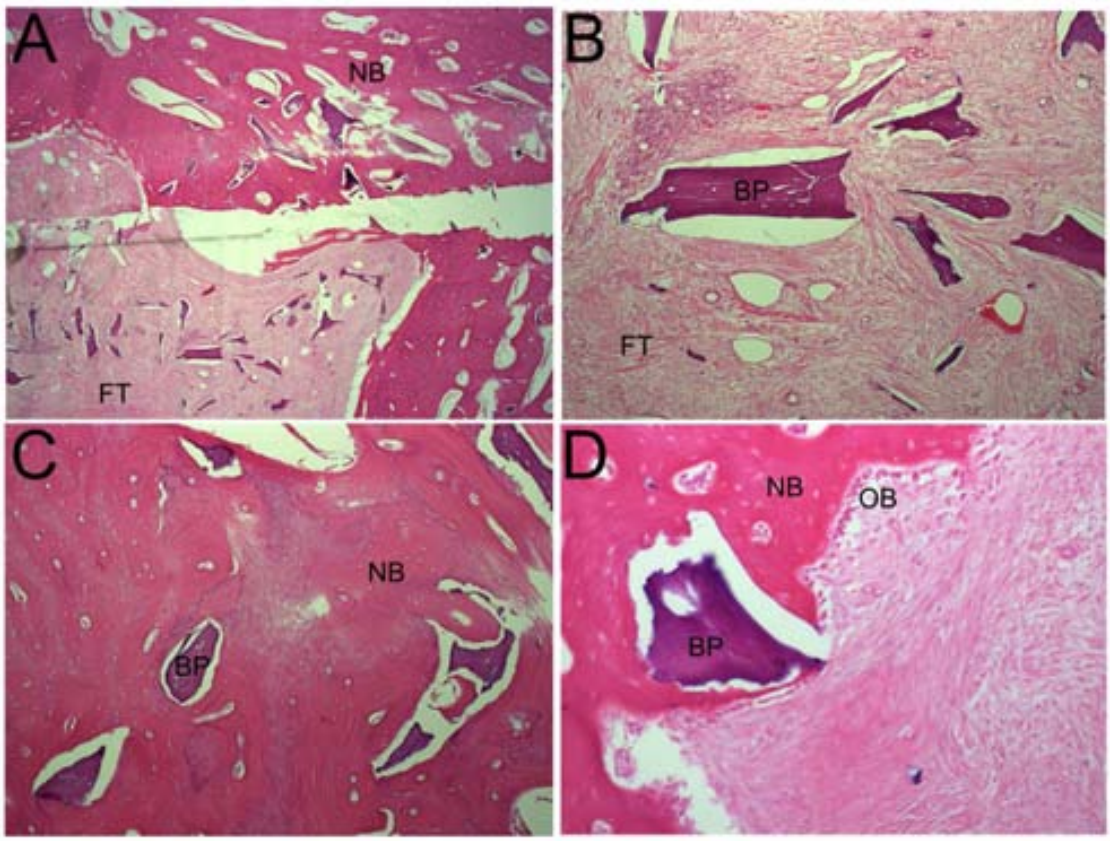

Fig. 4-14. Representative images of the results scaffold group showing staining with hematoxylin / eosin for histological sections of bone. A) Image showing part of construct with a fibroblastic tissue (FT) amplified in B) and a part of new bone (NB) surrounding bone particles (BP) from construct amplified in C). D) shows an osteoblast (OB) line producing NB around BP.

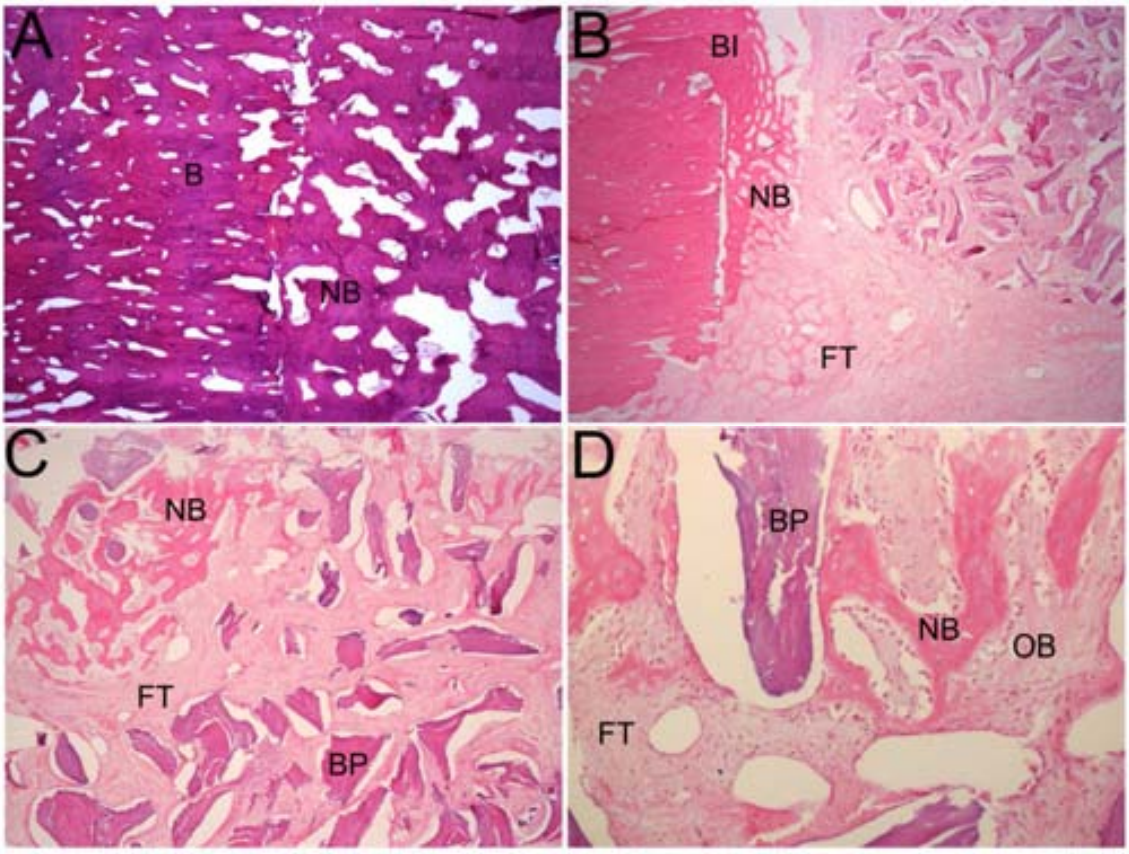

Fig. 4-15. Representative images of the results Tissue engineered product group showing staining with hematoxylin / eosin for histological sections of bone. A) Image showing bone integration between new bone (NB) and naïve bone (bone). B) Image also showing bone integration (BI) and part of the TEP, there is NB formed and fibroblastic tissue (FT). C) Shows NB formed around bone particles (BP) and a is a magnification is showed in D) were osteoblasts (OB) line forming new bone are shown.

CHAPTER V

Results: Osteonecrosis of Femoral Head

5. CHAPTER V: Results for osteonecrosis of femoral head

In the present PhD project a tissue engineered product (TEP) was developed, characterized and demonstrated its feasibility in a large animal model. After this TEP was evaluated in a relevant disease model of bone degeneration, the osteonecrosis of femoral head (ONFH) in a suitable established ovine model.

Osteonecrosis (ON) is caused by a lack or reduced blood flow to the bones and it causes a necrosis in that bone. Specifically, ON of femoral head (ONFH) affects either young or adults and its etiology could be multiple it can lead to a total hip replacement. The purpose of this study was to evaluate the efficacy of core decompression of the femoral head associated with a TEP for the treatment of ONFH in a sheep animal model. The ovine animal model was developed by Vélez (Vélez, Soldado et al. 2009) and was based on an emu ON model (Conzemius, Brown et al. 2002). The ONFH was induced by a ligature of the circumflex artery in combination with liquid nitrogen cryogenic injury. To assess bone regeneration a model of ONFH was chosen because it does not regenerate under normal conditions due to lack of blood supply and that can cause ischemia and cell death and can ultimately lead to structural collapse, articular incongruence and hip osteoarthritis.

In the present PhD project the ONFH was modeled in sheep hip in order to investigate how the MSC are involved in bone regeneration. The study was designed with three main goals: 1) evaluate the efficacy of a TEP in combination with a core decompression of the femoral head, 2) assess the safety of those TEP and 3) study the bone regeneration mechanisms.

The TEP developed in this PhD project consist of a particulate deantigenized human bone scaffold colonized by oMSC and blended with fibrin glue getting a three-dimensional structure. TEP was compared with two reference products: A) the gold standard (GS) consisted of a decompression of the femoral head and B) an acellular particulated deantigeneized human bone scaffold blended with fibrin glue.

5.1 Experimental design

A total of sixteen female sheep (*Ovis aries*, Ripollesa breed) were included in this study. All animals were 20 months old and weighted between 35.6 kg and 68.95 kg (48.8±8.6 kg). In addition, total of 10 sheep were used in the study to optimize the ON model by ligature of the circumflex artery in combination with liquid nitrogen cryogenic injury as shown in **Fig. 5-1** and ensure that osteonecrosis is maintained for 6 weeks (treatment time) and 12 weeks (euthanasia time) after the ON induction. Sheep were analyzed both by MRI and histology in order to ensure the ostenecrosis of the hip.

Fig. 5-1: ONFH model induction by ligature of the circumflex artery in combination with liquid nitrogen cryogenic injury.

All sixteen animals in the study were randomly distributed in three treatment groups described in **Table 5-1** and detailed in **Table 5-2**.

Treatment group	Treatment	Treated sheep number
CD	Core decompression (GS)	3
S	Scaffold	5
TEP	Tissue engineered product	8

Table 5-1. Study treatments summary. GS: Gold Standard.

Concerning the modeling of the ONFH in sheep, it was successful performed by identification and ligation of the circumflex femoral arteries and veins (medial and lateral). Then the femoral capsule was resected, drilled into the cervico-epiphyseal union. The anterior region of the femoral head where cryogenized for 3 cycles of 9 minutes each. The ON was allowed to establish for six weeks. Later the corresponding treatment was applied and a clinical follow up was performed for 6 weeks. At the end of the study sheep were euthanized and specimens were histological analyzed.

All sheep were euthanized as planned, on day 85±3.8 after the ON induction and 42±3.3 days from the treatment, with the exception of sheep 9 that was excluded from the study. Following euthanasia cesarean to sheep 4 was conducted to check the status of pregnancy, as fracture of the femoral head observed in this sheep could have been due to overweight supported by hind legs due to pregnancy that lasted the entire phase treatment. The sample was processed as any other but the fracture could have resulted in a higher response than the rest of sheep bone regeneration.

Sheep ID	Treatment group	Weight (Kg)	Observations
1	GS	49.75	8 mm decompression diameter
2	TEP	54.1	N/A
3	TEP	44.89	N/A
4	TEP	46	Pregnant
5	GS	N/A	Pregnant during ONFH establishment
6	TEP	35.6	N/A
7	TEP	42.8	Pregnant
8	TEP	N/A	N/A
9	GS	80.3	Non treated, trocar was broken inside the sheep and it has to be killed.
10	TEP	36.06	N/A
11	TEP	53.4	N/A
12	S	68.95	Pregnant during ONFH establishment
13	S	51.5	N/A
14	S	46.95	N/A
15	S	51.8	N/A
16	S	52.1	N/A

Table 5-2: Ovine specimens included in the study and the correspondent treatment group, initial weight and observations. GS:Gold Standard (Core Decompression), S: Scaffold, TEP: Tissue Engineered Product, ONFH: OsteoNecrosis of the Femoral Head and N/A: Not applicable.

5.2 TEP manufacturing

TEP was made of oMSC seeded a particulated deantigeneized human bone scaffold and 3D structured with fibrin glue.

5.2.1 Cell isolation and expansion

Sheep ID	Cell population doublings	Expansion factor
2	7	54
3	6	47
4	7	54
6	9	69
7	9	69
8	10	75
10	10	75
11	10	76
AVERAGE	9	64.9
Standard deviation	1.5	11.4

Table 5-3. Summary of oMSC expansion. All data is showed for the two passages of the expansion.

Cell population doublings to obtain the clinical dose was uniform along all the animal average of 9±1.5 duplications. Also expansion factor presented consistency with an average of 64.9±11.4 as shown in **Table 4-3**. Cell densities achieved at p-1 and p0 were shown in **Fig. 4-2**. Cellular density reached at p-1 is more variable than at p0 but no significant differences are shown between p-1 and p0 in the cellular density achieved.

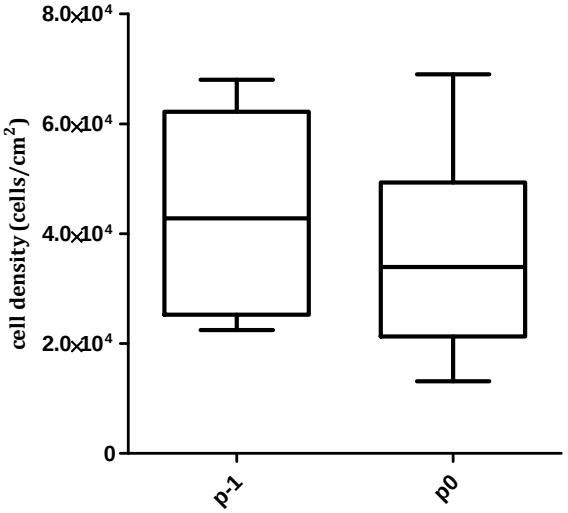

Fig. 5-2. Cellular densities achieved for each oMSC line during the study. Passage -1 (p-1) and passage 0 (p0).

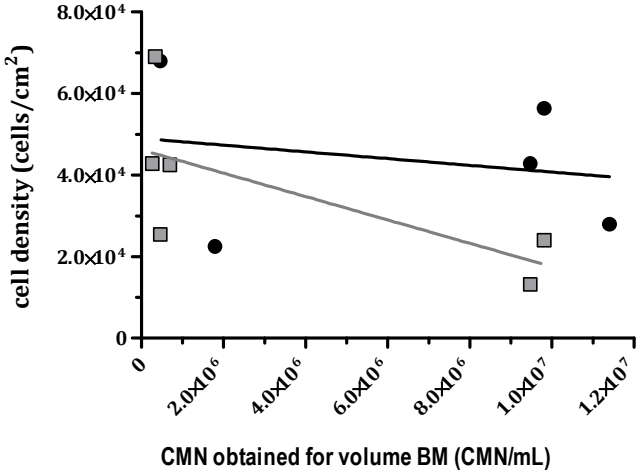

Fig. 5-3. Cellular densities achieved for each oMSC line during the study depending on the initial MNC concentration in BM. Passage -1 in black and passage 0 in gray.

We failed to show a correlation between the cell density reached in each passage and the MNC number in volume of BM is shown in **Fig. 4-2**. Since it is highly variable between different animals

5.2.2 Colonization

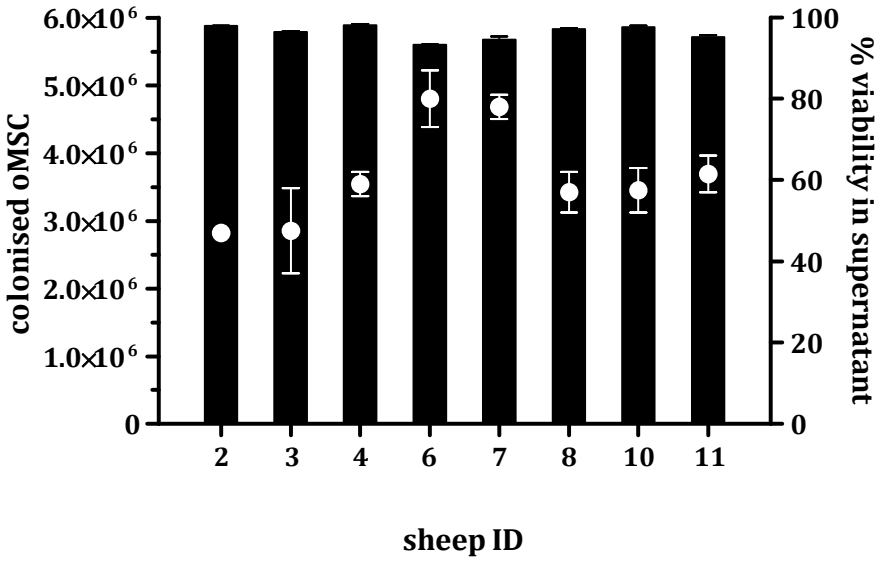

Fig. 5-4. oMSC number colonized for 1cc of scaffold, in each specimen that it was used to treat a ONFH of a sheep (black bars) and non-colonized (supernatant) cells viability (white points), for each manufactured TEP.

The cellular dose provided to seed the scaffolds was $6 \cdot 10^6$ cells/cm^3 of bone and the bone volume for the lesion to treat was 1 cm^3. Number of oMSC retained in 1cc of bone graft for each sample is shown in **Fig. 4-3**. Such numbers resulted from the subtraction cells in suspension at the end of the colonization reaction to the inoculated cells. An average of $5.4 \cdot 10^6 \pm 2.6 \cdot 10^5$ oMSC were attached to the scaffold after 21 hours whilst non-attached cells had a viability of 61%±13%. Low variability was observed between all samples, therefore ensuring high uniformity among all.

5.3 Manufacture of cell seeded and cell-free construct

After scaffold colonization and the respective washes, bone seeded particles or the respective non seeded bone, were blended together with fibrin glue, modeled in a

3-D cylindrical structure in the same trocar for the implantation as shows in **Fig. 5-5A**.

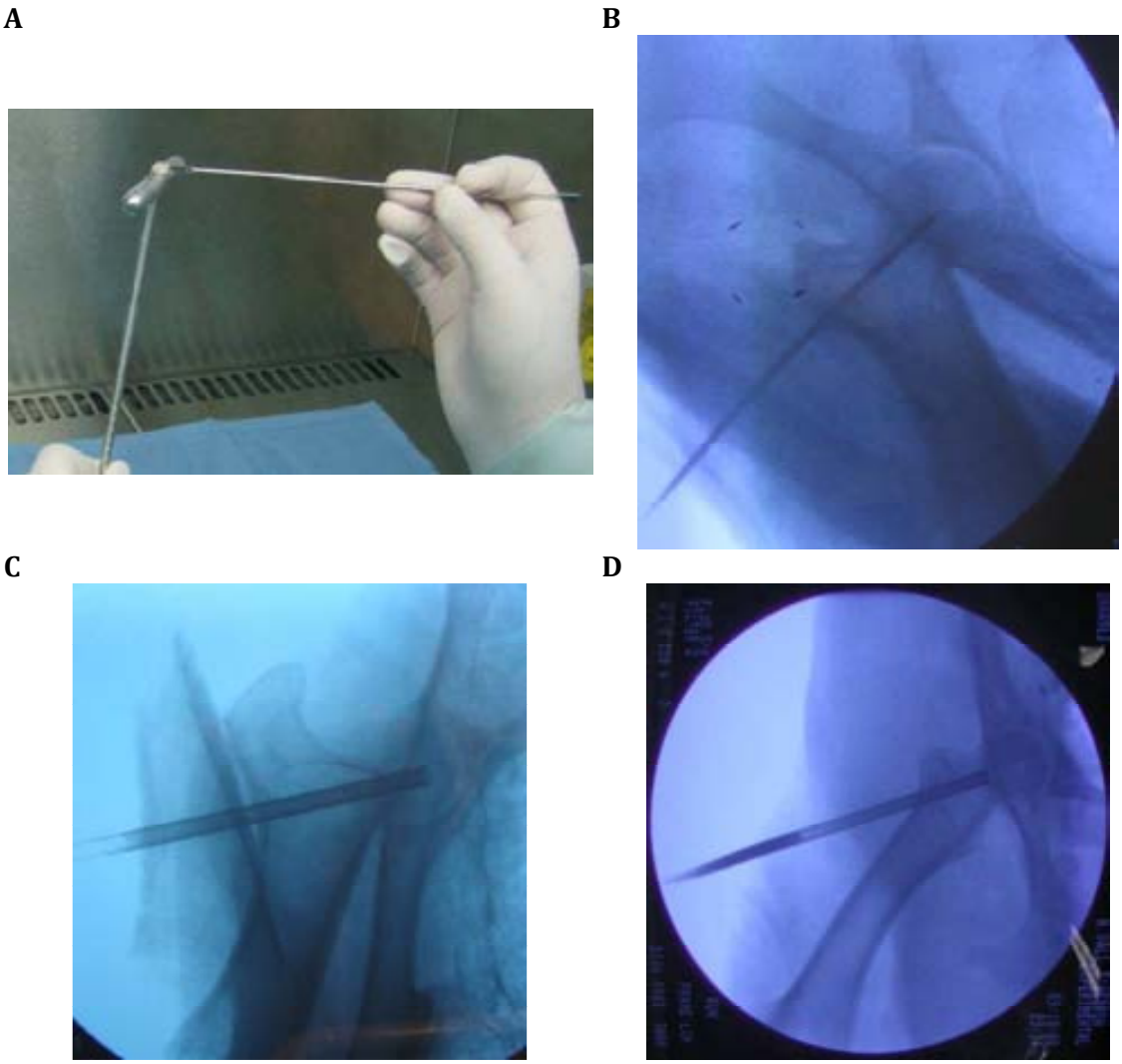

Fig. 5-5. A) TEP preparation in a sterile area, B) guide for the femoral head decompression, C) Femoral head decompression and D) TEP introduction.

Decompresion of femoral head was performed to all sheep, as shown in **Fig. 5-5B-C**, and groups treated with scaffold and TEP, the corresponding treatment was implanted as pictured radiographically in **Fig. 5-5D**.

5.4 Clinical follow up

After the first 48 h after surgery all sheep walked without evidence of limp. No surgical complications were evidenced during the first period of the study, the ON generation.

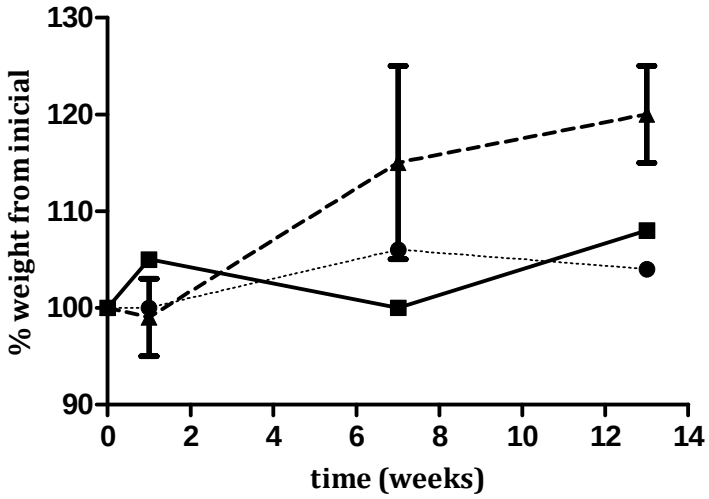

Fig. 5-6: Weight gain percentage representation throughout the study, with reference to the weight of the day 0 (surgery). GS: Gold Standard (▲), S: Scaffold (■), TEP: Tissue engineered product (●). No significant differences were found between any group ($p<0.05$).

Evolution of the percentage of variation of the initial weight (day of surgery) during all treatment period is shown graphically in **Fig. 5-6**. Although no significant differences were found ($p<0.05$) there is an evidence that TEP group and had higher weight gain compared with scaffold group and gold standard group that showed a slow weight recuperation.

Only one out of sixteen ewes (9: GS), had to be sacrificed before the end of the study, due to the impossibility to extract the broken trocar from the femoral head. Four sheep were found pregnant during the study (9: GS, 12: S and 5 and 8: TEP), therefore they were divided into the three groups described in **Table 5-1** and **Table 5-2**.

5.5 Macroscopical and histological results

Once animals were euthanasied, specimens for histological analysis were obtained as shown in **Fig. 5-7**.

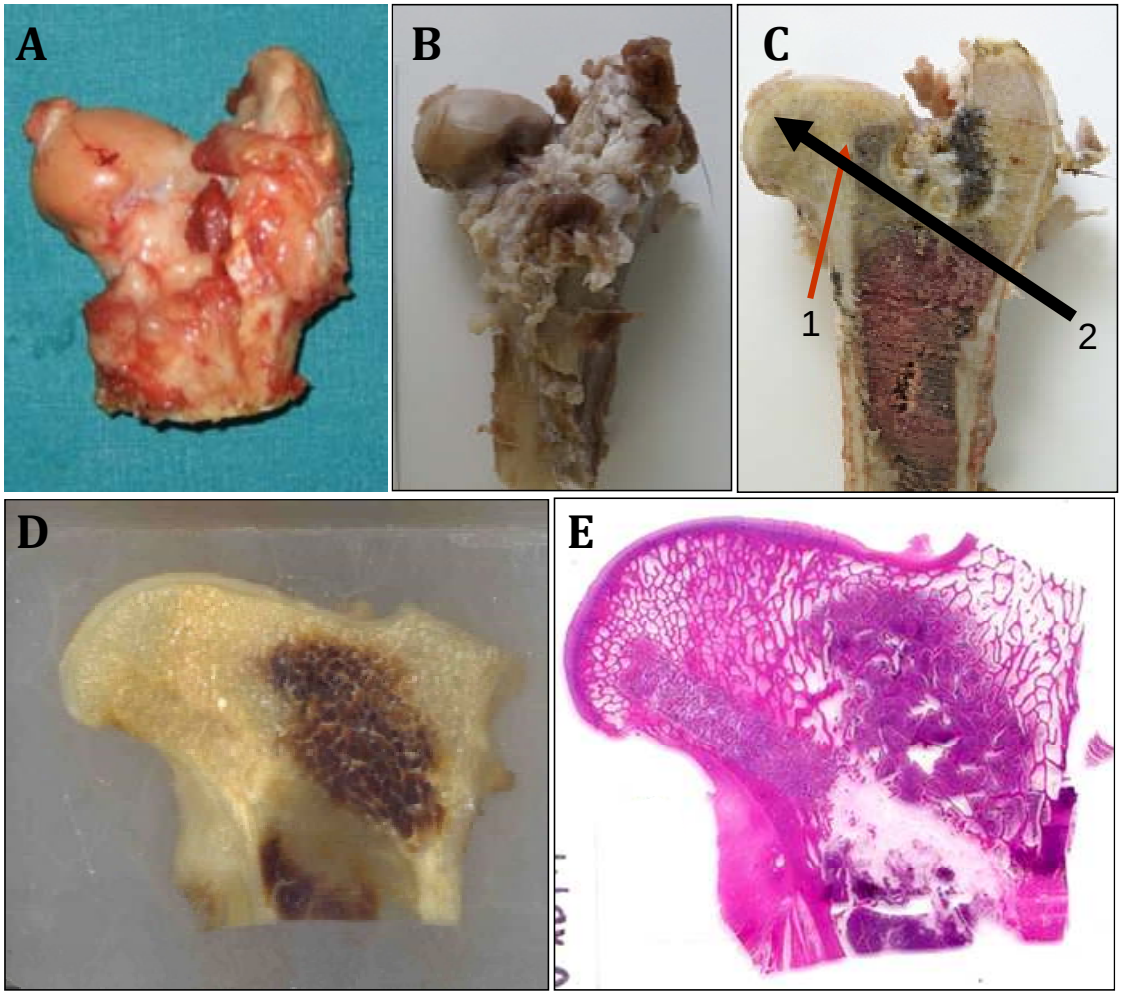

Fig. 5-7: Histological analysis. A) Femoral head was harvested from sheep, B) Decalcified, C) Sliced in half, showing the osteonecrotic area (1) and the treatment conduct (2), D) embebed in paraffin and finally E) stained.

In general it was observed in histological sections, intense bone remodeling activity accompanied by vascularization in GS and TEP, having superior bone regeneration degree in individuals belonging to the group TEP. Observing in all of cases osteoblastic line and in some cases osteoclasts indicating the bone remodelling (see **Fig. 5-8**, **Fig. 5-9** and **Fig. 5-10**).

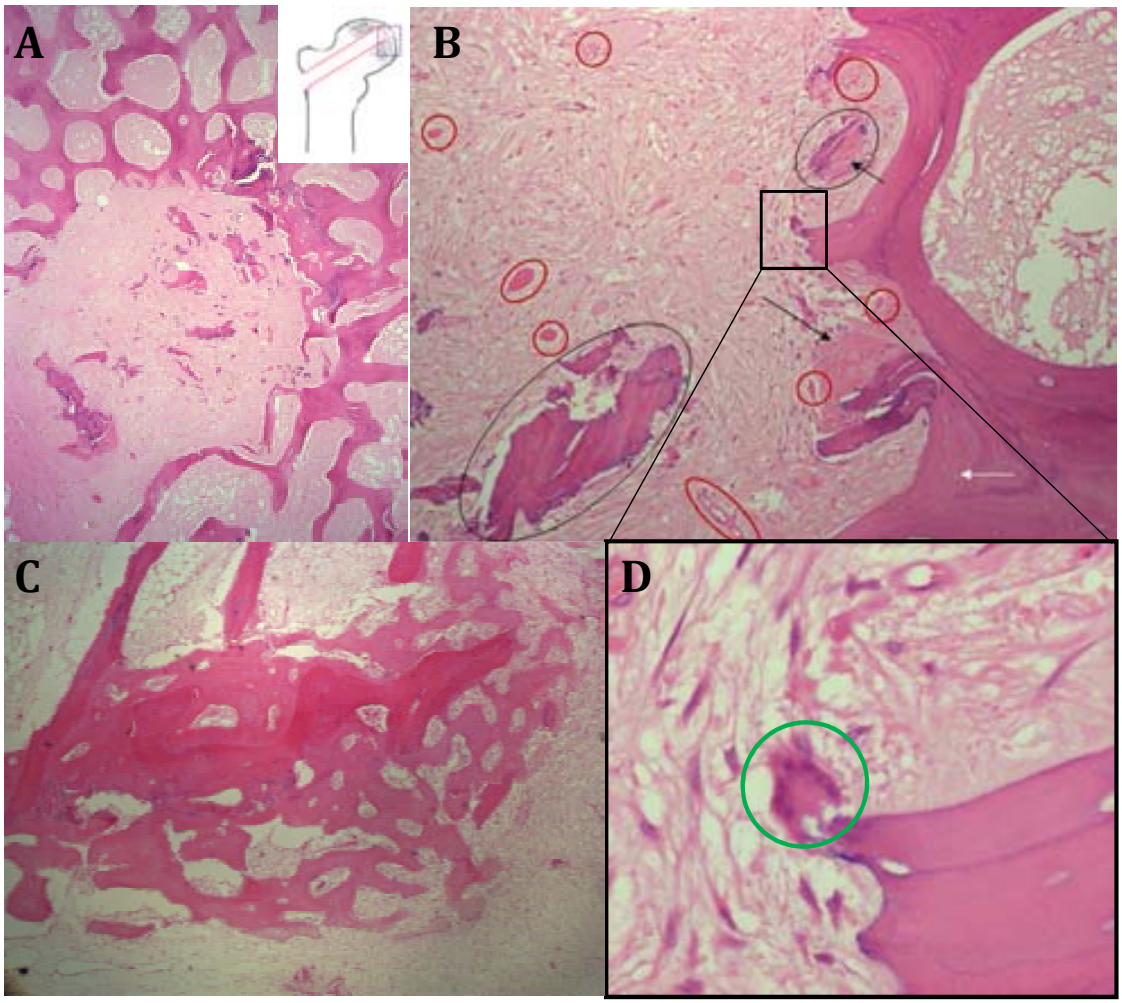

Fig. 5-8. Histological samples corresponding to gold standard treatment with H&E staining. A) corresponds to the end of the construct of the specimen 1 showing little regeneration, B is an amplification of A showing a bone particle dragged from another bone area (gray cirvle) and some vascularization (red circle). D is an amplification of B and shows an osteoclast remodeling the bone. C) corresponds to sheep 5 and shows a focus of bone formation.

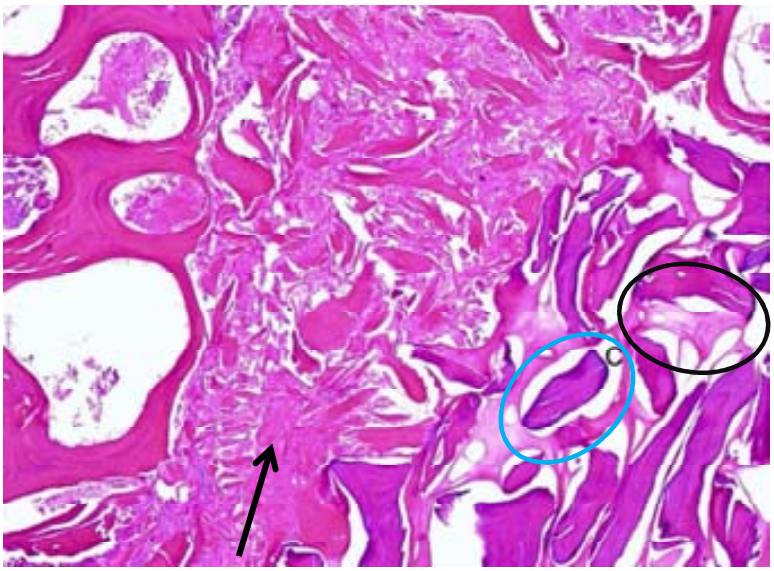

Fig. 5-9. Histological sample corresponding to scaffold treatment with H&E staining (sheep 12). At the right the treatment area with bone particles circled in blue and presence of fibrin circled in black. At the left fibrotic tissue pointed with a black arrow.

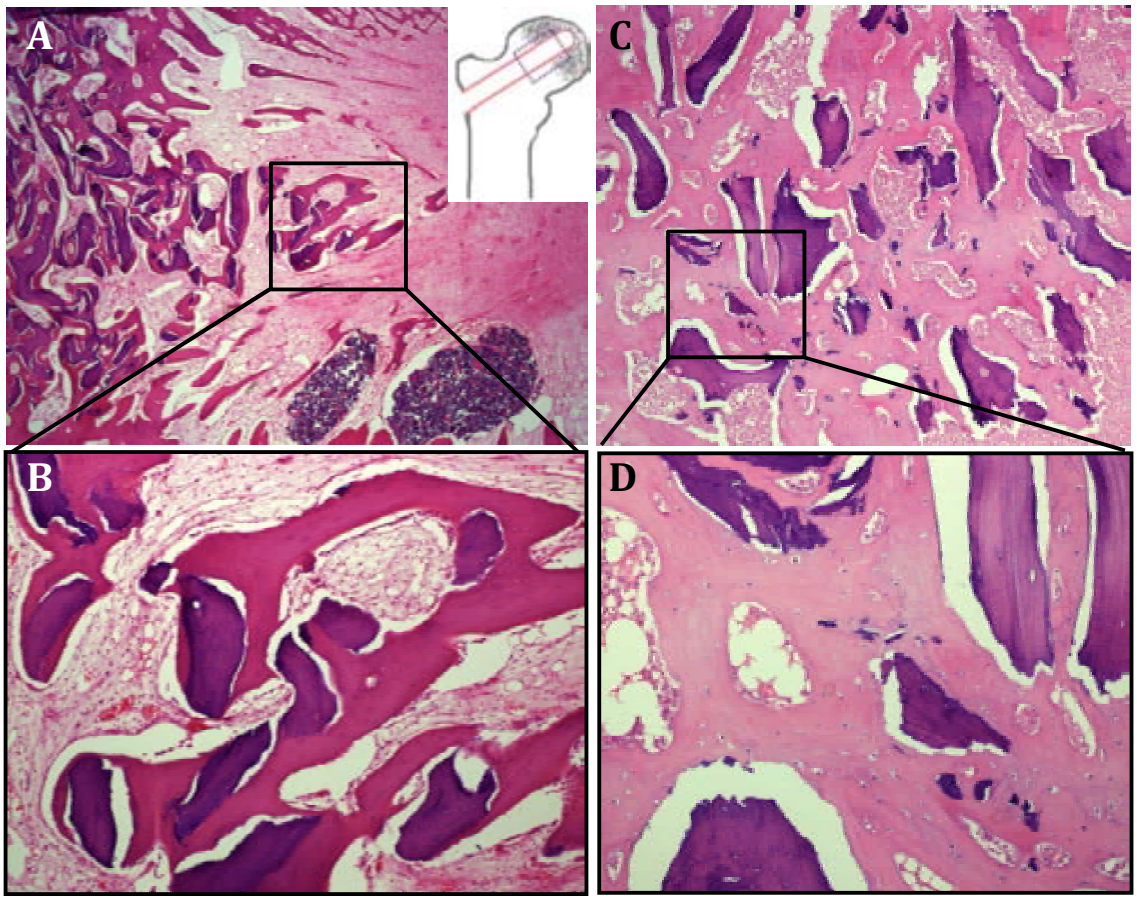

Fig. 5-10. Histological samples corresponding to TEP treatment with H&E staining. A and B corresponds to sheep 2 and C and D to sheep 4. Newly bone formed around particles it is shown in sheep 2 and mature bone newly formatted is also shown in sheep 4.

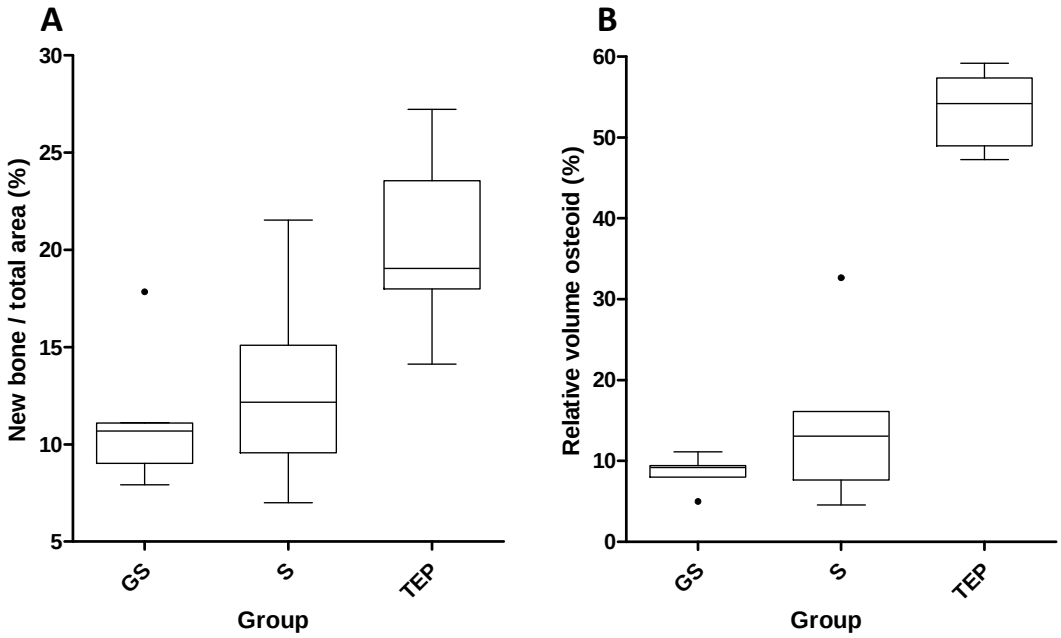

Fig. 5-11. Image software analysis of the histological samples with BoneJ A) box plot showing a higher tendency of newly formed bone in TEP group. B) box plot showing the augmentation in the TEP group of mean relative volume of immature osteoid through MSC.

The image software analysis of the histological samples revealed that the TEP group, has a tendency toward higher values of the relative surface of newly formed bone with a mean of 20.3% (14.0–27.2%) versus 11.3% (7.9–17.8%) in GS group and 13.0% (6.9–21.5%) in non seeded scaffold group, although no statistically significant differences were shown (see **Fig. 5-11A**). Osteoid production as measured by the relative volume of osteoid was dramatically increased in the TEP group. The mean relative volume of immature osteoid was 8.6% (5.2–11.2%) in GS group, 15.0% (4.8–32.7%) in S group, and 53.5% (47.5–59.3%) in TEP group ($p<0.05$) (see **Fig. 5-11B**).

5.6 MSC involved in the bone regeneration mechanism

Another sheep was included to the experiment and followed the same protocol. The treatment was TEP with eGFP labeled oMSC and the duration of the treatment was longer than those animals in experiment exposed before (107 days). After killing the animal, femoral head was harvested and treated at the same fashion and slides from femoral head were immunostained by eGFP. It was observed that transducted oMSC cells maintain GFP expression over the time *in vivo* (see **Fig. 5-12**). Moreover there are cells with osteoblastic morphology (see **Fig. 5-12B1**) and osteocyte morphology (see **Fig. 5-12B2**), both normal cells and eGFP expressing cells.

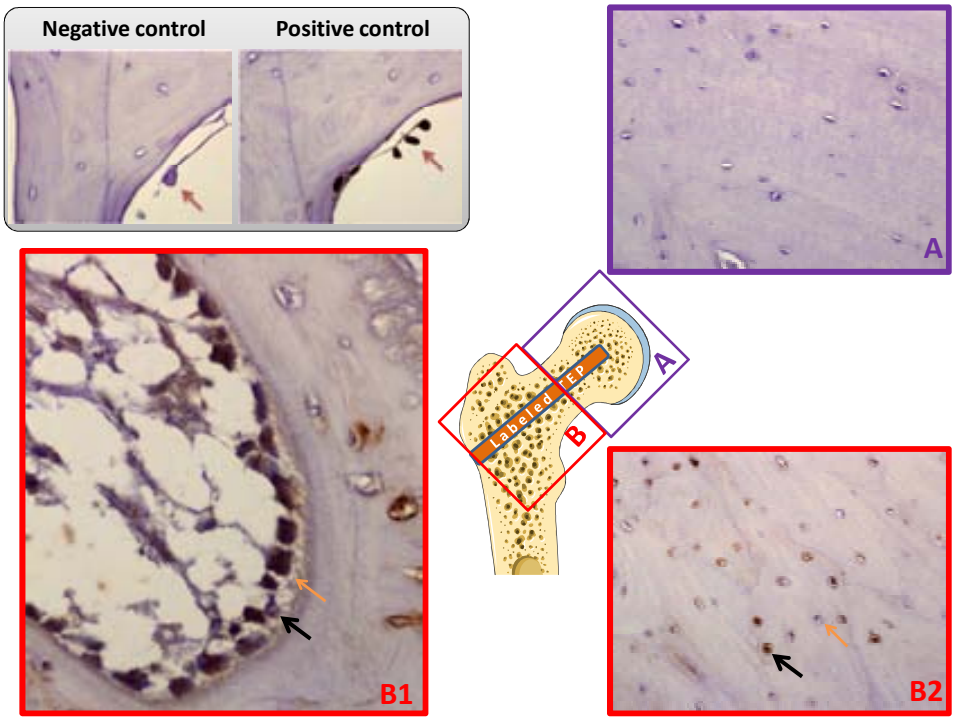

Fig. 5-12. eGFP immunohistochemistry of a sheep with a treatment of a TEP with eGFP labeled oMSC. A corresponds to the necrotic area and B1 and B2 corresponds to the normal area , showing labeled (black arrow) and non labeled (orange arrow) cells with osteoblastic morphology in B1 and labeled (black arrow) and non labeled (orange arrow) cells with osteocyte morphology in B2.

CHAPTER VI

Discussion

6. CHAPTER VI: DISCUSSION

Musculoskeletal diseases are the leading cause of chronic disability in the world (Connelly et al., 2006) also representing socioeconomic consequences and high economic burden (Vos et al., 2012). Therefore, in 2007 these were the leading cause of disability in Spain (Lázaro et al., 2014). Bone is one of the only adult tissues that retain its self-healing properties. However there are still great quantities of fractures that cannot heal spontaneously due to either interposition of soft tissue, unstable fixation, infection, deficiencies in blood supply and metabolic disturbances (Stevenson, 1998).

Recently, regenerative medicine and tissue engineering have shown huge potential to recover nearly–dead tissues that lost their functions after debilitating conditions such as myocardial infarction, spinal injury, skin burns, and bone diseases.

As it is described in the introduction, bone is a complex tissue and its regeneration involves a plethora of growth factors, MSC recruitment, three different mature cells (osteoblasts, osteoclasts and osteocytes), and a complex structural matrix. For overcoming this issues regenerative medicine provides a range of tools that could be used alone or in combination: A) *biomaterials*, which provide structural support; B) *signals* required to enhance cell proliferation and/or differentiation (i.e. growth factors and mechanical signals); and C) *cells*, such as tissue-specific cells or progenitor and stem cells (Langer and Vacanti, 1993). In terms of clinical translation into musculoskeletal disorders, a limited number of cases using strategies combining autologous cells with a variety of synthetic scaffolds have shown some efficacy for treating long bone defects (Marcacci et al., 2007), fracture

non-union (Quarto et al., 2001) and in spinal fusion surgery (Faundez et al., 2006; Putzier et al., 2008).

6.1 *In vitro* studies

Before reaching human clinical trials *in vitro* studies and preclinical trials should be conducted in animal models to confirm their safety and efficacy. Large animal models are used to asses and verify the practicability of tissue engineering approaches closer to the real clinical situations. Therefore in this PhD an autologous tissue engineering product (TEP) is assessing we develop the methodology for obtaining oMSC in order to repair bone defects in an ovine animal model.

One of the steps for developing an adequate TEP for the purpose of bone regeneration is to choose the appropriate cellular source that allows its isolation and expansion into high numbers. In fact, an ideal cell source should be easily expandable to higher passages, non-immunogeneic and have a protein expression pattern similar to the tissue to bone tissue. For that reason bone marrow (BM) derived mesenchymal stromal cells (MSC) are the most used cells both experimentally and in clinically (Bruder et al., 1998; Ohgushi et al., 2009; Quarto et al., 2001). For that reason we developed a TEP for bone regeneration purposes using BM derived MSC.

Currently there is a high interest in developing a sheep MSC model as a therapeutic agent for assaying new TEP in such a large animal model to treat many types of diseases and disabilities due to its capacity to differentiate into different lineages (Bianco and Robey, 2001). The properties of bone marrow (BM) derived MSC are

well characterized in human (Pittenger, 2008, 1999), but at a present the knowledge concerning the methods and sources to obtain ovine MSC (oMSC) and its proper characterization are limited. BM is found in flat bones, therefore oMSC were harvested from sheep sternum as it is covered by a thin layer of bone being the anatomical part more easily accessible that contains BM (Smith, 2014).

From different BM aspirates it was defined the conditions of oMNC obtaining from an adaptation of the procedure of the hMNC protocolized in our laboratory. We managed to obtain the highest amount of oMNC and the greatest location of the cell ring using 1:1 dilution with PBS, 1.077 g/mL of Ficoll density, centrifugal force of 1000 *g* during 35 minutes, although in the bibliography different protocols have been established, for example whole BM direct plating without gradient separation (Mareschi et al., 2011) or immunoseparation for different molecules as $CD105^+$ and $CD271^+$ (Jarocha et al., 2008). The ratio number of oMNC/BM volume was studied and high variability has been proven, this may be due to different persons who have extracted bone marrow that were also from different centers, therefore, extracted bone marrow volumes were variable and this as well as the age of the patients influence the number of cells obtained (Batinić et al., 1990; Stolzing et al., 2008). Furthermore we demonstrated that the proportion of oMSC in the BM is similar to those in human BM defined by Pittenger et al (Pittenger, 1999).

The chosen strategy for isolation of oMSC was a seeding density of $4 \cdot 10^5$ cells/cm^2 and wash 5 days post-seeding. There are different strategies to isolate MSC based on their ability to adhere to plastic surface, PBS washing performed at 24 hours post-seeding (Colter et al., 2000), 72 hours (Campagnoli, 2001) or up to 120 hours (Murphy et al., 2003), and with different cell seeding densities (P. a Sotiropoulou et

al., 2006) and a wide variety of media supplements, not having a clear consensus in the literature (Carrancio et al., 2008).

After MSC isolation cell expansion is a major stage in the process for obtaining the TEP, since a high cell number is required. Therefore it was convenient to choose a seeding density and culture supplement for obtaining a higher number of cells. In all culture conditions the growth pattern followed the typical sigmoid curve showing a latency stage in which cells are attaching to the surface, an exponential stage and finally the plateau. Previous reports, evaluating critical parameters for MSC expansion, have proposed that plating MSC at low density favors its proliferation (Colter et al., 2001, 2000; Prockop et al., 2001; Sekiya et al., 2002). From the experiments performed, we can indicate that initial plating densities of $2.5 \cdot 10^6$ cells/cm^2results in much higher numbers of MSC population. Because the proliferative capacity of MSCs is very high, the starting population is crucial for final numbers of cells to be obtained.

Further factors affecting the expansion of human MSC include the media supplements. We have tested autologous serum and pooled serum as alternatives for clinical scale manufacturing to fetal bovine serum (FBS). Although both media suplements supported MSC expansion, pool serum significantly accelerated MSC proliferation compared to autologous, is as effective as supplementing the culture medium with FBS. Several studies have concentrated on the use of autologous serum (Stute et al., 2004), although this approach is limited by the amount of autologous serum necessary to expand MSC for clinical use (P. A. Sotiropoulou et al., 2006) and the variability of serum. This variability is fixed by making a pool and some studies have been successful in isolating and expanding MSC using AB

serum (Yamaguchi et al., 2002), however, others reported MSC growth cessation after the first passage (Shahdadfar et al., 2005).

Referring to MSC characterization the minimal, our cells meet the minimal criteria defined by ISCT (Dominici et al., 2006). However, the lack of cross-reactivity with the standard antibodies (human) we failed to characterize oMSC with the standard antibodies panel, changing CD105 to CD44 (Godoy et al., 2014) and not using HLA-DR as it is specific for human cells. Moreover, the MSC heterogenic population holds the potential to differentiate into the three lineages. Some studies revealed the complexity of the MSC hierarchy and suggested CD146 as a marker of as proliferation capacity and CD146 expression diminish with loss of trilineage potential (Russell et al., 2010).

With the aim To augment the therapeutic effects MSC delivered locally, many efforts are focused on the design of scaffolds to create a biocompatible environment, to provide a surface for cell adhesion and migration and to promote osteoconduction,. Different types of scaffolds are used in bone regeneration TEP, Ceramics, such as hydroxyapatite or β-tricalcium phospate have been widely used (LeGeros, 2002) or other natural polymers like collagen I, PGA/PLA scaffolds, . Allogenic deantigeneized bone is one of the most frequently scaffold used ant its increasing availability made it possible to manufacture customized types, such as dowels, powder, and chips (Sandhu et al., 1999).

Regarding the scaffold colonization different bone graft manufactures were tested and it was shown that the powder format accepts more cells than the bone fragments possibly due to the more exposed surface by the powder as being smaller particles. Also different inoculi were tested proving that the maximum

capacity of the scaffolds are $2 \cdot 10^6$ cells as the highest cell concentration $1 \cdot 10^6$ cells were remained in the supernatant not colonizing the scaffold. Also different colonization systems were tested demonstrating the homogeneous cell distribution, but non stirred colonization was chosen for further experiments having into account the possibility to have high mortality due to the shear stress in stirred colonization (Yeatts and Fisher, 2011) and the feasibility it.

oMSC were successfully labeled with eGFP and its had the same characteristics than non-labeled cells, including the trilineage differentiation, immunophenotype and expansion patterns. Although eGFP expression decreases as the cell population accumulates cell divisions.

6.2 CSBD

Having the TEP developed, we evaluated the capacity of the tissue-engineered bone to repair critical-defects in a sheep animal model. The model was developed similar to the description of Reichert et al (Reichert et al., 2010, 2009), having smaller critical sizes but it could be considered as a good critical size as there was no-union in the control group during all the course of the study.

Before starting the experimental part, some tests were performed decide on the fixation and depurate the surgical technique, thus ensuring the stability of the structure and at the same time it was possible to reduce the number of live animals needed for the experiment, using the animal welfare standards (3Rs). Surgical operation always performed by the same surgeon who performed all experimental lesions, thus reducing the variability in surgical technique.

After the treatment weight evolution was recorded and the results can be interpreted as a reduced regenerative capacity of the scaffold group, reflected in the behavior of the animal, having a slow weight recovery compared to those that received gold standard or TEP treatment.

The degree of regeneration at the end of the study due to each treatment was different and there was even a large variability between animals of the same experimental group. Perhaps this could be because the animals had not reached skeletal maturity and that while at 20 months the sheep are considered adult, some authors recommend radiological check the closing of growth plates and check that it has stopped (Reichert et al., 2010, 2009). The growth plate is a sheet of cartilage located between the epiphysis and metaphysis and is known as growth plate. When growth slows, the cartilage gradually ossifies, what is called closure of the growth plate. A commonly used method to determine skeletal maturity is the radiological assessment of the closure of the epiphysial growth plates of various joints and could also be used in future studies. This is justified because as younger the animal, it has greater regenerative capacity. In addition, the sheep have greater regenerative capacity than humans, so the use of animals with greater skeletal maturity reliably reflects physiological conditions more similar between species.

In the study of segmental tibial defect was observed macroscopically with the integration of the construct adjacent the native bone. Subsequent pathologic examination confirmed this observation at the microscopic level.

The torsion test provided information regarding the sought resistance when normalized with the value of the torque of each animal untreated contralateral tibia bone was performed. Statistical analysis of the results of biomechanics using

the Kruskal-Wallis test revealed no significant differences between the groups treated with cells and the gold standard, while there are differences between the gold standard and the treatment without cells. Then the TEP could regenerate bone with similar mechanical properties to those obtained by the gold standard treatment, and avoiding the need to remove the graft from the patient that have associated morbidity in the donor site.

Regarding efficacy of the treatment, preferably bone formation was observed using the product loaded with MSC, and in the case of the studies in sheep diaphyseal model critical size defect, was comparable clinical and mechanically to that obtained after the use of autologous cancellous graft (gold standard in humans).

6.3 ONFH

Since at present there is no effective treatment to prevent progression in the early stages of necrosis of the femoral head and in the later stages, the options are limited to surgical techniques of articular reconstruction (Petrigliano and Lieberman, 2007). So, once TEP was tested in a model for bone regeneration an ONFH model, that is a real disease model, was developed in ostrich model by Conzemius (Conzemius et al., 2002) and then adapted to an to sheep by Velez (Vélez et al., 2011).

The group of sheep treated with the TEP was the only group that stimulated bone regeneration within the ischemic area of the femoral head. The addition of cultured stem cells really set the difference in osteoid production locally in an hypoxic environment. This higher osteoid concentration translated into an apparent higher tendency to definitive new bone formation. We believe that the

tendency to higher new bone formation would have been statistically significant if the treatment had been prolonged longer than the established 6 weeks. These results show that the addition of cultured and expanded MSC ex vivo through advanced cell therapy techniques to a standard core decompression of femoral head osteonecrosis stimulates immature bone formation de novo much more effectively than the other two techniques. The scaffold group did not stimulate osteoid production locally or induce bone maturation and it could be that its osteoconductive and osteoinductive properties are insufficient when used without cultured MSC for bone regeneration. Although, we evidenced efficacy and safety of the developed TEP.

Unfortunately, our study was unable to evaluate through MRI (the clinical standard) the therapeutic effects of the different treatment modalities. This could be due to the limited time between the surgical treatment and the follow-up MRI, where there was an important artifact of edema that prevented the proper display of the areas with viable bone or necrosis. Moreover, the low power of the apparatus used (0.2 T), thus other authors have used devices 7–8 times more powerful, allowing a detailed study of the lesion (Jaramillo et al., 2003).

A limitation in both in vivo the studies was the sample size, however 4 animals per group falls within the low range acceptable as reported in the literature (Reichert et al., 2010). But we took special attention in reduce variability by an established surgical protocol performed always by the same surgeon. Also all animals were the same breed, age and weight.

One sheep was treated with an equivalent TEP with MSC labeled with GFP proving that the MSC maintained in the lesion after the course of the treatment, although

mechanism is not described we can say that MSC are important for bone regeneration either by the cells or the paracrine effect (REF).

Finally it is necessary to translate this TEP to a GFP manufacture production in order to initiate clinical trials for test safety in humans.

CHAPTER VII

Conclusions

7. CHAPTER VII: CONCLUSIONS

This PhD project was to develop and characterize a 3D tissue engineered product (TEP) and further evaluate the feasibility of its implantation *in vivo* and assess the, efficacy of its use in a preclinical setting.

A consistent method for TEP production was developed and its identity, potency and impurities were determined.

Isolation and expansion of MSC were successfully performed from ovine sources.

oMSC produced this way displayed the mesenchymal stromal cells characteristics and ware analogous to hMSC.

oMSC were successfully labeled for the GFP reporter for *in vivo* tracing and showed the same characteristics seen in the unlabeled cells.

TEP was tested *in vivo* in a standard test of long critical size bone defect in a large animal model, demonstrating its ability to synthesize new bone and bone remodelling.

oMSC were involved in the synthesis of new bone as progenitors in a preclinical model of ONFH, although paracrine mechanisms can not be discarded.

The use of MSC loaded in bone matrix, for tissue engineering therapy of critical sized defects and osteonecrosi of femoral head, is safe even after 3 months post-administration.

Taking everything into account, a TEP for bone regeneration has been developed under GLP environment as a key step prior to transfer it to a GMP compliance bioprocess for testing its safety and efficacy in clinical trials.

CHAPTER VIII

Materials and Methods

8. CHAPTER VIII: MATERIALS AND METHODS

8.1 Overview: from MNC isolation to TEP manufacturing

Fig. 8-1 presents an overview of TEP manufacturing form MNC isolation going through MSC expansion and all quality tests performed.

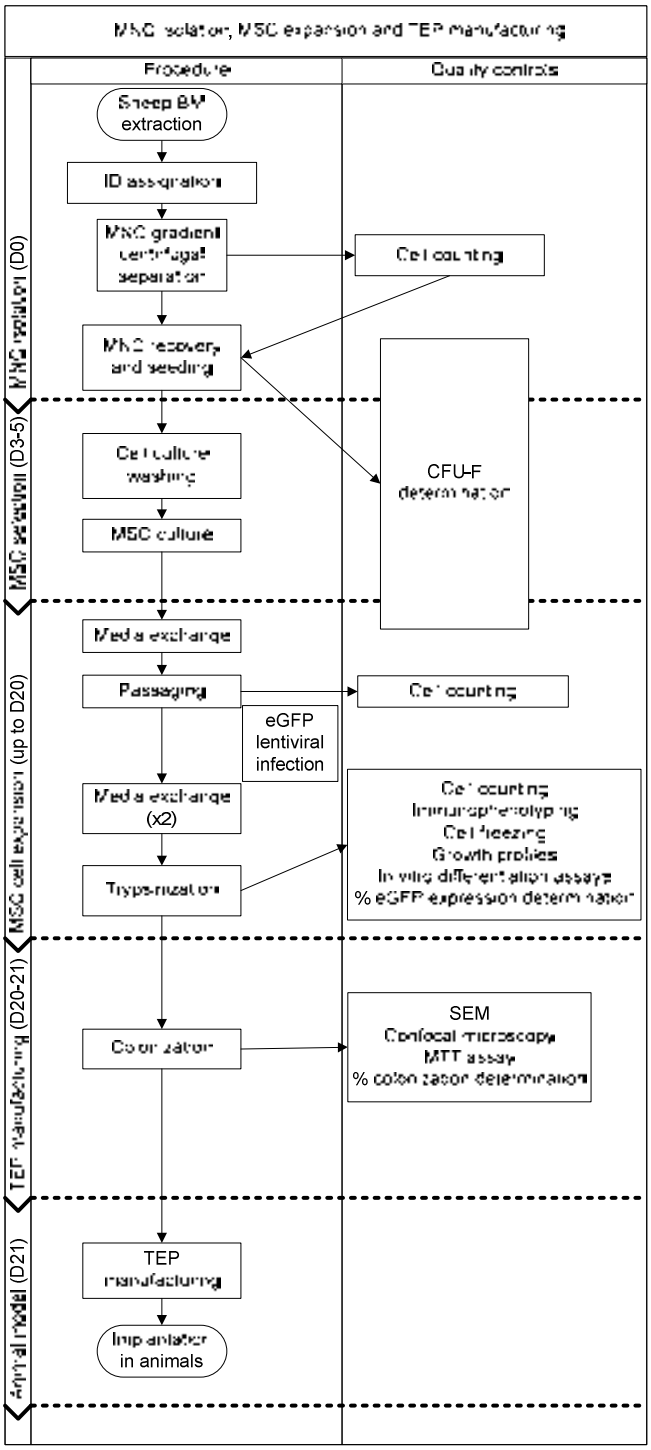

Fig. 8-1. TEP manufacturing overview.

8.2 Cell culture

Three types of cells were used in this PhD project; two of them were isolated from BM, which was aspirated either from sternum (for ovine cells), or from the iliac crest (for human cells). The third cell type was an established cell line called 293T (ECACC code 12022001), a variant of human derived embryonic kidney cells that contains the SV40 Large T-antigen, which allows episomal replication of transfected plasmids containing the SV40 origin, used for the production of lentivirus encoding the eGFP reporter.

8.2.1 Isolation of MNC from BM

Depending on the source (either animal or human). MNC were isolated following a different procedure after BM harvesting (see section **8.5.3 Bone marrow extraction**).

Prior to the isolation of MNC, sterility was confirmed by performing a specific test (see section **8.3.1. Sterility test**). Contaminated samples were discarded at this point, whereas sterile samples were further processed.

Either human or ovine BM was diluted 1:1 with PBS (Gibco, ref: 14190) and homogeneously mixed. In case that blood clots were present, these were discarded by either using a serological pipette or 100 μm filter, before proceeding to MNC isolation.

Next, a 1.077 g/mL density gradient medium was used to recover the MNC. To perform this procedure, 7.5 mL of 1.077 density gradient medium were placed in a 15 mL centrifugal tubes and other 7.5 mL of BM:PBS were dispensed in the tube slowly, in order to genera+te two separate phases. Two different gradient density

media were used depending on the cell source. For human cells, Ficoll-Paque™ PLUS (GE Healthcare Life Sciences, ref: 17-1440-02) was used, and Histopaque®-1077 (Sigma-Aldrich, ref: 10771) was used for the ovine source.

Tubes were then centrifuged in an Eppendorf 5804R under the following conditions (see **Table 8-1**).

	HUMAN SOURCE	OVINE SOURCE
Centrifugal force	330*g*	1000*g*
Time	25 minutes	35 minutes
Temperature	22ºC	22ºC
Acceleration	5	5
Break	0	0

Table 8-1. Centrifugal conditions for MNC isolation for two different sources.

After centrifugation, tubes presented the aspect shown in **Fig. 8-2**.

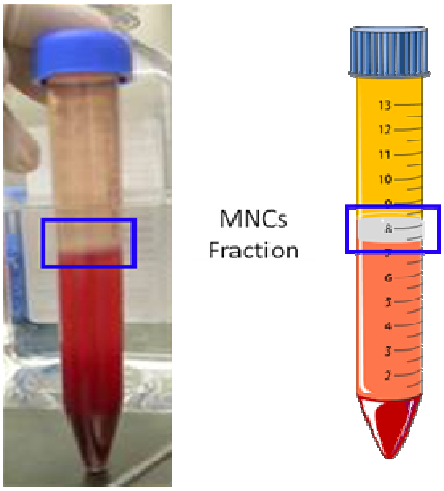

Fig. 8-2. Picture and schematic representation of the localization where MNC fraction must be located after centrifugation in a density gradient medium.

The MNC fraction was collected in two 50 mL sterile tubes, using a sterile Pasteur pipette, avoiding taking erythrocytes from the bottom phase. The two 50 mL tubes

were then filled with PBS, in order to dilute the gradient density media and were centrifuged 10 minutes at 400*g* and the supernatant was discarded.

For the purpose of lysing the erythrocytes, 1 mL of filtered lysing solution (160 mM NH_4Cl in sterile water; Sigma-Aldrich; ref: 254134) was added to each tube. After 10 minute incubation at room temperature, each tube was supplemented with 10 mL of PBS and centrifuged at 400*g* for 10 minutes. Supernatants were discarded and pellets from each sample were grouped together and resuspended with 10 mL of expansion media.

A sample of the cellular suspension was used for cell counting (as described in section **8.3.2. Cell counting, concentration and cell density calculation**).

Once nucleated cells were counted, BM yield was calculated as follows:

$$BM\ yield = \frac{Total\ nucleated\ cell\ number}{BM\ processed\ volume\ (mL)} \qquad \textbf{Equation 8-1}$$

8.2.2 MSC selection

MNC were seeded in culture flasks (T-25, T-75, T-150 or cell stacks) at $1{\cdot}10^5$ hMNC/cm^2 and $4{\cdot}10^5$ oMNC/cm^2 with expansion media (see **8.2.4 Expansion media** for media formulation and volumes in **Table 8-2**). Cells were maintained in a CO_2 incubator in an atmosphere of 5% CO_2, 95% humidity and at a temperature of 37ºC. After three to five days in culture, when MSC were adhered onto the plastic surface, the supernatants were discarded and adherent cells (MSC) were washed twice with PBS. MSC were further expanded (as described in section **8.2.3 Cell line maintenance**) in order to achieve a sufficient number of cells for the different experiments performed in this PhD project.

8.2.3 Cell line maintenance

D. Cell seeding and passaging

Cells were grown in the CO_2 incubator at the conditions specified in **8.2.2. MSC selection**. Medium was changed every 3-4 days. Media volumes are shown in **Table 8-2**. Typically, ten days after seeding, MSC reach confluence and need to be passaged, which involves harvesting and seeding new culture flasks.

Flask Type	Media volume (mL)
6 well plate (9.5 cm^2)	2
T-25 (25 cm^2)	6
T-75 (75 cm^2)	12
T-150 (150 cm^2)	20
Cell stack (636 cm^2)	80

Table 8-2. Media volumes depending on the culture flask.

E. Harvesting

MSC are adherent cells, and therefore they need to be detached from the surface. To do this, media was removed and cells washed with PBS in order to eliminate traces of serum that otherwise would inactivate trypsin. 0.05% Trypsin-EDTA solution (Gibco, ref: 25300) was added to the flask (see volumes in **Table 8-3**).

Flask Type (surface area)	Trypsin volume (mL)
6 well plate (9.5 cm^2)	0.5
T-25 (25 cm^2)	1
T-75 (75 cm^2)	3
T-150 (150 cm^2)	5
Cell stack (636 cm^2)	20

Table 8-3. Trypsin-EDTA volumes depending on the culture flask.

Culture flasks and plates were left in the CO_2 incubator for 5 minutes and cell detachment was checked visually using an inverted contrast phase microscope. If cells remained attached, the flasks were incubated for 5 extra minutes in the CO_2 incubator. The trypsin activity was inactivated with expansion media (twice the volume of trypsin).

A sample of the cellular suspension was taken for cell counting (see section **8.3.2. Cell counting, concentration and cell density calculation**).

MSC were reseeded at a cell density between $1{\cdot}10^3$ hMSC/cm^2 and $2.5{\cdot}10^3$ oMSC/cm^2 and maintained in a CO_2 incubator in an atmosphere of 5% CO_2, 95% humidity and at a temperature of 37ºC.

F. Cell freezing

Freezing media was prepared following this formulation:

- 20% expansion sera
- 10% Dimethyl Sulfoxide (DMSO) (Sigma-Aldrich, ref: 472301)
- 70% DMEM (see **1.A. Basal medium** for the formulation)

For optimal results MSC were harvested in the exponential phase of growth. Cells were trypsinized, counted and then centrifuged 10 minutes at 400*g. A*fter removal of the supernatant the cell pellet was gently resuspended in freezing media (1mL for each $1{\cdot}10^6$ MSC). The suspension was aliquoted in cryotubes containing $1{\cdot}10^6$ MSC in 1 mL of freezing media. Cryotubes were labeled indicating, at least, cellular type, cellular passage, date and initials of the person who performed the procedure.

Cryotubes were placed into the Mr. Frosty (Sigma-Aldrich, ref: C1562-1EA) filled with isopropanol (Sigma-Aldrich, ref: 190764) and then stored in a -80ºC freezer for at least 24 hours. Mr. Frosty is a device that allows a freezing ramp of 1ºC/minute. After 24 hours, cryotubes were transferred to a liquid nitrogen tank for long term storage.

G. Cell thawing

Thawing media was prepared following this formulation (equal volume as the thawing volume):

- 20% expansion sera
- 80% DMEM (see **1.A. Basal medium** for the formulation)

Thawing process and DMSO removal must be performed rapidly in order to remove DMSO quickly to preserve membrane cell structure.

One cryotube (1mL) was removed from the liquid nitrogen tank and maintained at 37ºC until the very moment that its contents started to melt (5 minutes approximately).

The volume of the cryotube was transferred into a 15mL tube and diluted 1:1 with the thawing media following these steps:

- 0.25 mL of thawing media addition→ 2 minutes at 4ºC (twice)
- 0.5 mL of thawing media addition → 2 minutes at 4ºC

Then cell suspension was diluted in 8 mL of expansion media. MSC from one cryotube were seeded in a T150 flask or equivalent surface area and media was

completely replaced after 24 hours in order to remove any residual traces of DMSO.

8.2.4 Expansion media

A. Basal medium

Both oMSC and hMSC were cultured using a basal medium DMEM either at low (1g/L) or high (4.5g/L) glucose concentration (Gibco, ref: 31885 and 41966 respectively). DMEM is a modification of Basal Medium Eagle (BME) containing four-fold concentrations of the amino acids and vitamins found in BME. DMEM is a widely used basal medium for supporting the growth of many different mammalian cells including MSC (Peterson, 1993).

B. Medium supplements

Supplements were added to media in order to offer essential compounds for cell activities such as cell adhesion, cell growth, extracellular protein transport, protease inhibitors and others.

Depending on the type of cells cultured, different sera supplements were used and these are detailed in **Table 8-4**.

Cell Type	Sera and concentration used
hMSC	10% AB human Serum (hSerAB)
oMSC	10% FCS (Fetal Calf Serum) or 10% ovine pool serum

Table 8-4: Sera used for each cell type.

Both hSerAB (Banc de Sang i Teixits) and FCS (Thermo Scientific, ref: SH3007103) are commercial products but ovine pool serum was produced in-house following the next protocol.

Blood bags without anticoagulants were used to extract blood. After extraction, blood bags were maintained at room temperature for 1-4 hours until the clot was formed. Bags were centrifuged in a vertical position in a Beckman J2-21 centrifuge according to the conditions listed in **Table 8-5**.

	SERUM CENTRIFUGATION
Centrifugal force	1300*g*
Time	25 minutes
Temperature	22ºC
Acceleration	2
Break	1

Table 8-5. Conditions for serum centrifugations.

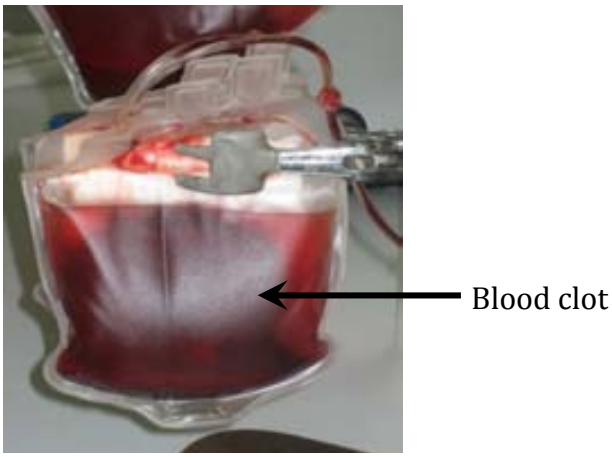

Fig. 8-3 Blood bag appearance after first centrifugation.

After centrifugation, blood bags presented the appearance shown in **Fig. 8-3**. Then serum from the blood bag was extracted with a serum extractor leaving the clot inside the bag. A second centrifugation was performed in order to eliminate blood cells from the sera. Conditions were the same as in the first centrifugation (see **Table 8-5**). After a second centrifugation serum presented the appearance shown in **Fig. 8-4**.

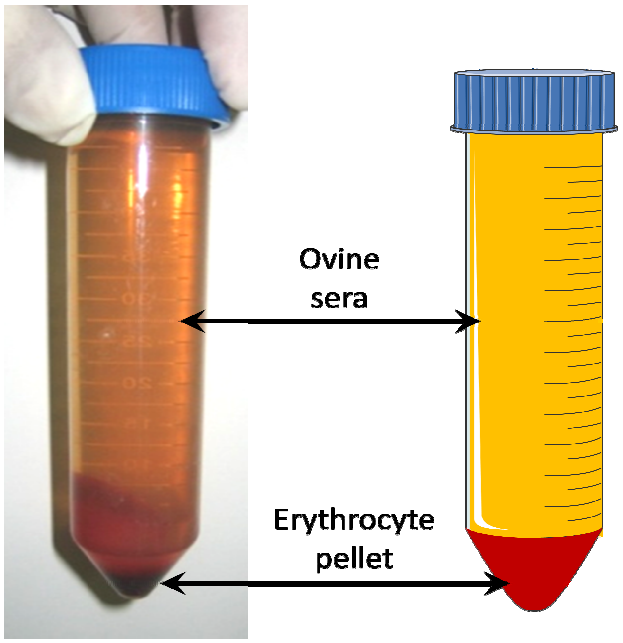

Fig. 8-4. Serum appearance after second centrifugation.

The supernatant was recovered avoiding taking the pellet and a third centrifugation was performed next following the same conditions (see **Table 8-5**). Serum was aliquoted in 50 mL tubes and sterility tests were performed for each aliquot (see section **8.3.1. Sterility test**). Tubes negative for contamination were then stored for at least 12 hours at -20ºC/-30ºC.

In order to generate a pool of sera, five different ovine autologous sera were thawed at room temperature and incubated in a water bath at 56ºC for 30 minutes to inactivate the complement. Pools were generated by mixing all sera in a sterile recipient, and then aliquoted in 50 mL tubes. Next, sterility tests were further performed (see section **8.3.1. Sterility test**) and aliquots were preserved at -20ºC/-30ºC until used.

8.2.5 Growth profile

Growth profile was performed to determine the growth kinetics parameters of the different cell types.

MSC were plated in two 6 well-plates (9.46 cm^2/well) at different densities ranging from $1 \cdot 10^3$ cell/cm^2 to $5 \cdot 10^3$cell/cm^2 and cultured for cell proliferation determination at 37ºC, 95% humidity and 5% CO_2. 3mL of 10% serum supplemented media.

Two wells were analyzed every 2-3 days, until the end of the growth curve. Cell culture supernatant was collected and used to determine the glucose and lactate's medium concentration using an automatic biochemical analyzer YSI 2700 (Yellow Spring Instruments) as an indirect test of cell growth (see section **8.3.2. Cell counting, concentration and cell density calculation**). Cell growth was followed by cell concentration determination. To do this, both wells were trypsinized (see section **E. Harvesting**), cells counted and cell density calculated (see section **8.3.2. Cell counting, concentration and cell density calculation**). Then cell kinetics parameters were determined. Batch culture cell growth is described by the next equation:

$$X = X_0 \cdot e^{(\mu \cdot t)} \qquad \textbf{Equation 8-2}$$

where X is the cell density (cells/cm^2) in a given time (t), X_0 is the initial cell seeding density (cells/cm^2) and μ is the specific growth rate ($days^{-1}$) and t represents the time in days.

During the exponential phase, specific growth rate is constant and maximum, μ_{max}. Its value was obtained from the slope of the linear regression corresponding to the exponential growth phase when ln X was plotted versus time.

$$\ln X = \ln X_0 + \mu_{max} \cdot t \qquad \textbf{Equation 8-3}$$

Cell population doubling time (DT) was calculated by:

$$DT = \frac{\ln 2}{\mu}$$ **Equation 8-4**

Cell population doublings (CPD) were calculated by:

$$CPD = \frac{\ln N}{\ln 2}$$ **Equation 8-5**

where N is the result of dividing the final number of harvested cells by the initial number of seeded cells. Then expansion factor (EF) was calculated as:

$$EF = PD \cdot e^2$$ **Equation 8-6**

The specific consumption rate (q_s, μmol/(10^6cells·day)) and production rate (q_p, μmol/(10^6cells·day)) were calculated by plotting either cumulative glucose consumption or cumulative lactate production versus the integral of viable cells (IVC) as described elsewhere (Bibila et al., 1994). And then slope of the regression lines corresponds to the consumption values. IVC was calculated as follows:

$$IVC = \int_0^t X dt = \sum_{i=0}^{n-1} [\bar{X}_i (t_{i+1} - t_i)]$$ **Equation 8-7**

where $\bar{X}_i = \frac{X_{i+1}+X_i}{2}$, X_i and X_{i+1} are the viable cell concentrations at times t_i and t_{i+1}, respectively, and $\overline{X}_i$ represents the average of viable cell concentration for the interval t_i - t_{i+1}.

8.2.6 MSC in vitro differentiation assay

A key feature of MSC is their capacity to differentiate to the Mesenchymal trilineage (Dominici et al., 2006). Thus, in order to demonstrate its identity by a functional assay, it's mandatory to differentiate MSC into osteoblasts, adipocytes and chondrocytes using the appropriate media.

A. Osteogenic differentiation

Cells were plated on 12-well plates at a density of $1 \cdot 10^4$ cells/cm^2 and incubated with expansion media at 37ºC, 95% humidity and 5% CO_2 for a minimum of 2 hours and up to 4 days allowing cells to adhere to the plastic surface. Then media was replaced by pre-warmed StemPro Osteogenesis kit medium (Gibco ref: A10072-01). Cultures were fed every 3-4 days with fresh pre-warmed medium avoiding cell detaching from the plastic surface by placing the medium slowly on the walls of the well.

After 7-14 days in Osteogenic environment, cells should express alkaline phosphatase 7 days later calcium depositions secreted by MSC can be detected by the Von Kossa staining procedure.

– Alkaline phospatase (AP) staining: AP activity was detected using a commercial kit TRACP&ALP double stain (Takara, ref: MK300), designed for the detection of bone-related cells, in which chromogenic substrates for alkaline phosphatase, an enzyme marker of osteoblasts, and tartrate-resistant acid phosphatase, an enzyme marker of osteoclasts, are combined with the reagent for nuclear staining that provides visualization of multinucleated osteoclasts (OC). Osteoclasts are derived from the differentiation of hematopoietic stem cells and share their lineage with monocytes and macrophages. Both acid and alkaline phosphatase activities in the cells can be stained simultaneously for comparison. However, MSC-derived osteoblasts progenitors only express alkaline phosphatase and that is the reason why only this staining was performed in this study.

The differentiation media was discarded and wells were washed once with PBS. Fixation solution was then added and the plate was left for 5 minutes at room temperature and after it was diluted with distilled water (1:10). Subsequently wells were emptied and washed once with sterile distilled water. Substrate solution for alkaline phosphatase was prepared according to the kit instructions and enough volume to cover the bottom was added to each well. Multiwell plates were incubated at 37ºC for at least 15 minutes and a maximum of 45 minutes for reaction (until coloring was detected). Staining solution was removed and discarded and wells were washed three times with sterile distilled water to terminate the reaction. Finally sterile distilled water was added to each well for the microscopic examination.

– Von Kossa functional assay: In studies using osteogenic cultures, mineralization is considered a functional in vitro endpoint reflecting advanced cell differentiation and von Kossa staining is used to visualize phosphate, within the deposited mineral (von Kossa, 1901). Von Kossa functional assay was performed at least 21 days after differentiation, since it is the time required for osteocytes to start the calcium deposition. Cell cultures were prefixed adding 4% paraformaldehyde (PFA) (Sigma-Aldrich, ref: 33220) solution and incubated for 10 minutes at room temperature. Media was removed and 4% PFA were added other time. After 10 minutes, wells were withdrawn and washed twice with distilled water. 5% Silver nitrate solution (Sigma-Aldrich, ref: S6506) w/v was added to the wells. Multiwell-paltes were left under UV light for 1 hour or until phosphate depositions appeared as a dark brown staining on the bottom of the wells. Wells were washed carefully with distilled water twice and one volume of water was added before

microscopic examination. Then macroscopic photographs of phosphate deposition were taken from each sample in order to easily compare different conditions.

B. Adipogenic differentiation

Cells were plated at a density of $1 \cdot 10^4$ cells / cm^2 on 12-well plates using expansion media and incubated at 37ºC, 95% humidity and 5% CO_2 for a minimum of 2 hours up to 4 days allowing cells to adhere to the plastic surface with the correspondent expansion media. Then media was replaced with pre-warmed StemPro Adipogenesis kit media (Gibco, ref: A10070). Cultures were fed every 3-4 days with fresh pre-warmed media avoiding cell detaching from plastic by placing the media slowly on the well walls.

– Oil Red-O staining: After a period of 7-14 days in adipogenic medium, cells accumulated lipid vacuoles and were ready for Oil red-O staining. Before the staining, cells were observed microscopically for the detection of lipid vacuoles in the cell cytoplasm. A prefixation was performed by adding 4% PFA without removing the culture media (1:1 volume ratio). After 10 minutes incubation, supernatants were removed and the fixation was performed by adding 4% PFA for 10 extra minutes. Wells were washed twice with PBS. Pure propylene glycol (1,2-propanediol) (Sigma-Aldrich, ref: 398039) was added to each well and cells were incubated for 2 minutes in order to permeabilize cell membranes. Then an Oil Red-O (Sigma Aldrich, ref: O0625) working solution was prepared by mixing 7 mL of 0.2% w/v Oil Red-O solution in methanol (Sigma-Aldrich, ref: 322415) with 2 ml of NaOH 1M solution (Sigma-Aldrich, ref: S2770) and was allowed to stand at room temperature for 20 minutes.

Isopropanol solution was then poured off and 0.5 mL of prewarmed Oil Red-O working solution was added to each well and was allowed to stain for 5 minutes. Wells were washed carefully with distilled water twice and one volume of water was added before microscopic examination in order to identify the intracellular lipid vesicles.

C. Chondrogenic differentiation

A cell suspension of $1.6 \cdot 10^7$ cells/mL was used for micromass generation. Cells were seeded in the center of each well by dispensing 5 µL droplets of the cell suspension. Micromasses were incubated for 2 hours at 37ºC, 5% CO_2 under high humidity conditions by adding PBS in the surrounding wells. Pre-warmed StemPro Chondrogenesis kit media (Gibco, ref: A10071) was added to each well very slowly. Cultures were fed every 3-4 days with fresh pre-warmed media avoiding micromass detachment from plastic by dispensing the media slowly on the well walls.

– Safranin O staining: After a period of at least 14 days, the extracellular accumulation of glycosaminoglycans (GAG) was detected by Safranin O staining. Differentiation media was withdrawn and wells were washed once with PBS. Then cells were fixed with 4% PFA for 30 seconds. Traces of PFA were eliminated by two PBS whashes. Then 1% acetic acid (v/v) (Fulka, ref: 34254) was added to the wells and incubated for 30 seconds and then aspirated. 0.01% Safranin O solution (w/v) was added to the micromass and incubated for 5 seconds. Excess of stain was removed by two PBS washes. Then distilled water was added and photographs of the stained micromass were taken using a microscope.

8.2.7 eGFP transduction

A. Lentiviral production

293T cells were seeded onto a 75 cm^2 culture flask (75cm^2) at 2.5·10^5 cells/cm^2 (80%-90% confluence) with DMEM + 10% FBS. On the next day, the transfection mix was prepared as follows (**Table 8-6**).

	T75	GENERAL
Filtered 150 mM NaCl	1500 µL	20 mL/cm^2
Envelope vector (VSVG)	1.5 µg	20 ng/cm^2
Rev expression vector (RTR2)	1.5 µg	20 ng/cm^2
Packaging vector (PKGPIR)	4.5 µg	60 ng/cm^2
eGFP vector	7.5 µg	100 ng/cm^2
1mg/mL PEI (Polysciences, ref 23966), pH 7.45	75 µL	1 µL/cm^2

Table 8-6. Quantities for the mix preparation. Plasmids for lentivirus production were prepared by Luigi Naldini (Hospital de San Rafaele, Milàn).and kindly provided by Dr. J. Barquinero (VHIR, Barcelona)

The mixture was let stand for 15-20 minutes at room temperature. Cell medium was withdrawn carefully and 25 mL of fresh medium was then added. Afterwards the DNA-PEI mixture was added slowly onto the cultured cells ensuring homogenization but avoiding shaking it. Then culture flasks were incubated at 37ºC, 95% humidity and 5% CO_2. After 12-16 hours, medium was replaced and cells were incubated at 37ºC, 95% humidity and 5% CO_2 for 48 hours more. On the third day after transfection, media was collected in sterile tubes and replaced by fresh media for three times (approximately every 12 hours). Collected media was conserved at 4ºC and then 0.45 µm filtration was performed. Cell suspension was ultracentrifugated 120 minutes at 25000 rpm at 4ºC (SORVALL Discovery 100 SE). Pellets were resuspended and hydrated for 18-24h at 4ºC. Viral suspension was aliquoted and preserved at -80ºC.

B. Viral titer

Viral titer was calculated by infecting 293T cells. Fourteen wells from 6 well plates were seeded with $1 \cdot 10^6$ 293T cells in each well with 2 mL of expansion medium and incubated at 37ºC, 95% humidity and 5% CO_2. Two wells were trypsinized and cells counted in order to determine cell density. Medium of the other wells was changed for fresh media and different volumes of viral suspension were added to each well (in duplicates), 0.1 µL, 0.5 µL, 1 µL, 2.5 µL, 5 µL and 10 µL. Plates were centrifuged at 1800 *g,* 90 minutes at 32ºC and then incubated for 72 hours at 37ºC, 95% humidity and 5% CO_2 replacing media every 24 hours. Cells were trypsinized and positive eGFP cells were quantified by flow cytometry (see **D eGFP fluorescence detection**). The number of viral particles was calculated using **Equation 8-8**, where *TU/mL* are the transductant units for each mL, *cells* is the number of cells counted at 24 hours, *eGFP* is the percentage of transducted cells and *V* is the volume of viral suspension added to the culture.

$$\text{viral titer (TU/mL)} = \frac{cells \cdot eGFP \cdot 10}{V} \qquad \text{Equation 8-8}$$

C. Lentiviral transduction

MSC were transducted in the day 6 to 8 of the culture before reaching confluence. Media was replaced for the minimum volume of fresh media that cover the surface of the culture (i.e., 6mL for a T-150). Then, a volume of virus calculated according the **Equation 1-9** was dispensed to the surface of the culture in horizontal position.

$$Virus\ volume\ 1(\mu L) = \frac{3.75 \cdot 10^6 \frac{virus}{cm^2} \cdot flask\ surface(cm^2)}{viral\ titer\ (virus/\mu L)} \qquad \textbf{Equation 8-9}$$

On the next day, medium was replaced for fresh media and between days 3 to 5 after the first transduction the procedure was repeated using **Equation 8-10** to calculate viral volume**.**

$$Virus\ volume\ 2\ (\mu L) = \frac{1{\cdot}10^6 \frac{virus}{cm^2} flask\ surface(cm^2)}{viral\ titer\ (virus/\mu L)} \qquad \textbf{Equation 8-10}$$

Ten days after the first transduction cells were subcultured as described in **8.2.3. Cell line maintenance**.

D. eGFP fluorescence detection

eGFP⁺ cells were detected by two techniques, 1) qualitatively by using fluorescence microscopy (excitation filter 470/40nm emission filter 515/30nm) and 2) quantitatively by using flow cytometry.

The percentage of transduced cells from the total number of cells was quantified by flow cytometry. A minimum of 30% eGFP positive cells was considered as an acceptable eGFP percentage for transplantation studies. Cultured cells were trypsinized and re-suspended in fresh medium and fluorescence was measured using a FACSCalibur flow cytometer (BD Biosciences). The fluorescence cutoff was chosen at the value that rendered a 1% or less positive events in the negative control (cells not transducted). The percentage of positive eGFP cells was calculated by **Equation 8-11**.

$$\%\ cells\ eGFP = \frac{concentration\ viable\ cells}{concenntration\ eGFP\ cells} \cdot 100 \qquad \textbf{Equation 8-11}$$

8.3 Analytical methods

8.3.1 Sterility test

All media were tested for sterility by placing 0.5 mL of the sample in 2 mL of rich media, such as Tryptose Phosphate Broth solution (Sigma-Aldrich, ref: T8159), and incubated at 37ºC, 95% humidity and 5% CO_2 for a minimum of 5 days. Then sterility was checked by observing the test under the microscopy. If no contamination was observed, the solution was considered sterile.

For cellular suspensions, the sterility test was performed by placing 0.1 mL of the testing solution in 2 mL of rich media, Tryptose Phosphate Broth solution, then 0.1 mL of this solution was placed in 2 mL of Tryptose Phosphate Broth solution and both tests were incubated at 37ºC, 95% humidity and 5% CO_2 for a minimum of 5 days. The test was checked and considered sterile just as explained above for media.

8.3.2 Cell counting, concentration and cell density calculation

Following trypsinization, a cell suspension was obtained and it was counted by either a direct method known as the trypan blue dye exclusion method (Phelan and Lawler, 2001), using a haemocytometer, or by an automated cellular counter (Scepter, Millipore).

A 1:1 dilution of the suspension of cells with 0.2% trypan blue (Sigma-Aldrich, ref: T8154) in PBS was performed (for example 100 µL trypan blue and 100 µL cell suspension). Then the haemocytometer was loaded by carefully touching the cover slip at its edge with the pipette tip allowing each chamber to overfill by capillarity.

Then cells were observed under a microscope at 100x magnification focusing in one of the 4 outer squares of the grid. A separate counting of viable (refractive and bright cells) and non-viable cells (blue and non-refractive) were performed for each square. The countings were performed in both chambers. A total of 8 squares were counted.

For an accurate determination, the total number of cells in one square should range between 5 and 100. If the number of cells exceeded 100, the sample was diluted and counted again, and if the number of cells was less than 10, a concentration of the sample was performed by centrifuging the sample 10 minutes at 400g and resuspending the cell pellet in a smaller volume.

Once cells were counted, for each chamber (see **Fig. 8-5**), the maximum and minimum values of each chamber were eliminated, having a total of four countings (n2a, n3a, n2b and n3b). Cellular concentration of the viable cells in the sample was determined by using the next equation.

$$Viable\ cell\ concentration\ (VCC)(cells/mL) = \frac{n1a+n2a+n1b+n2b}{2} \cdot 10^4 \qquad \textbf{Equation 8-12}$$

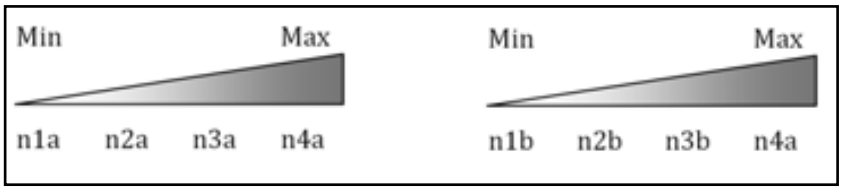

Fig. 8-5. Cell counting scheme of the Neubauer chamber. n1a, n2a, n3a and n4a for chamber a; n1b, n2b, n3b and n4b for chamber b.

Same procedure was performed for dead cells resulting in dead cell concentration (DCC).

Viability was determined by applying the next equation:

$$Viability\ (\%) = \frac{VCC}{VCC+DCC} \cdot 100 \qquad \textbf{Equation 8-13}$$

Total cell number was determinated by using the next equation:

$$Total\ cells\ (TC) = \ CC \cdot V\ (mL) \qquad \textbf{Equation 8-14}$$

Where CC is the cell concentration (either VCC or DCC) and V is the sample volume expressed in mL.

Cell density in the culture was calculated as follows:

$$cell\ density\ (CD)(cells/cm^2) = \frac{TC\ (viables)}{culture\ surface\ (cm^2)} \qquad \textbf{Equation 8-15}$$

8.3.3 Glucose and lactate concentration analysis

Supernatants of the cultures were analyzed using an YSI 27000 Select (Yellow Springs Instruments) to determine the glucose and lactate concentrations. This equipment has a very thin membrane with immobilized enzymes (glucose-oxidase and lactate-oxidase, respectively). Glucose and lactate undergo an enzymatic transformation producing hydrogen peroxide that passes through a membrane to a platinum electrode where the hydrogen peroxide is oxidized. The resulting number of electrons is proportional to the concentration of glucose and lactate, respectively.

Before analyzing the sample, this was centrifuged or filtered to remove cells or cellular debris. Samples were stored at -30ºC until the analysis was performed.

8.3.4 Colony-forming unit-fibroblast (CFU-F) assay

The capacity and efficiency for self-renewal of MSC was determined by seeding MNC at low density in 6-well culture plates and new fibroblast colonies derived from single cells were counted. For each condition 3 wells were seeded at a density of 1.5 and $3x10^5$ MNC/well. Seven after seeding, cultures were washed once with PBS and then fixed and stained with 0.5% crystal-violet solution (Sigma-Aldrich, ref: 32909) during 5 minutes at room temperature. Stained cultures were washed three times with distilled water to remove the residual dye. Violet colonies made up of more than 20 cells were scored as CFU-F and were counted. Calculation of the CFU-F efficiency was performed according to the **Equation 1-15** and the average were calculated for the triplicates.

$$CFU-F\ efficiency = \frac{counted\ CFU-F}{cells\ originally\ seeded} \cdot 100 \qquad \textbf{Equation 8-16}$$

8.3.5 Immunophenotypic analysis

MSC phenotypic analysis was performed by flow cytometry using a FACSCalibur flow cytometer (BD Biosciences). This equipment identifies the presence or absence of different molecules that were previously marked usually by antibodies or other fluorescent molecules with high affinity to the antigens to be detected.

One of the criteria recommended by the ISCT (International Society for Cellular Therapy) to define MSC is its immunophenotype determined by the expression of the antigens (Dominici et al., 2006). Such criteria were adapted to those antibodies

that cross-reacted with the ovine spice. For oMSC antibodies used for the cellular markers are the ones listed below (see **Table 8-7**)

Antibody	MSC	Fluorochrome	Isotype	Supplier	Reference	Clone
CD-45	h	PE	IgG1	BD Biosciences	556627	5H9
CD-44	o	FITC	IgG2bκ	BD Biosciences	555478	G44-26
CD-44	h	FITC	IgG1	AbD Serotec	MCA2219F	25.32
CD-90	o	PE	IgG1	Beckman Coulter	IM1840U	F15-42-1-5
CD90	h	APC	IgG1	BD Pharmingen	559869	5E10
HLA-DR	o	FITC	IgG2bκ	BD Biosciences	555560	TU36
CD140-α	h	AF647	IgG2aκ	BD Pharmingen	562798	αR1
CD166	h	PE	IgG1	BD Pharmingen	560903	3A6
CD105	h/o	PE	IgG1	Life Technologies	MHCD10504	SN6
Isotype control IgG1	h/o	PE	IgG1	BD Biosciences	340416	X40
Isotype control IgG2bκ	h/o	FITC	IgG2bκ	BD Biosciences	555742	27-35

Table 8-7: Cellular markers used to characterize hMSC (h) and hMSC (o).

100 µL of oMSC were labeled with 5 µL of each antibody for 15 minutes at room temperature in the darkness. Then 2 mL of PBS were added and suspension cells were centrifuged at 340 *g* during 10 minutes. Supernatant was discarded and the pellet then was resuspended with 100-150 µL of PBS before acquisition by flow cytometry.

8.4 Cell seeding of bone matrices

8.4.1 Bone matrix

Bone matrix used in all *in vivo* experiments was a clinical grade particulated cancellous bone dehydrated and deantigenized from human source (Bioteck ®, ref: Osteoplant).

8.4.2 Colonization without agitation

The bone matrix was transferred into a T-25 and oMSC were added to the flask in DMEM supplemented with 10% the corresponding sera. It was considered that all cells were attached to the scaffold within 18 to 24 hours.

In order to quantify the number of cells attached and thus the colonisation rate, a volume of supernatant was taken to perform a cellular counting (see section **8.3.2 Cell counting, concentration and cell density calculation**).

$$Attached\ Cells(AC) = initial\ cell\ number - cells\ in\ supernatant \quad \textbf{Equation 8-17}$$

$$Colonization\ Rate = \frac{AC}{initial\ cell\ number} \cdot 100 \quad \textbf{Equation 8-18}$$

8.4.3 Stirred colonization

Colonisation was performed in an agitated minibioreactor (Hexascreen ®) (shown in **Fig. 8-6**) sterilized by gamma radiation at 15 – 25 KGy. Bone scaffolds and resuspended cells were transferred to the bioreactor in a final volume of 10 mL. The minibioreactor was then placed onto a magnetic plate set at 120 -200 for 18 to 24 hours.

Fig. 8-6: Hexascreen ® Minibioreactor

In order to quantify the number of cells attached, a sample from the supernatant was harvesteded to perform a cell counting (see section **8.3.2 Cell counting, concentration and cell density calculation**).

8.4.4 Scanning Electron Microscopy (SEM)

Samples were fixed in 2.5% glutaraldehyde and 2% paraformaldehyde in PBS (pH 7) and dehydrated in ethanol series (15 minutes in each 30–50–70–90–100–100%) to absolute ethanol and immediately transferred to acetone before being critical-point dried and gold-coated using a Sputter Coater (K550, Coating Attachment, Emitech Ashford). Samples were examined with a HITACHI S-570 electron microscope at a voltage of 15 kV.

8.4.5 Confocal microscope

To stain the cells colonising bone the matrix it was incubated in 1 µg/mL Hoechst 33342 (Invitrogen, ref: H1399) solution for 10 minutes at 37ºC. Then 5µg/mL CellMask Deep Red (Invitrogen, ref: C10046) solution was added and incubed for 5 minutes at 37ºC. The bone matrix was washed with PBS twice and images were taken and analysed using a confocal microscope system (Leica, ref: TCS SP5).

8.4.6 Indirect cell growth determination

Indirect determination of cell growth was done by measuring the activity of living cells via mitochondrial dehydrogenase activity of immobilized cells in bone matrix. The key component is 3-[4,5-dimethylthiazol-2-yl]-2,5-diphenyl tetrazolium bromide (MTT). Mitochondrial dehydrogenases of viable cells cleave the tetrazolium ring, yielding purple MTT formazan crystals which are insoluble in aqueous solutions. The crystals can be dissolved in acidified isopropanol resulting in a purple solution that can be spectrophotometrically measured. An increase in cell number results in an increase in the amount of MTT formazan formed and an increase in absorbance.

The MTT method was performed using commercially cell growth determination kit (Sigma-Aldrich, CGD-1). MTT solution was added to the colonized bone scaffolds aseptically in a 1:10 ratio. Cultures were incubated for 3 hours at 37ºC, 5% CO2 and 95% humidity. After the incubation period, the resulting MTT formazan crystals were dissolved with an equal amount to the original culture volume of MTT solvent and cultures were agitated gently to completely dissolve the MTT formazan crystals. 100 µL of each sample were transferred to a 96 well plate and absorbance was measured spectrophotometrically at a 570 nm wavelength and background at 690 nm was substracted.

8.5 Animal models

8.5.1 Animal facilities

All experimental procedures adhered to the recommendations of local, national, and European laws (Decret 214 of 1997, Real Decreto 223 of 1988, European

directive 86/609/CEE of 1986, respectively). The two procedures on animals performed here received the approval by the Ethics Committee on Animal Experimentation of the Institut de Recerca de l'Hospital Universitari Vall d'Hebron.

8.5.2 Anaesthesia and post-operative care

All procedures were performed using aseptic techniques and under general anaesthesia. After premedication with an IM injection of 0.01mg/kg of buprenorphine (Buprex, Schering-Plough, S.A.) and 0.2 mg/kg of midazolam (Dormicum, Roche), IV access was established at cephalic vein. Sheep were pre-oxygenated and induced with 4 mg/kg IV propofol (Propofol-Lipuro 1%, BBraun Melsungen AG). The animals were under general anaesthesia intubated and maintained on isoflurane 2% (Isoflo, Abbott laboratories Ltd) with 100% oxygen. Esophageal intubation was made to prevent ruminal bloat. A continuous infusion of Ringer lactate (Ringer lactate, BBraun Melsungen AG) was administered at 10 mL/kg/h during surgery. Intraoperative monitoring consisted of electrocardiography, pulse oximetry, non invasive blood pressure and capnography. All animals received one dose of SC meloxicam (Metacam, Boehringer) 0.2 mg/kg daily for 10 days and a single dose of transdermal fentanyl (Durogesic, Janssen-Cilag) 100 μg for post-operative pain relief. For peri-operative infection prophylaxis the animals received 22 mg/kg of cefazolin IM (Kurgan, Normon Laboratories) every 12 hours during 10 days.

8.5.3 Bone marrow extraction

Sheep were placed in decubitus position and the sternum was aseptically prepared and draped. Using an 11G trochar (Sterylab, ref: BEN 1110), 2 mL of bone marrow

was aspirated before redirectioning the trochar and re-aspirating. A total of 65 cc of bone marrow aspirate was obtained and collected in a flask pre-filled with 8 mL of ACD-A (Grifols, ref: 721781).

8.5.4 Whole blood extraction

Sheep were first immobilized and then the neck of the animal was shaved and kept in hyperextended position. A 20G needle (BD Biosciences, ref: 303007) connected to a sterile 600mL transfer bag (TerumoBCT, ref: BB*T060CM) whithout anticoagulant was inserted into jugular vein in the caudocephalic direction and blood was withdrawn slowly. After extracting 100 to 250 mL of blood (a maximum of 10% of the whole blood total volume) the needle was withdrawn and jugular vein was pressed with the finger in order to stop bleeding. The blood transfer bag was sealed to preserve the sterility and immediately transported to the laboratory to proceed with sera extraction (see section **1.B Medium supplements**).

8.5.5 Critical size defect

The study was approved by the Ethics Committee on Animal Experimentation of the Institut de Recerca de l'Hospital Universitari Vall d'Hebron (Register number: 47/09 CEEA).

Sixteen sheep (*Ovis aries,* Ripollesa breed) were obtained from a licensed provider of experimental animals (A.M. Animalia S.L., Vall de Bianya) and then were divided in three groups listed in **Table 8-8**.

Group	Treatment	N (sheep number)
I	autologous bone replacement (gold standard; GS)	4
II	bone scaffold without oMSC	5
III	bone scaffold with oMSC	7

Table 8-8. Description of the experimental groups with the corresponding number of sheep treated in each group.

The temporality of each procedure performed in this study was listed in **Table 8-9**. Prior to starting the experiment sheep were included in the study and X-Ray and blood analysis were performed, and blood was extracted for sera production (see section **1.B. Medium supplements**).

	pre	D0	D7	D21	D41	D42	D49	D57	D133	D140
Animal selection	■									
Acclimatization, anamnesis		■→	■							
Blood extraction			■							
Serum obtaining			■							
Bone marrow extraction				■						
MSC expansion				■→	■					
MSC colonization					■					
CSD modelling						■				
Construct implantation						■				
Blood analysis	■					■		■	■	
X-Ray	■					■			■	
Weight						■	■	■	■	
Euthanasia									■	
Histological evaluation										■

Table 8-9. Critical size defect (CSD) study chronogram of the different phases of the experiment. MSC: Mesenchymal Stromal Cells, Pre: Time before the start of the study.

A critical size segmental tibial defect (2.2-2.5mm) was surgically produced and each experimental group was treated as follows:

- **Group I** (gold standard): followed the methodology and treatment described by Dias et al (Dias et al., 2007). Autografting spongy bone from humerus were applied to the critical size segmental tibial defect.

- **Group II** (scaffold without cells): 3 cm^3 of bone graft (Osteoplant; Bioteck, Vicenza, Italy) were hydrated and mixed with fibrin glue, Tissucol Duo (Baxter, ref: 690511.1) to mold the construct in a cylindrical shape. Then the construct was applied to the critical size segmental tibial defect.

- **Group III** (scaffold colonized with oMSC): 3 weeks prior to the critical size tibial resection, bone marrow cells were harvested from the sternum and MNC isolated on a Ficoll density gradient (see section **8.2.1 Isolation of MNC from BM**). Subsequently, adherent oMSCs were expanded for twenty days. Then 3 cm^3 of bone graft (Osteoplant; Bioteck, Vicenza, Italy) were colonised by the $6 \cdot 10^6$cells/cm^3 *ex vivo* expanded cells. The construct was molded by using fibrin glue (Baxter, ref: 690511.1) and immediately introduced into critical size segmental tibial defect.

Then all critical size segmental tibial defects were stabilized by a contralateral fixation using two limited contact dynamic compression plates (LC-DCP) per tibia. Eight holes LC-DCP (Synthes, ref: 224.580) with a total of 6 cortical screws between 18 and 22 mm long (Synthes, ref: 214.822, 214.820 or 214.818) were

used in the medial side and six holes LC-DCP (Synthes, ref: 224.580) with a total of 4 cortical screws between 18 and 22 mm long were used in the medial side, as depicted in **Fig. 8-7**.

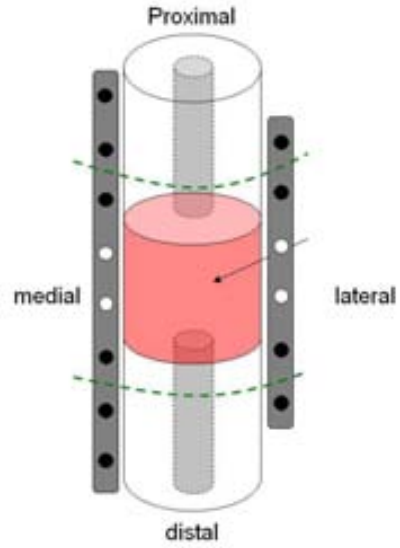

Fig. 8-7. Osteosynthesis plate fixation draw. The area enclosed with the dashed line was recoverd after the treatment for histological analysis. Arrow points the area of treatment.

After each of the treatments, surgical approach was closed. Remaining cells of group III were used in quality controls, differentiation assays (chondrogenic, osteogenic and adipogenic) and phenotypical characterization.

8.5.6 Osteonecrosis of the Femoral Head (ONFH)

The study was approved by the Ethics Committee on Animal Experimentation of the Institut de Recerca de l'Hospital Universitari Vall d'Hebron (register number 04/07 CEEA). 15 mature sheep (*Ovis aries*, Ripollesa breed) were obtained from a licensed provider of experimental animals (A.M. Animalia S.L., Vall de Bianya). Sheep were divided into three treatment groups as described in **Table 8-10**.

Group	Treatment	N (sheep number)
I	femoral head core decompression (gold standard; GS)	4
II	bone scaffold without oMSC	5
III	bone scaffold with oMSC	8

Table 8-10. Description of the experimental groups with the corresponding number of sheep treated in each group.

	pre	D0	D7	D28	D48	D49	D91	D97
Animal selection		■						
Acclimatization, anamnesis		■	■					
Blood extraction			■					
Serum obtaining			■					
ONFH modeling			■					
Bone marrow extraction				■				
MSC expansion				■	■			
MSC colonization					■			
Construct implantation						■		
Blood analysis	■						■	
Euthanasia							■	
X-Ray	■					■	■	
Histological evaluation								■

Table 8-11. Temporality of the different phases of the ONFH experiment. MSC: Mesenchymal Strmoal Cells. Pre: Time before the start of the study.

The temporality of the procedures performed in the osteonecrosis stufy is shown in **Table 8-11**. Prior to starting the experiment, sheep were included in the study and XR and blood analysis were performed. 6 weeks prior to the treatment, osteonecrosis was induced in the right hip according to a published ONFH method adapted to sheep (Vélez et al., 2011) and blood was extracted for sera obtaining (see section **1.B. Medium supplements**). For the osteonecrosis treatment, a small percutaneous incision was made just distal to the greater trochanter accessing the lateral femoral cortex. Using an image intensifier, a 2-mm guide wire was advanced

from the lateral cortex to the anterosuperior region of the femoral head reaching the periphery of the necrotic lesion. A 5 mm trephine was then introduced through the tunnel and advanced through the necrotic lesion. The trephine was removed and the bone cylinder extracted. Each experimental group was treated as follows:

- **Group I** (core decompression): no additional procedures were done.
- **Group II** (scaffold without cells): One cm^3 of lyophilized cancellous bone graft (Osteoplant; Bioteck, Vicenza, Italy) scaffold was introduced within a sterile 5 mm trephine mixed with fibrin glue, Tissucol Duo (Baxter, ref: 690511.1) to consolidate the construct. Then the trephine was introduced through the tunnel reaching the periphery of the necrotic lesion and an obturator was pushed through the trephine expelling the bone graft within the necrotic lesion and finally the empty trephine was then removed.
- **Group III** (scaffold colonized with oMSC): bone marrow cells were harvested from the sternum and MNC isolated on a Ficoll density gradient (see section **8.2.1 Isolation of MNC from BM**). Subsequently, adherent oMSCs were expanded for twenty days and then $6 \cdot 10^6$ cells were loaded in one cm^3 of bone graft (Osteoplant; Bioteck, Vicenza, Italy) and combined with fibrin glue in a 5 mm trephine which was then applied to the necrotic lesion in similar fashion as group II.

After each of the treatments, surgical approach was closed. Remaining cells of group III were used in quality controls, differentiation assays (chondrogenic, osteogenic and adipogenic) and phenotypical characterization.

8.5.7 Blood analysis

Several times during the experimental phase (**Table 8-9** and **Table 8-11**), blood samples were taken for analysis using a flow cytometry haematological system ADVIA 120 Analyzer (Bayer Lab, NY, USA) and on an Olympus AU400 auto analyzer (Hamburg, Germany).

8.5.8 Radiograohic (X-Ray) Immaging

Radiographic (X-Ray) imaging was performed in the latero-lateral and antero-posterior planes using Sedecal APR-Vet Console (Sedecal, Madrid, Spain) at 50KVp/5mAs/ 100mA/0.05s with a digital flat-panel detector system (Regius cassette 14 × 17, Konica Minolta, Tokyo, Japan).

8.5.9 Euthanasia

All animals were euthanatized by an overdose of Pentobarbital after previous sedation.

8.5.10 Mechanical test

Mechanical tests of tibiae were performed at a final point for the study of critical size defect. After culling the animals (6 weeks after the treatment), treated and contralateral tibiae were harvested and all muscle and tendon tissues were cleared out, avoiding damaging periosteum and the callus formed. Radiographs were taken from treated tibiae with the osteosynthesis plates positioned so that it could be properly evaluated the fracture callus. Then, osteosynthesis material was removed. Again radiographs were taken to visualize clearly the neoformation of bone at the osteotomy level.

The mechanical test consisted on a torsion test as described previously (Avery et al., 2007), which gave information related to the bone strength. Once the animals were euthanized, dissected tibiae were attached to both ends of the measuring equipment using bone polimetilmetraquilate surgical cement paste (Biomet, ref: Refobacin® Bone Cement R). The proximal end of the tibia was fixed and attached to a workbench. The distal end of the tibia was fixed to a torsion wrench. The tibia was aligned with the axis of rotation and the strength reader device was adjusted to zero. The bottom element was tightly fixed to the workbench. The torsion wrench was operated manually applying torsion force slowly and progressively ascending up to the fracture of the tibia. The torsion dynamometer (FA 500, Mecmesin) registered the torsion forces applied and all data were analyzed using Dataplot software (Mecmesin). The test was finished when the bone fractuded. Then tibiae were segmented just above and below the defect section and immersed in 4% PFA for later histological analysis.

8.5.11 Histological analysis

Femoral heads, tibiae and colonised bone were fixed in 4% PFA solution at room temperature for between 24 hours and 1 week, decalcified with 5 % formic acid for at least 24 hours and up to 12 weeks (depending on the calcification of the initial segment) and embedded in paraffin for subsequent histological and immunohistochemical procedures. At least 4 microtome sections of 4 μm thick were cut in the sagittal plane and stained with haematoxylin/eosin (H&E, Sigma-Aldrich; ref: H3136 and E4009).

For the ONFH study the sections were then digitalized and analyzed using ImageJ software (National Institutes of Health, US Government) and the plug-in BoneJ

(Copyright Michael Doube and licensed under General Public License version 3). The relative surface of newly formed bone of the total area of tissue was calculated, using a 8-bit image input with the command Optimise Threshold. The total bone area (BA) was divided by the total area of tissue (TA), after the lamelar bone area (LBA) was substracted by thresholding from the total bone surface (BA) to obtain the non-lamelar relative surface (NB/TA), thus, to estimate the rate of newly formed bone. The relative volume of immature osteoid was also measured using a 100 point reticle in which all points presenting immature osteoid were added and expressed as a percentage (Doube et al., 2010).

8.6 Data analysis

All data was expressed as the media ± standard deviation. All data calculation was performed using Microsoft Office Excel 2007 and data representation and statistical analysis using non-parametric tests (Kruskal-Wallis), 1way ANOVA and linear regressions, was performed by GraphPad Prism (GraphPad software).

8.7 Good Laboratory Practice

Compliance with the Organisation for Economic Co-operation and Development (OECD) Principles of Good Laboratory Practice (GLP) is concerned with the organisational process and the conditions under which laboratory studies are planned, performed, monitored, recorded, reported and archived (OECD, 2003). Some of the studies included in the present PhD project were performed according to the GLP regulations. In this respect, approved study plans and established Standard Operating Procedures (SOP) were followed for the execution of the

studies and assays. Moreover our Quality Assurance Unit (QAU) carried out periodical inspections.

CHAPTER IX

Bibliography

9. CHAPTER IX: Bibliography

Abad, M., Mosteiro, L., Pantoja, C., Cañamero, M., Rayon, T., Ors, I., Graña, O., Megías, D., Domínguez, O., Martínez, D., Manzanares, M., Ortega, S., Serrano, M., 2013. Reprogramming in vivo produces teratomas and iPS cells with totipotency features. Nature 502, 340–5. doi:10.1038/nature12586

Avery, C.M.E., Best, a, Patterson, P., Rolton, J., Ponter, a R.S., 2007. Biomechanical study of prophylactic internal fixation of the radial osteocutaneous donor site using the sheep tibia model. The British journal of oral & maxillofacial surgery 45, 441–6. doi:10.1016/j.bjoms.2006.10.010

Batinić, D., Marusić, M., Pavletić, Z., Bogdanić, V., Uzarević, B., Nemet, D., Labar, B., 1990. Relationship between differing volumes of bone marrow aspirates and their cellular composition. Bone marrow transplantation 6, 103–7.

Bianco, P., Robey, P.G., 2001. Stem cells in tissue engineering. Nature 414, 118–21. doi:10.1038/35102181

Bibila, T. a, Ranucci, C.S., Glazomitsky, K., Buckland, B.C., Aunins, J.G., 1994. Monoclonal antibody process development using medium concentrates. Biotechnology progress 10, 87–96. doi:10.1021/bp00025a011

Bruder, S.P., Jaiswal, N., Ricalton, N.S., Mosca, J.D., Kraus, K.H., Kadiyala, S., 1998. Mesenchymal stem cells in osteobiology and applied bone regeneration. Clinical orthopaedics and related research S247–56.

Campagnoli, C., 2001. Identification of mesenchymal stem/progenitor cells in human first-trimester fetal blood, liver, and bone marrow. Blood 98, 2396–2402. doi:10.1182/blood.V98.8.2396

Carrancio, S., López-Holgado, N., Sánchez-Guijo, F.M., Villarón, E., Barbado, V., Tabera, S., Díez-Campelo, M., Blanco, J., San Miguel, J.F., Del Cañizo, M.C., 2008. Optimization of mesenchymal stem cell expansion procedures by cell separation and culture conditions modification. Experimental hematology 36, 1014–21. doi:10.1016/j.exphem.2008.03.012

Colter, D.C., Class, R., DiGirolamo, C.M., Prockop, D.J., 2000. Rapid expansion of recycling stem cells in cultures of plastic-adherent cells from human bone marrow. Proceedings of the National Academy of Sciences 97, 3213–3218. doi:10.1073/pnas.97.7.3213

Colter, D.C., Sekiya, I., Prockop, D.J., 2001. Identification of a subpopulation of rapidly self-renewing and multipotential adult stem cells in colonies of human marrow stromal cells. Proceedings of the National Academy of Sciences of the United States of America 98, 7841–5. doi:10.1073/pnas.141221698

Connelly, L.B., Woolf, A., Brooks, P., 2006. Cost-Effectiveness of Interventions for Musculoskeletal Conditions, in: Jamison, D., Breman, J., Measham, A., Alleyne, G., Claeson, M., Evans, D., Jha, P., Mills, A., Musgrove, P. (Eds.), Disease Control Priorities in Developing Countries. 2nd Edition. World Bank, Washington (DC).

Dias, M.I., Lourenço, P., Rodrigues, A., Azevedo, J., Viegas, C., 2007. Utilizado na Regeneração Óssea num Modelo Experimental de Osteotomia da Tíbia. Acta Med Port 20, 37–46.

Dominici, M., Le Blanc, K., Mueller, I., Slaper-Cortenbach, I., Marini, F., Krause, D., Deans, R., Keating, a, Prockop, D., Horwitz, E., 2006. Minimal criteria for defining multipotent mesenchymal stromal cells. The International Society for Cellular Therapy position statement. Cytotherapy 8, 315–7. doi:10.1080/14653240600855905

Doube, M., Kłosowski, M.M., Arganda-Carreras, I., Cordelières, F.P., Dougherty, R.P., Jackson, J.S., Schmid, B., Hutchinson, J.R., Shefelbine, S.J., 2010. BoneJ: Free and extensible bone image analysis in ImageJ. Bone 47, 1076–9. doi:10.1016/j.bone.2010.08.023

Faundez, A.A., Taylor, S., Kaelin, A.J., 2006. Instrumented fusion of thoracolumbar fracture with type I mineralized collagen matrix combined with autogenous bone marrow as a bone graft substitute: a four-case report. European spine journal : official publication of the European Spine Society, the European Spinal Deformity Society, and the European Section of the Cervical Spine Research Society 15 Suppl 5, 630–5. doi:10.1007/s00586-006-0162-4

Godoy, R.F., Alves, A.L.G., Gibson, A.J., Lima, E.M.M., Goodship, A.E., 2014. Do progenitor cells from different tissue have the same phenotype? Research in veterinary science 96, 454–9. doi:10.1016/j.rvsc.2014.02.013

Jaramillo, D., Connolly, S.A., Vajapeyam, S., Robertson, R.L., Dunning, P.S., Mulkern, R. V, Hayward, A., Maier, S.E., Shapiro, F., 2003. Normal and ischemic epiphysis of the femur: diffusion MR imaging study in piglets. Radiology 227, 825–32. doi:10.1148/radiol.2273011673

Jarocha, D., Lukasiewicz, E., Majka, M., 2008. Adventage of mesenchymal stem cells (MSC) expansion directly from purified bone marrow CD105+ and CD271+ cells. Folia histochemica et cytobiologica 46, 307–14. doi:10.2478/v10042-008-0046-z

Langer, R., Vacanti, J., 1993. Tissue engineering. Science 260, 920–926. doi:10.1126/science.8493529

Laurencin, C.T., Ambrosio, A.M., Borden, M.D., Cooper, J.A., 1999. Tissue engineering: orthopedic applications. Annual review of biomedical engineering 1, 19–46. doi:10.1146/annurev.bioeng.1.1.19

Lázaro, P., Parody, E., García-Vicuña, R., Gabriele, G., Jover, J.Á., Sevilla, J., 2014. Cost of temporary work disability due to musculoskeletal diseases in Spain. Reumatología clinica 10, 109–12. doi:10.1016/j.reuma.2013.07.001

LeGeros, R.Z., 2002. Properties of osteoconductive biomaterials: calcium phosphates. Clinical orthopaedics and related research 81–98.

Marcacci, M., Kon, E., Moukhachev, V., Lavroukov, A., Kutepov, S., Quarto, R., Mastrogiacomo, M., Cancedda, R., 2007. Stem cells associated with macroporous bioceramics for long bone repair: 6- to 7-year outcome of a pilot clinical study. Tissue engineering 13, 947–55. doi:10.1089/ten.2006.0271

Mareschi, K., Rustichelli, D., Calabrese, R., Gunetti, M., Sanavio, F., Castiglia, S., Risso, A., Ferrero, I., Tarella, C., Fagioli, F., 2011. Multipotent mesenchymal stromal stem cell expansion by plating whole bone marrow at a low cellular density: a more advantageous method for clinical use. Stem cells international 2012.

Murphy, J.M., Fink, D.J., Hunziker, E.B., Barry, F.P., 2003. Stem cell therapy in a caprine model of osteoarthritis. Arthritis and rheumatism 48, 3464–74. doi:10.1002/art.11365

Nerem, R.M., 1992. Tissue engineering in the USA. Medical & Biological Engineering & Computing 30, CE8–CE12. doi:10.1007/BF02446171

OECD, 2003. Principles on Good Laboratory Practice.

Ohgushi, H., Goldberg, V.M., Caplan, A.I., 2009. Repair of bone defects with marrow cells and porous ceramic: Experiments in rats.

Parenteau, N., Naughton, G., 1999. Skin: the first tissue-engineered products. SCIENTIFIC AMERICAN-AMERICAN EDITION- 280, 83–85.

Peterson, J., 1993. Animal Cell Culture: A Practical Approach. The Yale journal of biology and medicine 66, 336–337.

Phelan, M.C., Lawler, G., 2001. Cell counting. Current protocols in cytometry Appendix 3, Appendix 3A. doi:10.1002/0471142956.cya03as00

Pittenger, M.F., 1999. Multilineage Potential of Adult Human Mesenchymal Stem Cells. Science 284, 143–147. doi:10.1126/science.284.5411.143

Pittenger, M.F., 2008. Mesenchymal stem cells from adult bone marrow. Methods in molecular biology (Clifton, NJ) 449, 27–44. doi:10.1007/978-1-60327-169-1_2

Prockop, D.J., Sekiya, I., Colter, D.C., 2001. Isolation and characterization of rapidly self-renewing stem cells from cultures of human marrow stromal cells. Cytotherapy 3, 393–6. doi:10.1080/146532401753277229

Putzier, M., Strube, P., Funk, J., Gross, C., Perka, C., 2008. Periosteal cells compared with autologous cancellous bone in lumbar segmental fusion. Journal of neurosurgery Spine 8, 536–43. doi:10.3171/SPI/2008/8/6/536

Quarto, R., M, M., R, C., SM, K., V, M., A, L., E, K., M, M., 2001. Repair of Large Bone Defects with the Use of Autologous Bone Marrow Stromal Cells — NEJM. new england journal of medicine 344, 385–6.

Reichert, J.C., Epari, D.R., Wullschleger, M.E., Saifzadeh, S., Steck, R., Lienau, J., Sommerville, S., Dickinson, I.C., Schütz, M. a, Duda, G.N., Hutmacher, D.W., 2010. Establishment of a preclinical ovine model for tibial segmental bone defect repair by applying bone tissue engineering strategies. Tissue engineering Part B, Reviews 16, 93–104. doi:10.1089/ten.TEB.2009.0455

Reichert, J.C., Saifzadeh, S., Wullschleger, M.E., Epari, D.R., Schütz, M. a, Duda, G.N., Schell, H., van Griensven, M., Redl, H., Hutmacher, D.W., 2009. The challenge of establishing preclinical models for segmental bone defect research. Biomaterials 30, 2149–63. doi:10.1016/j.biomaterials.2008.12.050

Russell, K.C., Phinney, D.G., Lacey, M.R., Barrilleaux, B.L., Meyertholen, K.E., O'Connor, K.C., 2010. In vitro high-capacity assay to quantify the clonal heterogeneity in trilineage potential of mesenchymal stem cells reveals a complex hierarchy of lineage commitment. Stem cells (Dayton, Ohio) 28, 788–98. doi:10.1002/stem.312

Sandhu, H.S., Grewal, H.S., Parvataneni, H., 1999. BONE GRAFTING FOR SPINAL FUSION. Orthopedic Clinics of North America 30, 685–698. doi:10.1016/S0030-5898(05)70120-6

Sekiya, I., Larson, B.L., Smith, J.R., Pochampally, R., Cui, J.-G., Prockop, D.J., 2002. Expansion of human adult stem cells from bone marrow stroma: conditions that maximize the yields of early progenitors and evaluate their quality. Stem cells (Dayton, Ohio) 20, 530–41. doi:10.1634/stemcells.20-6-530

Shahdadfar, A., Frønsdal, K., Haug, T., Reinholt, F.P., Brinchmann, J.E., 2005. In vitro expansion of human mesenchymal stem cells: choice of serum is a determinant of cell proliferation, differentiation, gene expression, and transcriptome stability. Stem cells 23, 1357–66. doi:10.1634/stemcells.2005-0094

Smith, B.P., 2014. Large Animal Internal Medicine. Elsevier Health Sciences.

Sotiropoulou, P. a, Perez, S. a, Salagianni, M., Baxevanis, C.N., Papamichail, M., 2006. Characterization of the optimal culture conditions for clinical scale production of human mesenchymal stem cells. Stem cells (Dayton, Ohio) 24, 462–71. doi:10.1634/stemcells.2004-0331

Sotiropoulou, P.A., Perez, S.A., Salagianni, M., Baxevanis, C.N., Papamichail, M., 2006. Cell culture medium composition and translational adult bone marrow-

derived stem cell research. Stem cells (Dayton, Ohio) 24, 1409–10. doi:10.1634/stemcells.2005-0654

Stępien, E., 2011. Coronary Angiography - Advances in Noninvasive Imaging Approach for Evaluation of Coronary Artery Disease. InTech. doi:10.5772/1812

Stevenson, S., 1998. Enhancement of fracture healing with autogenous and allogeneic bone grafts. Clinical orthopaedics and related research S239–46.

Stolzing, A., Jones, E., McGonagle, D., Scutt, A., 2008. Age-related changes in human bone marrow-derived mesenchymal stem cells: consequences for cell therapies. Mechanisms of ageing and development 129, 163–73. doi:10.1016/j.mad.2007.12.002

Stute, N., Holtz, K., Bubenheim, M., Lange, C., Blake, F., Zander, A.R., 2004. Autologous serum for isolation and expansion of human mesenchymal stem cells for clinical use. Experimental hematology 32, 1212–25. doi:10.1016/j.exphem.2004.09.003

Takahashi, K., Tanabe, K., Ohnuki, M., Narita, M., Ichisaka, T., Tomoda, K., Yamanaka, S., 2007. Induction of pluripotent stem cells from adult human fibroblasts by defined factors. Cell 131, 861–72. doi:10.1016/j.cell.2007.11.019

Takahashi, K., Yamanaka, S., 2006. Induction of pluripotent stem cells from mouse embryonic and adult fibroblast cultures by defined factors. Cell 126, 663–76. doi:10.1016/j.cell.2006.07.024

Vélez, R., Soldado, F., Hernández, A., Barber, I., Aguirre, M., 2011. A new preclinical femoral head osteonecrosis model in sheep. Archives of orthopaedic and trauma surgery 131, 5–9. doi:10.1007/s00402-010-1084-5

Von Kossa, J., 1901. Über die im Organismus künstlich erzeugbaren Verkalkungen. Beitr path Anat 29, 163–202.

Vos, T., Flaxman, A.D., Naghavi, M., Lozano, R., Michaud, C., Ezzati, M., Shibuya, K., Salomon, J.A., Abdalla, S., Aboyans, V., Abraham, J., Ackerman, I., Aggarwal, R., Ahn, S.Y., Ali, M.K., Alvarado, M., Anderson, H.R., Anderson, L.M., Andrews, K.G., Atkinson, C., Baddour, L.M., Bahalim, A.N., Barker-Collo, S., Barrero, L.H., Bartels, D.H., Basáñez, M.-G., Baxter, A., Bell, M.L., Benjamin, E.J., Bennett, D., Bernabé, E., Bhalla, K., Bhandari, B., Bikbov, B., Bin Abdulhak, A., Birbeck, G., Black, J.A., Blencowe, H., Blore, J.D., Blyth, F., Bolliger, I., Bonaventure, A., Boufous, S., Bourne, R., Boussinesq, M., Braithwaite, T., Brayne, C., Bridgett, L., Brooker, S., Brooks, P., Brugha, T.S., Bryan-Hancock, C., Bucello, C., Buchbinder, R., Buckle, G., Budke, C.M., Burch, M., Burney, P., Burstein, R., Calabria, B., Campbell, B., Canter, C.E., Carabin, H., Carapetis, J., Carmona, L., Cella, C., Charlson, F., Chen, H., Cheng, A.T.-A., Chou, D., Chugh, S.S., Coffeng, L.E., Colan, S.D., Colquhoun, S., Colson, K.E., Condon, J., Connor, M.D., Cooper, L.T., Corriere,

M., Cortinovis, M., de Vaccaro, K.C., Couser, W., Cowie, B.C., Criqui, M.H., Cross, M., Dabhadkar, K.C., Dahiya, M., Dahodwala, N., Damsere-Derry, J., Danaei, G., Davis, A., De Leo, D., Degenhardt, L., Dellavalle, R., Delossantos, A., Denenberg, J., Derrett, S., Des Jarlais, D.C., Dharmaratne, S.D., Dherani, M., Diaz-Torne, C., Dolk, H., Dorsey, E.R., Driscoll, T., Duber, H., Ebel, B., Edmond, K., Elbaz, A., Ali, S.E., Erskine, H., Erwin, P.J., Espindola, P., Ewoigbokhan, S.E., Farzadfar, F., Feigin, V., Felson, D.T., Ferrari, A., Ferri, C.P., Fèvre, E.M., Finucane, M.M., Flaxman, S., Flood, L., Foreman, K., Forouzanfar, M.H., Fowkes, F.G.R., Franklin, R., Fransen, M., Freeman, M.K., Gabbe, B.J., Gabriel, S.E., Gakidou, E., Ganatra, H.A., Garcia, B., Gaspari, F., Gillum, R.F., Gmel, G., Gosselin, R., Grainger, R., Groeger, J., Guillemin, F., Gunnell, D., Gupta, R., Haagsma, J., Hagan, H., Halasa, Y.A., Hall, W., Haring, D., Haro, J.M., Harrison, J.E., Havmoeller, R., Hay, R.J., Higashi, H., Hill, C., Hoen, B., Hoffman, H., Hotez, P.J., Hoy, D., Huang, J.J., Ibeanusi, S.E., Jacobsen, K.H., James, S.L., Jarvis, D., Jasrasaria, R., Jayaraman, S., Johns, N., Jonas, J.B., Karthikeyan, G., Kassebaum, N., Kawakami, N., Keren, A., Khoo, J.-P., King, C.H., Knowlton, L.M., Kobusingye, O., Koranteng, A., Krishnamurthi, R., Lalloo, R., Laslett, L.L., Lathlean, T., Leasher, J.L., Lee, Y.Y., Leigh, J., Lim, S.S., Limb, E., Lin, J.K., Lipnick, M., Lipshultz, S.E., Liu, W., Loane, M., Ohno, S.L., Lyons, R., Ma, J., Mabweijano, J., MacIntyre, M.F., Malekzadeh, R., Mallinger, L., Manivannan, S., Marcenes, W., March, L., Margolis, D.J., Marks, G.B., Marks, R., Matsumori, A., Matzopoulos, R., Mayosi, B.M., McAnulty, J.H., McDermott, M.M., McGill, N., McGrath, J., Medina-Mora, M.E., Meltzer, M., Mensah, G.A., Merriman, T.R., Meyer, A.-C., Miglioli, V., Miller, M., Miller, T.R., Mitchell, P.B., Mocumbi, A.O., Moffitt, T.E., Mokdad, A.A., Monasta, L., Montico, M., Moradi-Lakeh, M., Moran, A., Morawska, L., Mori, R., Murdoch, M.E., Mwaniki, M.K., Naidoo, K., Nair, M.N., Naldi, L., Narayan, K.M.V., Nelson, P.K., Nelson, R.G., Nevitt, M.C., Newton, C.R., Nolte, S., Norman, P., Norman, R., O'Donnell, M., O'Hanlon, S., Olives, C., Omer, S.B., Ortblad, K., Osborne, R., Ozgediz, D., Page, A., Pahari, B., Pandian, J.D., Rivero, A.P., Patten, S.B., Pearce, N., Padilla, R.P., Perez-Ruiz, F., Perico, N., Pesudovs, K., Phillips, D., Phillips, M.R., Pierce, K., Pion, S., Polanczyk, G. V, Polinder, S., Pope, C.A., Popova, S., Porrini, E., Pourmalek, F., Prince, M., Pullan, R.L., Ramaiah, K.D., Ranganathan, D., Razavi, H., Regan, M., Rehm, J.T., Rein, D.B., Remuzzi, G., Richardson, K., Rivara, F.P., Roberts, T., Robinson, C., De Leòn, F.R., Ronfani, L., Room, R., Rosenfeld, L.C., Rushton, L., Sacco, R.L., Saha, S., Sampson, U., Sanchez-Riera, L., Sanman, E., Schwebel, D.C., Scott, J.G., Segui-Gomez, M., Shahraz, S., Shepard, D.S., Shin, H., Shivakoti, R., Singh, D., Singh, G.M., Singh, J.A., Singleton, J., Sleet, D.A., Sliwa, K., Smith, E., Smith, J.L., Stapelberg, N.J.C., Steer, A., Steiner, T., Stolk, W.A., Stovner, L.J., Sudfeld, C., Syed, S., Tamburlini, G., Tavakkoli, M., Taylor, H.R., Taylor, J.A., Taylor, W.J., Thomas, B., Thomson, W.M., Thurston, G.D., Tleyjeh, I.M., Tonelli, M., Towbin, J.A., Truelsen, T., Tsilimbaris, M.K., Ubeda, C., Undurraga, E.A., van der Werf, M.J., van Os, J., Vavilala, M.S., Venketasubramanian, N., Wang, M., Wang, W., Watt, K., Weatherall, D.J., Weinstock, M.A., Weintraub, R., Weisskopf, M.G., Weissman, M.M., White, R.A., Whiteford, H., Wiersma, S.T., Wilkinson, J.D., Williams, H.C., Williams, S.R.M., Witt, E., Wolfe, F., Woolf, A.D., Wulf, S., Yeh, P.-H., Zaidi, A.K.M., Zheng, Z.-J., Zonies, D., Lopez, A.D., Murray, C.J.L., AlMazroa, M.A., Memish, Z.A., 2012. Years lived with disability (YLDs) for 1160 sequelae of 289 diseases and injuries

1990-2010: a systematic analysis for the Global Burden of Disease Study 2010. Lancet 380, 2163–96. doi:10.1016/S0140-6736(12)61729-2

Yamaguchi, M., Hirayama, F., Wakamoto, S., Fujihara, M., Murahashi, H., Sato, N., Ikebuchi, K., Sawada, K., Koike, T., Kuwabara, M., Azuma, H., Ikeda, H., 2002. Bone marrow stromal cells prepared using AB serum and bFGF for hematopoietic stem cells expansion. Transfusion 42, 921–927.

Yeatts, A.B., Fisher, J.P., 2011. Bone tissue engineering bioreactors: dynamic culture and the influence of shear stress. Bone 48, 171–81. doi:10.1016/j.bone.2010.09.138

APPENDIX

Scientific contributions

List of publications

1. Pla A, Sarró E, **Caminal M**, et al. Scaffolds for Articular Joint Tissue Engineering. In: Noll T, ed. *Cells and Culture SE -126*. Vol 4. ESACT Proceedings. Springer Netherlands; 2010:727-733.
2. Vélez R, Hernández-Fernández A, **Caminal M**, et al. Treatment of femoral head osteonecrosis with advanced cell therapy in sheep. *Arch Orthop Trauma Surg*. 2012;132(11):1611-1618.
3. **Caminal M**, Moll X, Codina D, et al. Transitory improvement of articular cartilage characteristics after implantation of polylactide:polyglycolic acid (PLGA) scaffolds seeded with autologous mesenchymal stromal cells in a sheep model of critical-sized chondral defect. *Biotechnol Lett*. 2014:1-11.
4. Fonseca C, **Caminal M**, Peris D, et al. An arthroscopic approach for the treatment of osteochondral focal defects with cell-free and cell-loaded PLGA scaffolds in sheep. *Cytotechnology*. 2014;66(2):345-354.
5. **Caminal M**, Fonseca C, Peris D, et al. Use of a chronic model of articular cartilage and meniscal injury for the assessment of long-term effects after autologous mesenchymal stromal cell treatment in sheep. *N Biotechnol*. 2014;31(5):492-498.

Congress contributions

1. Pla A, Sarró E, **Caminal M**, de la Fuente N, Cervera L, Vidal L, Cairo JJ, Gòdia F. Scaffolds for articular joint tissue engineering (2007). Poster. 20th ESACT Meeting. (Dresden, Germany).
2. Fonseca C, Morist A, **Caminal M,** Peris D, Fábregas PJ. Regeneración de lesión osteocondral en rodilla mediante la implantación artroscópica de polímero de ácido poliláctico colonizado con células madre: Estudio experimental en oveja (2008). Poster. Secive. (Zaragoza, Spain).

3. **Caminal M**, Vives, J Aguirre M, Esteves M, Rosal M, Fernández A, Martínez MJ, Pacha D, Huguet P, Garcia J, Pla A. Bone tissue engineered construct for the treatment of critical size segmental tibial defect in sheep (2010). Poster. Bone-Tec International Bone-Tissue-Engineering Congress (Hannover, Germany).

4. **Caminal M**, Vives J, Vélez R, Aguirre M, Esteves M, Rosal M, Huguet P, Garcia J, Pla A. Treatment of avascular necrosis of femoral head in an ovine model using autologous mesenchymal stem cells (2010). Poster. Bone-Tec International Bone-Tissue-Engineering Congress (Hannover, Germany).

5. Casamayor-Genescà A, Marín-Gallén S, Oliver-Vila I, **Caminal M**, Vives J, Pujol-Autonell I, Carrascal J, Vives-Pi M, Garcia J, Pla A. Expansión a escala clínica de células CD34+ de sangre de cordón umbilical con capacidad de injerto y repoblación en ratones NOD-Scid IL.2Rg null (2012). Poster. 23 Congreso Nacional de la Sociedad Española de Transfusión Sanguínea y Terapia Celular (SETS). (Saragossa, Spain). Condecoración con el Premio a la Mejor Comunicación en el área de "Tejidos y Terapia Celular".

6. Pujals-Fonts N, Casamayor-Genescà A, Marín-Gallén S, Oliver-Vila I, **Caminal M**, Vives J, Garcia J, Pla A. Desarrollo de un producto de terapia celular: Expansion a escala clínica de células CD34+ de sangre de cordón umbilical con capacidad de injerto y repoblación en ratones NOD-scid IL2rγnull (2013). Poster. Congreso de la Societat Catalana del Trasplantament (SCT). (Barcelona, Spain)

7. **Caminal M.** Situación actual de sustitutos sanguíneos (2013). Oral symposium. 24 Congreso Nacional de la Sociedad Española de Transfusión Sanguínea y Terapia Celular (SETS). (Murcia, Spain)

8. **Caminal M**, Pujals-Fonts N, Vives J, Codinach M, Oliver-Vila I, Casamayor-Genescà A, Coll R, Pla A, Garcia J. Development of a new advanced theraphy medicinal product for bone regeneration treatment; from bench to bedside. (2014). Poster. 20th ISCT Congress. (Paris, France).

9. Pujals-Fonts N, **Caminal M**, Vives J, Codinach M, Oliver-Vila I, Casamayor-Genescà A, Blanco M, Coll R, Pla A, Garcia J. (2014). Advanced cell therapy indicated for gonarthrosis treatment: the way to the completed clinical trial. Poster. 20th ISCT Congress. (Paris, France).

10. Coll R, Aguirre M, Hernandez A, **Caminal M**, Vives J, Oliver-Vila I, Codinach M, Blanco M, Pla A, Garcia J. (2014). Poster. Mesenchymal stromal cells for osteonecrosis of the femoral head (ONFH). data from ongoing clinical trial. Poster. 20th ISCT Congress. (Paris, France).

Patents

1. Pla A, **Caminal M**, Vives J, Oliver I, Garcia J. "Procedimiento para la obtención de un producto de ingeniería tisular orientado a la regeneración de tejido cartilaginoso". 2012. Ref. No.: 201030238/9. Applicant: Banc de Sang i Teixits.

2. Pla A, **Caminal M**, Vives J, Oliver I, Garcia J "Procedimiento para la obtención de un producto de ingeniería tisular orientado a la regeneración de tejido cartilaginoso" (2011). Ref. No.: P201130871. Applicant: Banc de Sang i Teixits.

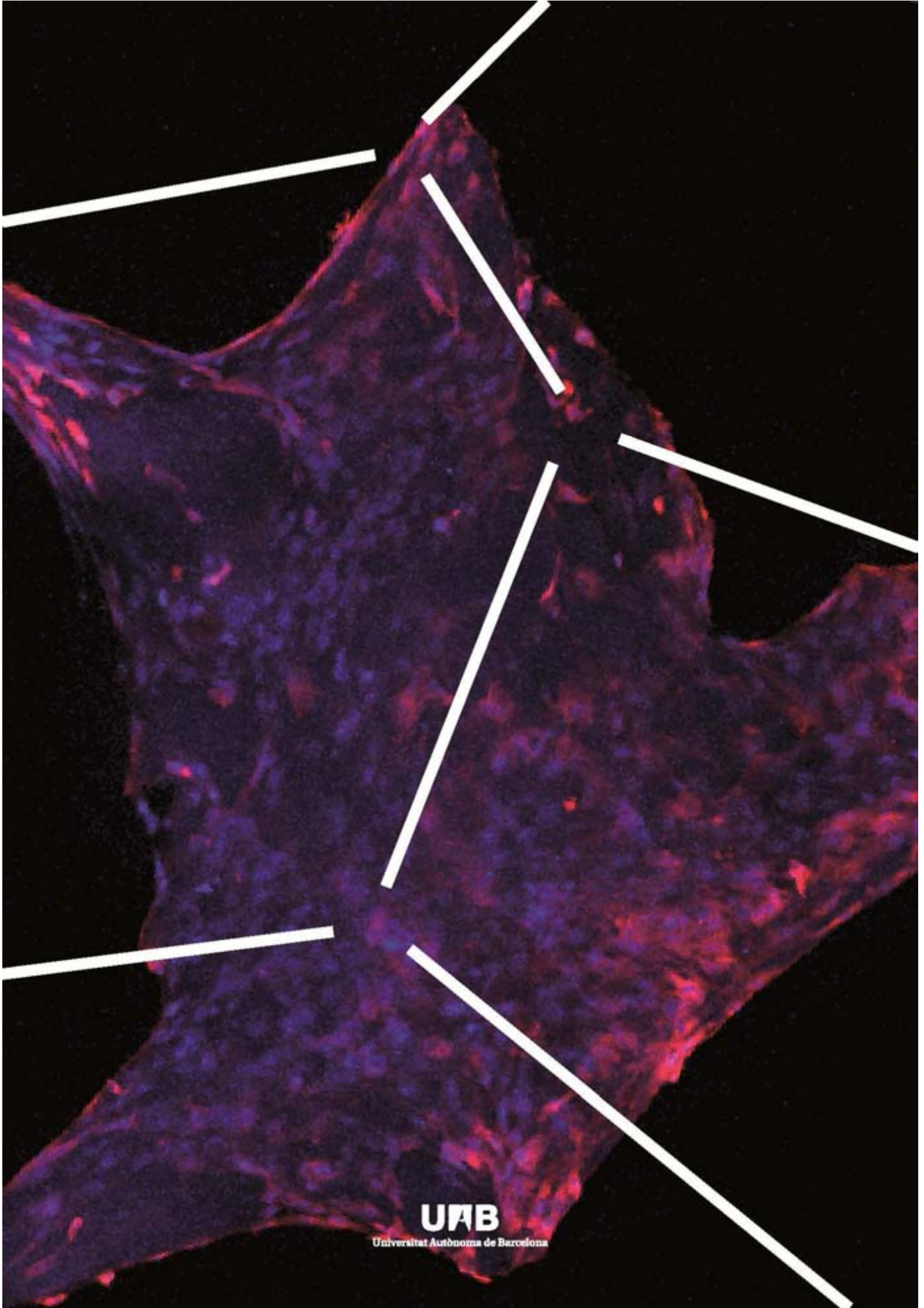

UAB
Universitat Autònoma de Barcelona